

**Mining University of Leoben / Montanuniversität Leoben**

**Master Thesis**

**Timur Cimitoğlu**

---

**Drilling in Hot Environments –**

**Causes and Effects of High Circulating Temperatures**



Department of Mineral Resources and Petroleum Engineering  
Chair of Drilling Engineering

**University supervisor:**

Univ.-Prof. Dipl.-Ing. Dr.mont. Gerhard Thonhauser, Head of Department of Drilling Engineering

**External supervisor:**

Dipl. Ing. Ralf Glettler, DrillTec GUT GmbH

## **Affidavit**

I declare in lieu of oath, that I wrote this thesis myself, using only literature cited in this volume.

## **Eidesstattliche Erklärung**

Ich erkläre an Eides statt, dass ich diese Arbeit selbständig verfasst, andere als die angegebenen Quellen und Hilfsmittel nicht benutzt und mich auch sonst keiner unerlaubten Hilfsmittel bedient habe.

.....  
Timur Cimitoğlu, Juni 2011

## **Acknowledgement**

I would like to take this opportunity to thank everybody who has helped me conducting this thesis. My particular gratitude goes to Univ.-Prof. Dipl.-Ing. Dr. mont. Gerhard Thonhauser, for his profound guidance and advice as my supervisor.

Moreover, I want to thank DrillTec GUT GmbH for giving me the chance to use their infrastructure and knowledge base. My special thanks hereby go to Dipl. Ing. Ralf Glettler, whose encouragement and support from the initial to the final level enabled me to develop my thesis.

Further, I offer my regards to all of those who supported me with valuable information and insight throughout the research and writing process. Namely I want to thank Oliver Kuchar, in place of STEP Offshore AS, Michael L. Drnec, in place of Halliburton, Ulrich Höfer, in place of Baker Hughes, and Dr. Thomas Kerk, in place of Weatherford International.

Last, but definitely not least, I would like to thank my beloved parents, for their good nature and care as well as their great effort they have put into my education.

## Abstract

Drilling in hot environments is becoming more and more common throughout the industry. The need to assure the growing energy supply asks for intensive development of demanding oil and gas fields as well as investments in alternative energy sources like geothermal energy. Either way, both have in common, that high temperatures are frequently encountered during drilling and production operations, thus causing concerns for operations, tools, well integrity and safety.

The scope of this work is to give a general understanding about the temperature development during drilling and to point out consequences for the involved operations.

In the introduction an overview about the actual activities and demands for high temperature drilling applications is presented. Common implementations, such as in HP/HT fields and geothermal hot spots as well as future technologies like the Hot Dry Rock technology are described briefly.

Thereafter an outline is given about subsurface heat-flow and the according static temperature situation down-hole. Further, a profound description about the development of the dynamic temperature profile during the hole-construction process is illustrated.

In a second step the attempt is to determine the relation and the impact of the various interacting parameters, affecting the temperature development during the drilling process. Therefore available data of a geothermal well drilled by DrillTec GUT GmbH was used and processed with the aid of a numerical simulator as well as an analytical method. Temperature profiles for the different operations were generated and compared to the actual sensor data, to verify the results.

As a next step, parameter studies were conducted, with both models, in order to get an overview of the impact and interaction of the single operational parameters. The results are discussed and further estimates are conducted.

The deteriorating influence of excessive heat on materials such as electronics, polymers, fluids, cement and metal is discussed in an additional chapter. General limits for tools and components involved in the whole construction process are identified and tabulated. Moreover, DrillTec GUT GmbH's rigs were investigated for potential improvements and limits regarding high temperature.

In a last step potential cost drivers for drilling operations in high temperature environments were evaluated and presented.

## Kurzbeschreibung

Bohroperationen in heißer Umgebung finden in der Industrie immer mehr Verbreitung. Der Bedarf, den heutzutage ständig wachsenden Energieverbrauch zu bedienen, verlangt nach einer intensiven Entwicklung von anspruchsvollen Öl- und Gasfeldern genauso wie nach Investitionen in alternative Ressourcen wie der Geothermie. Beiden genannten Fällen ist gemein, dass während der Bohrung und Produktion häufig hohe Temperaturen angetroffen werden, die in Problemen bezüglich der Operation, der Bohrlochintegrität und des verwendeten Equipments resultieren.

Das Ziel dieser Arbeit ist es, ein generelles Verständnis über die Entwicklung der Temperatur während dem Bohrprozess zu vermitteln und die Konsequenzen auf die entsprechenden Arbeiten aufzuzeigen.

Als Einführung wird dazu ein Überblick über die aktuellen Aktivitäten und Notwendigkeiten der Hochtemperaturoperationen präsentiert. Verschiedene Anwendungen, wie in HP/HT Feldern und geothermal aktiven Regionen, sowie zukunftssträngige Technologien wie Hot Dry Rock, werden kurz beschrieben.

Weiters wird eine Zusammenfassung über den Wärmefluss unter Tage gegeben und die damit zusammenhängende statische Temperaturentwicklung beschrieben. Danach wird eine detaillierte Beschreibung über die dynamische Temperaturentwicklung während des Bohrprozesses dargelegt.

In einem zweiten Schritt wird das Verhältnis und den Einfluss der verschiedenen, interagierenden Parameter, welche die Temperaturentwicklung im Bohrprozess beeinflussen, dargestellt. Dafür wurden verfügbare Daten einer Geothermiebohrung, durchgeführt von der Firma DrillTec GUT GmbH gesammelt und aufbereitet und dann mit Hilfe eines numerischen Simulators sowie einer analytischen Methode weiter bearbeitet. Temperaturprofile des Bohrloches wurden erstellt und mit den tatsächlichen Sensorwerten auf ihre Richtigkeit überprüft.

In einem weiteren Schritt wurde mit beiden Methoden eine Parameterstudie durchgeführt, um eine Übersicht über den Einfluss und die Interaktion der einzelnen Operationsparameter zu bekommen. Die Resultate werden diskutiert und weitere Vermutungen werden angeführt.

Der schädliche Einfluss exzessiver Hitze auf die Materialien wie Elektronik, Polymere, Fluide, Zement und Metall wird in einem weiteren Kapitel behandelt. Generelle Limits der für die Bohrung benötigten Komponenten werden identifiziert und tabellarisch aufgeführt. Bei dieser Gelegenheit wurden auch die Bohrtürme der Firma DrillTec auf potentielle Verbesserungen im Zusammenhang mit hohen Temperaturen untersucht.

Als ein letzter Schritt werden Kostentreiber für Bohroperationen in heißen Umgebungen evaluiert und präsentiert.

# Table of Contents

<b>Abstract</b> .....	<b>iv</b>
<b>Kurzbeschreibung</b> .....	<b>v</b>
<b>Table of Contents</b> .....	<b>1</b>
<b>Indices</b> .....	<b>2</b>
Index of figures .....	2
Index of tables.....	6
<b>Introduction</b> .....	<b>6</b>
<b>1. Temperature profiles</b> .....	<b>12</b>
1.1 The static temperature profile.....	12
1.2 The dynamic temperature profile.....	15
<b>2. Temperature development during drilling process</b> .....	<b>21</b>
2.1 Numerical simulation of a geothermal well .....	22
2.2 Analytical description of a geothermal well .....	31
2.3 Parameters affecting the temperature profile .....	38
2.4 Analysis of the drilling system energy balance .....	60
<b>3. Impact on materials &amp; equipment</b> .....	<b>65</b>
3.1 Metallurgy.....	66
3.2 Polymers.....	75
3.3 Fluids .....	91
3.4 Electronics .....	103
3.5 Review on limits and potential price drivers .....	110
3.6 Cost versus depth comparison.....	114
<b>Conclusion</b> .....	<b>117</b>
<b>References</b> .....	<b>120</b>
<b>Appendix</b> .....	<b>126</b>
A. Temperature limitations of fluid additives .....	126
B. Temperature limitations of various down-hole tools.....	129

# Indices

## Index of figures

Fig. 1: HP/HT fields around the world .....	9
Fig: 2 High temperature applications worldwide.....	9
Fig.3: Temperature distribution in Europe in 1000 meters depth .....	10
Fig.4: Resource base and power cost of the various geothermal energy systems for USA [12] .....	11
Fig.5: Left: Temperature-depth profiles near a salt dome, Right: Close to surface temperatures found in Bavaria [23] .....	13
Fig.6: Temperature gradient comparison of conductive vs. convective system; right: Temperature model of a real, virgin geothermal reservoir [12] .....	14
Fig.7: Subsurface temperature distribution in Germany at 3000 meters depth [36] .....	14
Fig.8: Temperature profile in the wellbore when circulating mud .....	16
Fig.9: Transient temperature behavior with time [88] .....	17
Fig.10: Temperature and pressure cycle of drilling mud [17] .....	18
Fig.11: Calculated temperature distribution at the close to wellbore formation at various depths .....	19
Fig.12: Theoretical temperature distribution for different shut-in times [33] .....	20
Fig.13: Theoretical bore-face temperature disturbance [33] .....	20
Fig.14: Wellbore schematics.....	23
Fig.15: Temperature distribution in the close subsurface .....	25
Fig.16: Diagrams of the sensor-data from the drilling operations.....	26
Fig.17: Diagrams of the down-hole temperature situation while constructing the 23” section.....	28
Fig.18: Diagrams of the down-hole temperature situation while constructing the 17 ½” section.....	29
Fig.19: Diagrams of the down-hole temperature situation while constructing the 12 ¼” section.....	30

---

Fig.20: Diagrams of the down-hole temperature situation while constructing the 8 ½" section open hole .....	30
Fig.21: Schematic of heat balance for tubular and formation <sup>[2]</sup> .....	33
Fig.22: Comparison of analytical method and numerical simulation results.....	34
Fig.23: Comparison of results of analytical method with and without energy input .....	35
Fig.24: Down-hole temperature development in annulus according the analytical method.....	36
Fig.25: Sensor data at flow-line from drilling operation 1.2 .....	36
Fig.26: Comparison of measured data and analytic tank model for drilling operation .....	37
Fig.27: Profiles for exact and linear gradient .....	41
Fig.28: Profiles for different temperature gradients.....	42
Fig.29: Temperature profiles depending on temperature and rock properties .....	43
Fig.30: Wellbore trajectories and vertical section of simulated wells: vertical well (left), J-shaped, S-shaped, build and hold profile.....	44
Fig.31: Temperature profiles of various well-paths .....	46
Fig.32: Annular temperature profiles for various well-geometries .....	48
Fig.33: Temperature profiles different pipe diameters .....	49
Fig.34: Temperature profiles of different flow-rates .....	50
Fig.35: Temperature profiles of different flow-rates in a deep well.....	51
Fig.36: Temperature profiles for water-based and oil-based mud .....	52
Fig.37: Temperature profiles for different nozzle sizes .....	53
Fig.38: Comparison of mud inlet Temperatures for a deep well given in a paper <sup>[2]</sup> (upper), and for the shallower drilling operation 3.2 (lower) .....	54
Fig.39: Temperature profiles different surface conditions .....	56
Fig.40: Possibility of temperature changes .....	57
Fig.41: Temperature ranges when changing specific properties .....	58
Fig.42: Control Volume of the well.....	60
Fig.43: Energy balance in the well .....	63



Fig.44: Components causing concerns at high temperatures .....	65
Fig.45: Yield Strength and Modulus of Elasticity vs. Temperature <sup>[71]</sup> .....	66
Fig.46: Degradation Chart of a Vallourec & Mannesmann S 135 6 3/8" drill pipe .....	67
Fig.47: Aluminum D16T alloy: Yield Point vs. temperature at different exposure times (left), creep vs. temperature at different exposure stress ranges (right) <sup>[50]</sup> .....	68
Fig.48: Thermal stresses in cemented casing <sup>[73]</sup> .....	70
Fig.49: Casing cross-section before and after thermal expansion <sup>[74]</sup> .....	71
Fig.50: Casing buckling with heating and elongation <sup>[73]</sup> .....	72
Fig.51: Rate of oxidation according to the Arrhenius-law <sup>[41]</sup> .....	73
Fig.52: Definition of the Rubber plateau <sup>[65]</sup> .....	75
Fig.53: Polymer network arrangement in elastomers <sup>[76]</sup> .....	76
Fig.54: Selection-table for natural rubber <sup>[76]</sup> .....	77
Fig.55: Temperature resistance of different natural rubbers .....	77
Fig.56: Temperature dependence of compression set <sup>[76]</sup> .....	79
Fig.57: Cross-section of a modern bi-material seal <sup>[52]</sup> .....	80
Fig.58: Typical roller cone bit lubrication reservoir <sup>[52]</sup> .....	81
Fig.59: Comparison of two 5:6 stators: Full rubber (left), rubber coated (right) <sup>[77]</sup> .....	82
Fig.60: Problem areas for massive heat development in the stator rubber <sup>[77]</sup> .....	82
Fig.61: Scaling factors for down-hole motors <sup>[77]</sup> .....	83
Fig.62: Bed material probes (left) and stinger protector probes (right) with allowed temperatures .....	85
Fig.63: Cost drivers for the reconfiguration of the rig .....	88
Fig.64: Rheological behavior „shear stress vs. shear rate... of the drilling mud at two different temperatures (20 and 49°C)... tested at the viscometer <sup>[95]</sup> .....	92
Fig.65: Example of the rheology of xanthan in sodium formate brine at different temperatures <sup>[58]</sup> .....	94
Fig.66: Price development with temperature for inhibited KCl water based systems .....	95

---

Fig.67: Effect of temperature on hydration time on Class G Portland cement observed in a calorimeter <sup>[53]</sup> (right), Effects of Temperature on thickening time <sup>[55]</sup> .....	97
Fig.68: Cement phases for various lime to silica ratios at different temperatures <sup>[53]</sup> .....	98
Fig.69: Hypothetical graph to show the influence of the retarder selection (left), Retardation of lignosulfonates at different Temperatures (right) <sup>[53]</sup> .....	99
Fig.70: Effect of sodium chloride on thickening time and compressive strength/development of cement [53].....	99
Fig.71: Effect of bentonite on compressive strength .....	100
Fig.72: Example of the temperature increase of cement with time .....	101
Fig.73: Annular pressure and temperature measurements during cementing <sup>[54]</sup> .....	102
Fig.74: Estimated price development of cement vs. temperature .....	102
Fig.75: Structure of the most common plastic encapsulated microcircuit .....	105
Fig.76: Temperature effect on a logging tools circuite board <sup>[88]</sup> .....	105
Fig.77: Difference in electronics module housing thickness between a normal (upper) and an HP/HT acoustic tool (lower) <sup>[90]</sup> .....	106
Fig.78: Dewar flask housing example <sup>[88]</sup> .....	106
Fig.79: Distribution of temperature limitations of wire-line logging tools .....	107
Fig.80: Temperature limitations of MWD/LWD tools available .....	108
Fig.81: Distribution of temperature limitations of MWD/LWD tools .....	109
Fig.82: Limits of down-hole tools and components .....	110
Fig.83: Limits of surface equipment .....	112
Fig.84: Maximum service temperature of materials according to the Ashby chart <sup>[96]</sup> ....	113
Fig.85: Cost vs. Depth of a well with different gradients .....	114
Fig.86: Comparison of temperature gradient of a hypohetic well with and without mud-cooler .....	116

## Index of tables

Table 1: Basic data of the geothermal well .....	22
Table 2: Physical properties of the formations drilled <sup>[15], [34]</sup> .....	24
Table 3: Impact of the different parameters in drilling operation 3.4 at 1 hour of drilling.....	38
Table 4: Impact of the different parameters in drilling operation 3.4 at the end of the operation .....	39
Table 5: Results for exact and linear gradient .....	41
Table 6: Results for various temperature gradients .....	42
Table 7: Results for different well-paths .....	43
Table 8: Input trajectories.....	45
Table 9: Results for different well-paths .....	47
Table 10: Pumping rates for the different derivations .....	48
Table 11: Results for different well-paths .....	48
Table 12: Results for different well-paths .....	50
Table 13: Results for different well-paths .....	52
Table 14: Results for different nozzle sizes.....	53
Table 15: Results for different surface conditions.....	56
Table 16: Sensor parameters at the end of drilling operation 1.2 .....	61
Table 17: Comparison of input and output power distribution of a well.....	63
Table 18: Elongation for different temperature profiles.....	68
Table 19: Stress resistance ratio for some common steel grades with P-110 as reference <sup>[62]</sup> .....	70
Table 20: Frequent polymeric materials in the oilfield .....	78
Table 21: Temperature sensitive elastomeric components of the DrillTec rigs.....	90
Table 22: Impact of the equipment on the total costs .....	115
Table 23: Limits for mud system, base fluids and additives and their limits found in the literature .....	127

Table 24: Limits for cement additives found in the literature ..... 128

Table 25: Temperature limits of MWD/LWD tools..... 138

## Introduction

Predicting the temperature profile throughout a wellbore is a difficult and highly complex procedure. Nevertheless, the knowledge of temperature present through the wellbore is essential for many aspects of drilling, completion, production and injection operations. Many operations and applications exist, that require an accurate knowledge and planning of the present temperature situation like: Drill bit design, BHA-layout, drilling mud and annular completion fluid formulation, determination of equivalent circulating/static density, corrosion and thermal stresses in casings and tubing, cement composition, placement, determination of setting time, logging tool design and log interpretation, detection of zones with poor casing cement, elastomer and seal selection for various tools (down-hole and surface), maximum allowable pumping rate, packer design and selection, wellhead and production equipment design, wax deposition in production tubing, permafrost thawing and refreezing, pressure/volume/temperature modelling of hydrocarbons, correlation between wells, understanding of temperature dependent geological processes such as cementation/dissolution of minerals, altering of maturation indicators and generation of hydrocarbons. <sup>[1], [2], [3]</sup>

All in all, overall planning of projects needs to be conducted more carefully as the additional factor of elevated down-hole temperature comes along. In today's drilling operations engineers have to deal more often with temperature induced problems by drilling deeper wells or wells that encounter high geothermal gradients. From 120°C (250°F) special attention should be put towards the drilling process, the fluids, the equipment and the tubular.

Although faced quite often, there is no general definition of the term "high temperature" through the industry. As a general rule, temperatures above 150°C (300°F) are referred to as "High Temperature" (HT). As in deep wells high temperatures are often faced in conjunction with high pressures, the term HP/HT is used to describe wells with temperatures over 300°F and pressures over 10 000 psi (690bar). This definition comes from the UK Department of Trade and Industry which stated for the first time a definition for a HP/HT well:

*"...where the undisturbed bottom hole temperature at prospective reservoir depth is greater than 149°C (300°F) and the maximum anticipated pore pressure of any porous formation to be drilled through exceeds 18 000 Newton/meter<sup>2</sup> (0.8 psi/ft) or around 10, 000 psi". <sup>[7]</sup>*

Above these values much more sophisticated design is needed due to smaller design margins of components, frequent upcoming tool limitations and to maintain well integrity. More recently, further separations developed: Normal HP/HT wells (Tier I) reach up to 1 334 bar/ 177°C, Extreme HP/HT (Tier II) up to 1 379 bar/ 204°C and Ultra HP/HT (Tier III) up to 2068 bar/ 260°C. <sup>[7]</sup>

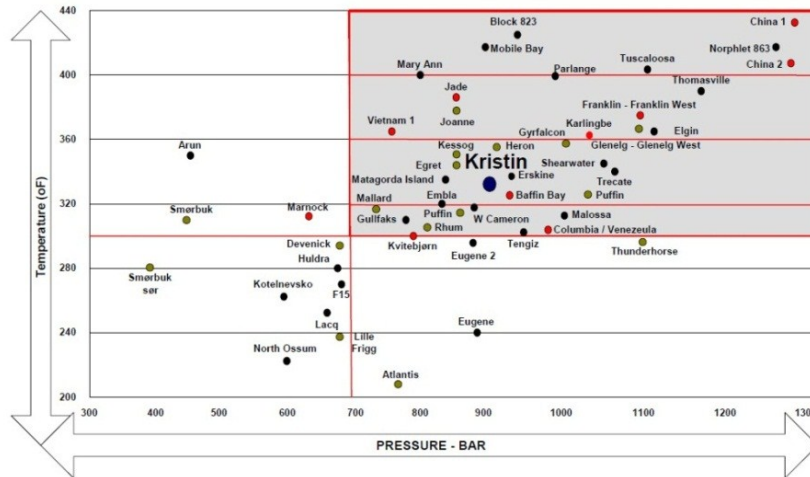


**Fig. 1:** HP/HT fields around the world

In recent years the amount of drilling operations conducted in high temperature environments increased noticeably. The need to satisfy the increasing energy demand requires an advance of drilling in more and more delicate areas, such as high gradient shale gas fields or the deep HP/HT fields. Operators were developing such fields for more than 20 years now, but due to increasing oil price and decreasing conventional resource base activities widened up and increasingly high temperatures are faced. Also the technology standard plays a major role in this very expensive exploration of such fields. A steep learning curve was observed supplied by enhanced key technologies in electronics, metallurgy, fluid systems and sealing.

Historically, exploration efforts for HP/HT formations started around Jackson Mississippi in the Gulf of Mexico and the North Sea in the seventies. Other earlier HP/HT basins are situated in Indonesia, Thailand and Northern Malaysia. Nowadays also the deep Gulf of Mexico Continental shelf, Northern India, Saudi Arabia and Brunei are involved in this increasing activity. The most severe conditions in Europe are found in the fields in the Central Graben of the North Sea, which represent mainly Trier II conditions. Bottom-hole temperatures over 200°C set technological and engineering requirements. [4], [5], [6], [7]

Below is a map showing HPHT plays across the world.

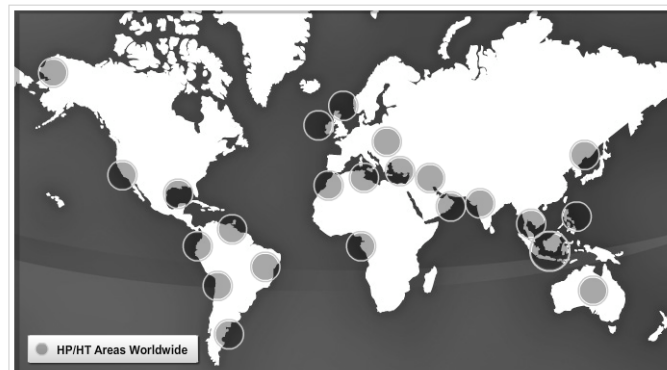


**Fig. 2** High temperature applications worldwide

Another situation in which high temperature environments are faced during drilling is geothermal exploration. The usage of geothermal energy sources gained increasing popularity lately, again driven by high energy prices and the desire for diversification of energy supply. Geothermal energy, compared to other alternative energy sources, is not dependent on weather conditions and is referred to as a “base load energy”.

Nevertheless, quickly changing energy prices, uncertainty of drilling costs, the actual water heat, production rates, and therefore the dimensioning of the surface facilities, influence the payout time and the critical overall economics of geothermal installations. As drilling costs represent about a half of the overall project costs it is essential to reduce operational hazards and to optimize the drilling process also for the elevated temperatures.

The development of geothermal resources began in 1904 with a geothermal power plant in Larderello, Italy. In the seventies the application increased rapidly, especially in the United States, caused by the oil crisis, followed by a phase of practical stagnation during the following decades. Currently, geothermal installations gain more attention worldwide again, for electricity production as well as for heating installations. The largest electricity generation is conducted by the United States (39%), Mexico, Italy, New Zealand, Iceland and Japan. Countries like Germany and Austria, with a moderate geothermal gradient, use the resource mainly for district heating applications which require less heat and often shallower wells. Electricity generation is hardly efficient here and thus needs more sophisticated technology (Organic Rankine and Kalina cycles) and governmental funding. In Europe currently the fastest developing market for geothermal electricity generation is in Western Turkey, benefiting from extremely high geothermal gradients and new governmental regulations. In direct geothermal applications like district heating, greenhouse heating and balneological use the country is already among the world leaders. [8], [9], [10], [11]

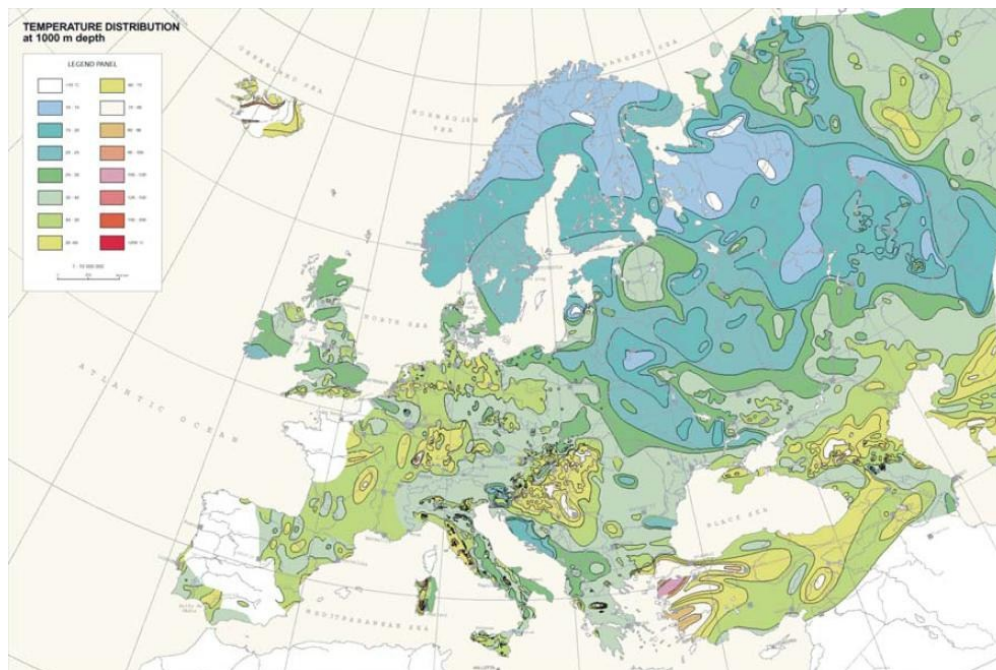


**Fig.3:** Temperature distribution in Europe in 1000 meters depth

Hot Dry Rock (HDR, Enhanced Geothermal System, EGS) represent a comparatively new type of geothermal power technology, which started in the seventies. Deep wells are drilled as a doublet into a hard rock formation, like granite. The temperatures faced are reasonably higher than with conventional geothermal drilling processes. By fracturing the hot, low-porosity rock and subsequent injection and production of water from the doublet an artificial heat reservoir is created. Currently in France, Australia, Japan, Germany, the U.S. and Switzerland such systems are being developed and tested. There is no widespread use until now, although a very large resource base exists worldwide.

The following figure presents an example of the approximate range of levelized power cost (in Dollar-¢/kWh) versus resource base (in kJ) for each of the potential geothermal resource types in the U.S. <sup>[12], [13]</sup>

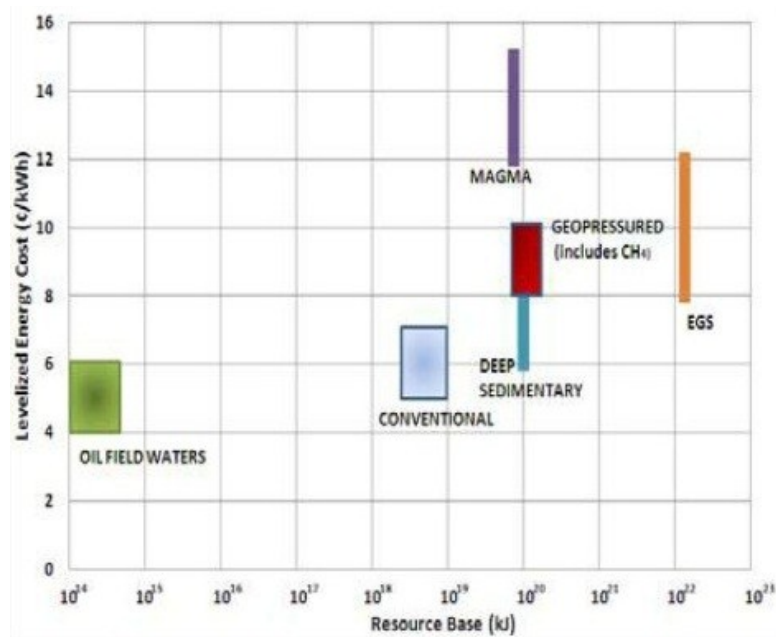


**Fig.4:** Resource base and power cost of the various geothermal energy systems for USA <sup>[12]</sup>

The economics are critical in geothermal projects, especially for HDR projects with their high fracturing costs. Seismic events, such as the induced seismicity during the HDR project in Basel or the damage caused by the geothermal plant in Landau in der Pfalz as well as the reduction of state subventions during the financial crisis of 2008/2009 represented a drawback for the development of geothermal resources. Also expensive HP/HT drilling projects were affected by the accompanying low oil price. Nevertheless, the strong increase of the price observed recently again increases the potential for a recurrence of widespread drilling activities for geothermal applications as wells as for HP/HT fields. <sup>[25]</sup>



# 1. Temperature profiles

Due to the heat flowing from the Earth's warm interior to its cooler surface temperature changes with depth are observed, which is an important engineering aspect particularly for drilling & production engineering. As a first step of approaching the temperature problem down-hole a clear separation must be established between the *static temperature profile*, also referred to as undisturbed/virgin/true formation temperature, and the circulating or *dynamic temperature profile*, which is a result of the working process.

The static temperature profile is the temperature present in the formations prior to the confrontation with the drilling process and is established over many millennia in a large time scale. The dynamic temperature profile is established within the drilling and production processes. Depending on the operation, the profiles develop mostly in a short term, transient way and influence the rock only in the vicinity of the wellbore.

## 1.1 The static temperature profile

The static temperature profile of the formation is expressed by the geothermal gradient, which is generally defined as the change of temperature by the change of vertical depth.

$$\text{Downhole Temperature} = \text{Surface Temperature} + \text{Vertical Depth} \cdot \frac{\text{Change of Temperature}}{\text{Change of Depth}}$$

### Equation 1

The geothermal gradient is the result of heat flow (convective or conductive) from the Earth's interior to the surface plus the thermal energy generated from radioactive decay of isotopes in the Earth's crust. Depending on the location there are huge discrepancies between gradients as heat flow depends on geology, mineralogy, morphology and especially volcanic/ activity. As a worldwide average the temperature increases about 25-30°C/km kilometer in depth. However, within ancient continental crust gradients as low as 10°C/km can be observed. A lower concentration of isotopes, as well as the presence of thicker impermeable sediment layers, shutting off thermal convection by deep waters, is the reason for the reduced heat flow. On the other hand the "Ring of Fire" around the pacific, spreading centres, continental rift zones and other hot spots, contain the hottest subsurface areas with high-temperature hydrothermal-convection systems that offer gradients larger than 100°C/km. <sup>[12], [14], [35]</sup>

The geothermal gradient is not increasing linearly in vertical. Temperatures at the close surface, which is needed to calculate the starting point of the geothermal gradient, are influenced considerably by seasonal temperature changes. Regional formulations of an average surface zone temperature through the year are needed. In the zone between the near surface down to several hundred meters the gradient is variable because it is affected by past climate changes and circulating ground waters. Below that zone

temperatures tend to increase with depth. However, the rate of increase varies considerably with the Earth's interior-terrestrial heat flow, the thermal properties of the rock and the tectonic setting.

Heat conduction from the underground heat sources can be observed by a more or less linear increase of temperature with depth. The intensity of increase depends mainly on the thermal conductivity of the formation. High formation conductivities result in low gradients and vice versa. Depending on the local geological setting temperature notable variations can occur as rocks conductivity may differ extensively. In the picture below an example is shown with a highly conductive salt dome formation and a lower conductive surrounding rock. Although the heat flow from the base sediments is the same, the different wells observe different gradients due to the deviations in the convective heat flow of the different rocks.

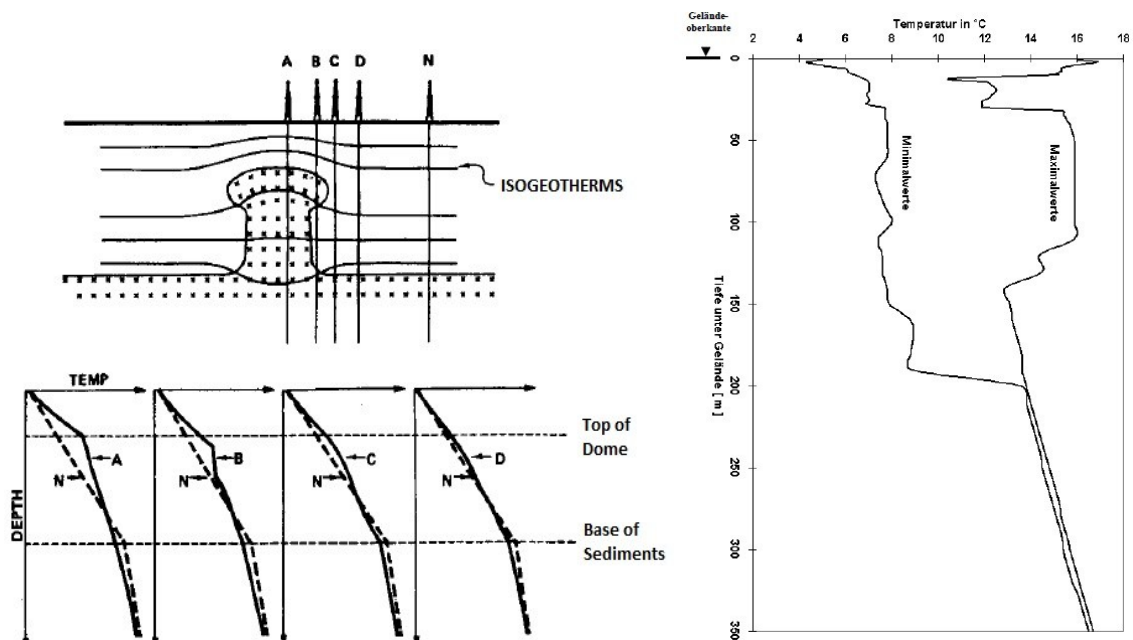


**Fig.5:** Left: Temperature-depth profiles near a salt dome, Right: Close to surface temperatures found in Bavaria <sup>[23]</sup>

Also the close presence of a terrain relief, like a mountain range, or water, in a close lake or sea, distorts the geothermal gradient for shallower subsurface regions. The lower temperatures of water will tend to affect the isogeothermal lines and decrease the temperature in adjacent formations. Elevations generally increase the isogeothermal lines. <sup>[23], [24]</sup>

Another way of heat transport is by convection due to deep water streams which transport heat up through faults, fractures and fissures. Heat convection can be observed by the temperature remaining more or less constant with depth. Such situations are especially interesting for geothermal energy applications, as larger amounts of heat are brought into shallower formations.

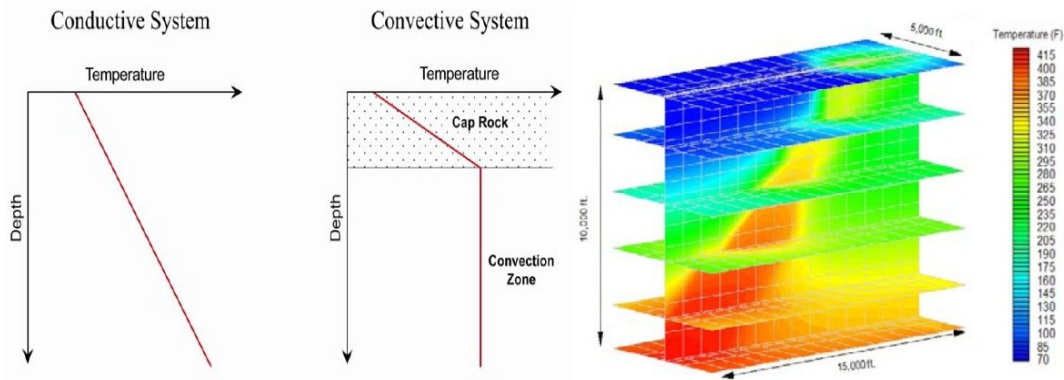


**Fig.6:** Temperature gradient comparison of conductive vs. convective system; right: Temperature model of a real, virgin geothermal reservoir <sup>[12]</sup>

Convection from fractured rock explains the high geothermal gradients observed for example in the Styrian Basin with their famous balneological accommodations. The observed average gradient for deep wells of around 30°C/km is not too high. Nevertheless, shallow wells show a much higher gradient due to the convective heat support from deep waters. <sup>[19]</sup>

Generally, in Germany and Austria the geothermal gradient is on a low average. A gradient of 30°C/km or slightly above can be found in the Malm formation in Bavaria and the Rhine rift. A slightly higher gradient can be found around Speyer which is up to 40°/km. <sup>[20]</sup> Also wells in the North, in the areas of Walsrode and Soehlingen, observed bottom hole temperatures up to 160°C.

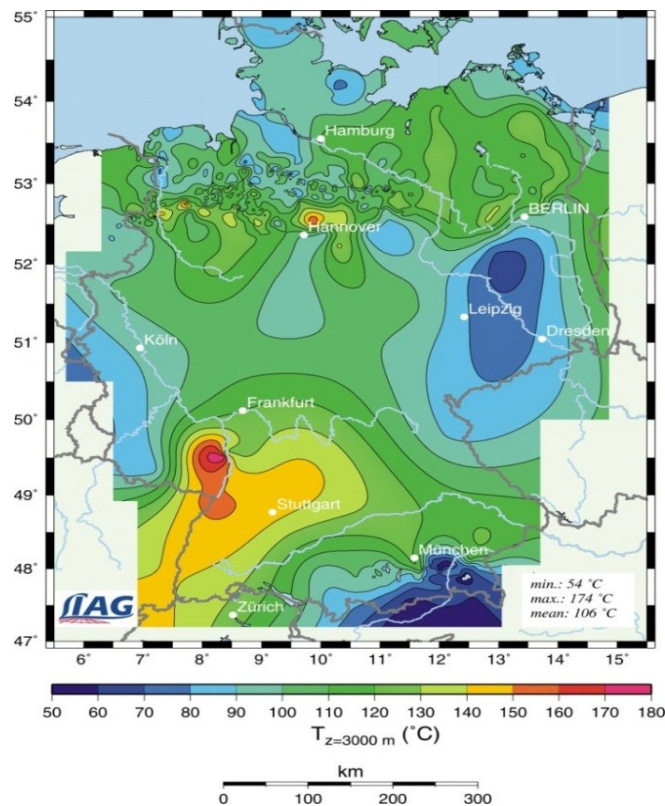


**Fig.7:** Subsurface temperature distribution in Germany at 3000 meters depth <sup>[36]</sup>

Iceland, which is famous in Europe for its geothermal power generation, water is extracted from areas with geothermal gradients larger than 40°C/km. Also some deep HP/HT wells in the North Sea showed such a gradient resulting in a virgin reservoir formation temperature of 250°C.

In Turkey several regions offer gradients up to 100°C/km and more. The Kızıldere Geothermal Field in the Büyük Menderes Graben for example contains temperatures of 240°C at a depth of 2300 meters and several very hot shallower convective reservoirs. [16]; [21]

Virgin rock temperatures are important for hydrocarbon exploration, as they are necessary for hydrocarbon generation computations and the estimation of the oil window.

Especially for the feasibility analysis of geothermal resources the knowledge of the exact down-hole temperatures is essential, as small changes in temperatures may lead to a large change of profitability of a project. The energy theoretically extractable from a reservoir can be shown by the basic equation: [22]

$$\text{Energy Produced} = \text{Mass} \cdot \text{Specific Heat Capacity} \cdot (\text{inlet Temp.} - \text{outflow Temp.}),$$

**Equation 2**

where the inlet temperature represents the reservoir temperature minus the heat losses of the fluid on the way to the surface installation, and the outflow the temperature behind the energy-extracting installations (injection temperature to the reservoir or district heating temperature).

## 1.2 The dynamic temperature profile

During various well operations like drilling, completion, production and injection a deviation of temperatures in the wellbore and the adjacent formations is caused. Any temperature difference between the formation and the circulating fluid causes a heat transfer. Though, the drilling fluid acts as a heat transmitter and tends to balance out the temperature difference between surface and down-hole.

When the virgin formation is penetrated in the drilling process it gets cooled by the drilling fluids. The drilling fluid on the contrary is heated up by the elevated temperatures present in the formation. Hydraulic and mechanical friction further increases the fluid temperature.

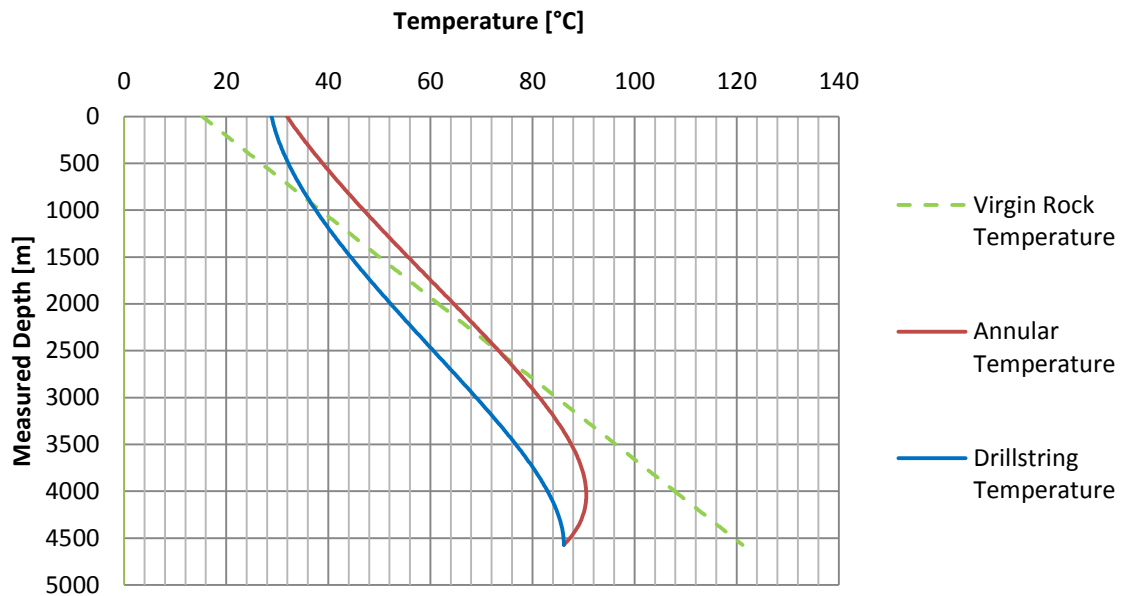


**Fig.8:** Temperature profile in the wellbore when circulating mud

The following parameters affect the heat exchange and the development of the dynamic temperature profile during circulation:

a.) Physical properties of fluid and formation:

- i. Specific heat capacity
- ii. Thermal conductivity
- iii. Mud Rheology
- iv. Density

b.) Heat sources:

- i. Formation heat determined by the geothermal gradient
- ii. Heating due to mechanical friction (Drill string, BHA, Bit),
- iii. Heating due to hydraulic friction/pressure drop,

c.) Heat losses:

- i. Cooling at surface installations (Tank volume, air temperature..),
- ii. Cooling in riser at offshore applications,
- iii. Cooling with mud coolers,

d.) Agitation from mud agitators or string vibration has a cooling (agitating) and a heating (hydraulic energy) effect.

e.) Fluid influx from the formation

f.) Operational parameters and timing

- i. Flow rate, pressure, ROP
- ii. Wellbore Geometry
- iii. Operational sequence (drilling, circulating, logging, shut-in...)
- iv. Mud additives added

Depending on the parameters, the actual dynamic down-hole temperature profile varies between the lowermost possible temperatures reached during long circulation on one side, and the static formation temperature on the other. The circulation time of the operation is thereby a major factor: Heat conduction from the formation to the annulus is a rather slow process, so that short term operations (like short drilling or circulation, cementing, completion, fracturing or production start-up) will be in a transient state. Long term operations (like long drilling intervals, production or injection operations) result in a more steady state temperature dynamic equilibrium.

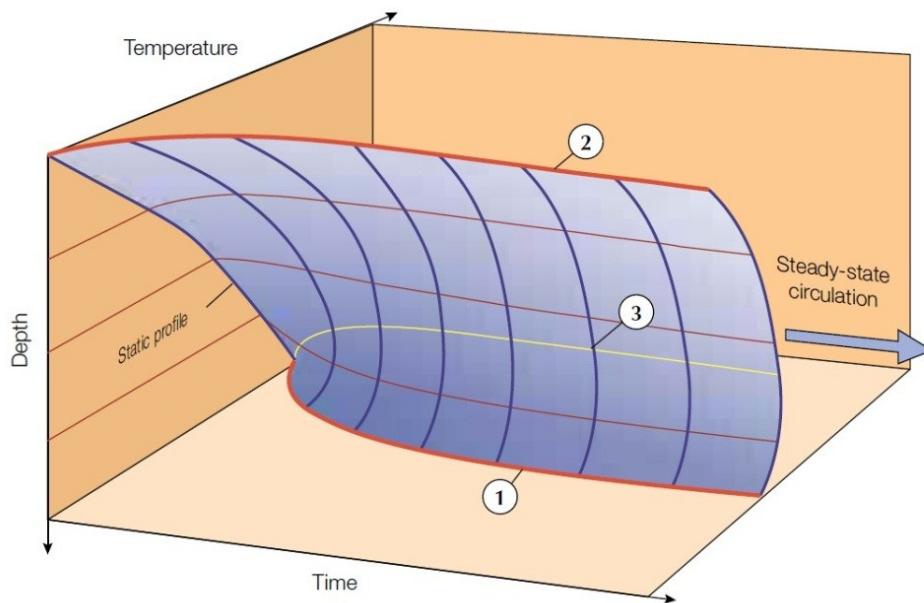


**Fig.9:** Transient temperature behavior with time <sup>[88]</sup>

In the transient state the fluid temperature is strongly sensitive to the flow-rate. In figure 9 the deviation of the annular temperature distribution with time can be seen. While the bottom hole temperature (1) decreases, after establishing circulation, the flow-line temperature (2) increases. Depending on the formation temperature the hottest point in the mud column may move from the lowest section to some place in the lower third of the wellbore. A dynamic equilibrium is reached in the matter of hours. Vice versa when interrupting the fluid flow the temperature profile will tend to shift back to the static conditions, which it can get close to in the matter of more than a day. <sup>[3], [17]</sup>

As the temperature profile depends on many interacting operational parameters mentioned above, the time needed to reach steady state temperature conditions can therefore not be globally stated.

When analysing the temperature profile one has to keep in mind, that the heat transfer of the mud is convective, while the transfer through the formation is mainly conductive. The formation gets cooled or heated continuously by the bypassing fluid. The drilling mud on the other side flows through the whole wellbore for many cycles. For a volume unit of circulating mud the following temperature development with time can be observed during one circulation cycle:

The drilling mud is stored at the suction tanks, where it reaches its lowest temperature. When passing the suction pump and the mud pump it gets loaded with hydraulic energy. Small heating occurs in the range of deci-degrees, depending on the hydraulic efficiency of the pump. The heat generated on the surface in pumps and pipes, however, is small and the effect of heat losses to the atmosphere is probably in the same range or higher. While circulating down the drill-string the heat exchanged with the annulus results in an increase of temperature. Also the fluid friction heat has a small impact. While passing restrictions in the end of the drill-string (bit nozzles, mud motor, MWD/LWD etc.) the temperature increases again sufficiently.

In the annulus the lower part of the formation still transfers additional heat energy to the mud. At a certain point in the lower part of the annulus the mud reaches its highest temperature in the cycle. Above this point the hotter mud transfers heat to the cooler formation.

At the bell nipple the drilling mud exits the well to the flow line and is exposed to the surface temperatures. Cooling occurs at the shakers, where the surface area is maximised and heat exchange with air and vaporisation of water is facilitated. In the mud tank heating from pumping as well as cooling effects from agitation, wind and weather or from additives happen.

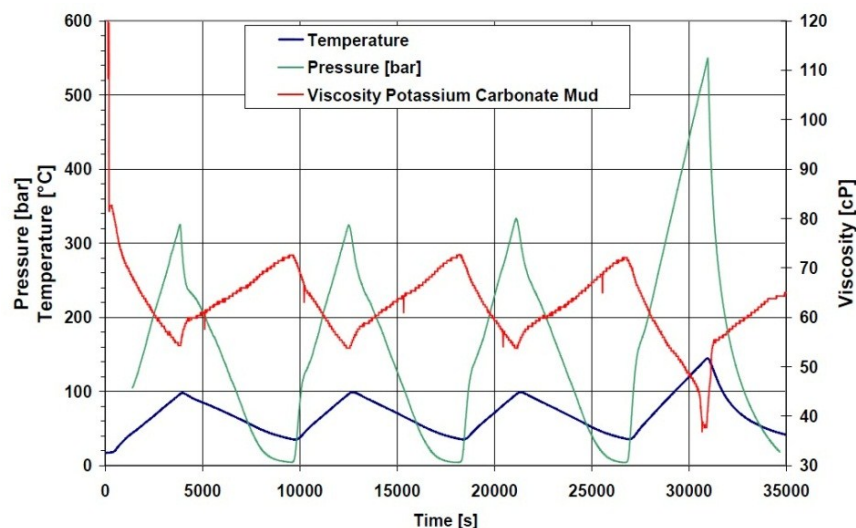


**Fig.10:** Temperature and pressure cycle of drilling mud <sup>[17]</sup>

An important consequence of the dynamic temperature gradient is the development of a certain radial temperature distribution in the formation around the wellbore. When heat conduction only is considered, the formation temperature is a function of circulation time, shut-in time, temperature difference between the formation and drilling mud, well radius, thermal properties of formations, and the radial distance from the wellbore. The knowledge of the exact temperature distribution is valuable for improving the well log readings, namely those of resistivity logs. Furthermore formation strength is influenced around the borehole as well as cementing rheological properties, compressive strength development and setting time. In theory the drilling process affects the temperature field of formations at very long radial distances. However, there is a practical limit which is stated with the radius of thermal influence (RTI). At this radius the temperature, is practically equal to the formation temperature for a given circulation time. <sup>[23]</sup>

$$\frac{T(r, t) - T_f}{T_w - T_f} = 1 - \frac{\ln\left(\frac{r}{r_w}\right)}{\ln\left(\frac{r_{in}}{r_w}\right)}, \quad r_w \leq r \leq r_{in}$$

**Equation 3:**

$T_f$  = Formation temperature [K]

$T_w$  = Wellbore temperature [K]

$r_{in}$  = Radius of thermal influence [m]

$r_w$  = Wellbore radius [m]

The following diagram shows the calculated temperature distribution of the formation close the wellbore in different depths. In the shallow section the adjacent formation is heated by the drilling mud while in deep sections the formation is cooled.

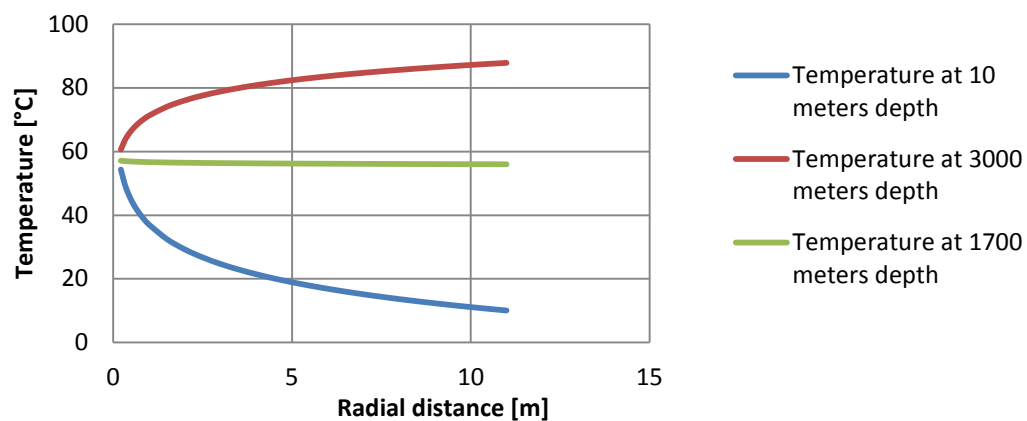


**Fig.11:** Calculated temperature distribution at the close to wellbore formation at various depths

A formation with a higher heat capacity will change its temperature slower than one with a lower one. A larger thermal conductivity will cause more heat flux from the formation to the wellbore or vice versa, thus causing a steeper gradient. Strong fluid losses into the formation, resulting in conductive transfer, will accelerate and increase the temperature disturbance. The thermal properties of rock vary strongly, depending on the properties of the single minerals in the composition and the internal structure as well as on fractures. Also the actual pressure and temperature situation influence the thermal rock properties. Measurement of the actual rock properties is a delicate issue, especially due to the porosity and anisotropy of rocks. Samples are best measured in a laboratory, as there are no reliable down-hole methods. Various representative values as a guideline can be found in the literature, but their usage will cause larger errors. <sup>[33], [34], [35]</sup>

When circulation ceases, the temperature distribution will gradually reverse back to static conditions with time. Complete equilibrium may be reached in a matter of days or weeks, depending on circulation time, contrast between mud and formation temperature during the cycle and the thermal properties of the formation.



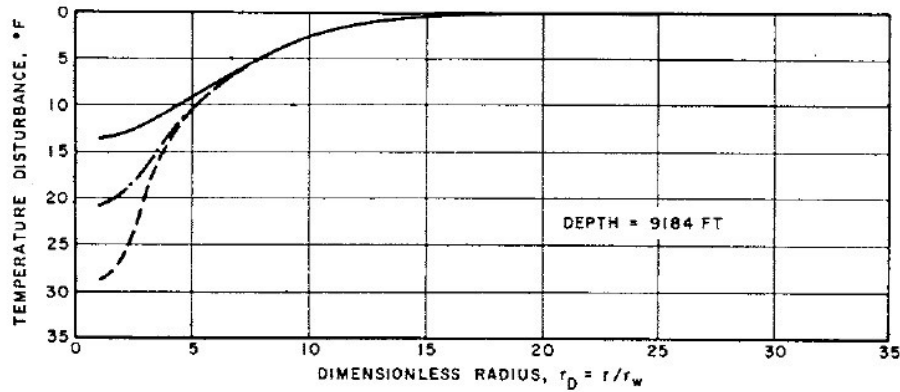


**Fig.12:** Theoretical temperature distribution for different shut-in times<sup>[33]</sup>

It should be mentioned here, that the temperature profile will actually not return completely back to the virgin conditions, even when the well is completely shut-in for a long period. This is due to the very small distorting influence of convective fluid movement in the annulus and the high conductivity of metal casing.

Multiple circulation and shut in intervals disturb the formation temperature contrarily, especially at the bore-face. As the time to gain static conditions is not sufficient the bore-face will have a somewhat saw-tooth like shape with time, and it is difficult to obtain the actual temperature accurately.<sup>[23]</sup>

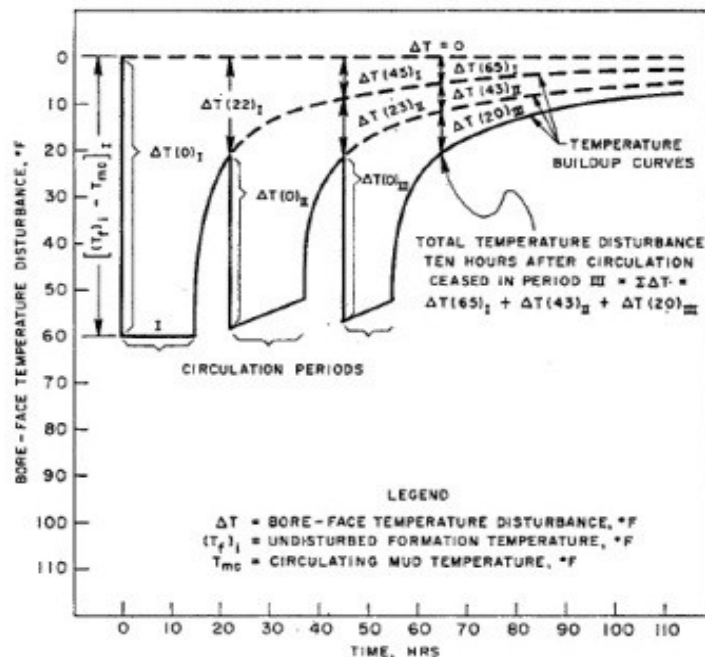


**Fig.13:** Theoretical bore-face temperature disturbance<sup>[33]</sup>

As can be seen, the borehole wall, as all down-hole components, are subjected to a temperature cycle with the dynamic circulation and the static temperatures being the two extremes.

## 2. Temperature development during drilling process

The description of the temperature development is a complex process, as many properties affect the heat flow, which are variable and interacting. Basically the wellbore acts like a heat exchanger, supplying heat from the formation to the tank.

An easy method to estimate the bottom hole circulating temperature is by API specification 10 (“specification for materials and testing for well cements”) which contains temperature schedules. However, the results are said to give only a very rough and conservative estimate.

Various papers have been published for the correct determination of the down-hole temperatures. Besides the early papers describing the basic principle of wellbore heat transfer, they can be separated into two groups: Numerical simulators and analytical approaches.<sup>[37]</sup>

Both approaches have special advantages and disadvantages. Numerical simulators are frequently used in the industry, especially for more delicate wells. They solve the governing equations for energy exchange with finite-difference methods over specific volume elements. So they can provide a detailed description of the heat transfer in a well and provide a reliable approximation of the actual down-hole temperatures. Nevertheless, the numerical models require extensive data input and can be very time-consuming. They also prove problematic for parameter studies, due to the large amounts of required input. First order and second order effects (effects of dominating impact or additional impact) are difficult to separate from each other.

Analytical models require only very basic input, which makes them very interesting for general parameter studies. Unfortunately, these models are limited to very simple wellbore geometries and simplifying assumptions. Another major limitation is the general negligence of hydraulic and friction heat generated along the wellbore for most models.

To get an idea about the impact of the various parameters as well as their interaction, actual field data was further processed with a numerical simulator and an analytical method.

## 2.1 Numerical simulation of a geothermal well

In this section the available operational data from a well construction were used to re-simulate the construction process with an analytical and a numerical procedure. The observed results were then compared with the sensor data taken.

### 2.1.1 Temperature profile of a geothermal well

For a first analysis of the temperature issue in drilling a geothermal well in Germany was chosen for simulation. This well represents a typical geothermal well in that region, and is the production well of the production-injection doublet installed. The given geothermal conditions cannot be referred to as “High Temperature”, due to the very average gradients in that region. Unfortunately for this study there was no data of wells with higher gradients available.

The whole drilling operations lasted for three months and were conducted from November to February. The project costs were almost six million Euros.

Phase	40"	33 ½"	23"	17 ½"	12 ¼"	8 ½"
Measured Depth [m]	27	200	625	1681	2427	3142
TVD [m]	27	200	625	1684	2460	2770
Casing	36" J-55	26" J-55	18 5/8" X-56	13 3/8" L-80	9 5/8" Liner K-55	O.H.
Cement	PZ 275 1,85 kg/l	PZ 275 1,70 kg/l	PZ 275 1,75 kg/l	PZ 275 1,75 kg/l	PZ 275 1,85 kg/l	-
Drilling Mud	Bentonite 1,05 kg/l	Bentonite 1,05 kg/l	Bentonite 1,10 kg/l	KK-Polymer 1,15 kg/l	KK-Polymer 1,2 kg/l	Water-Polymer 1,02 kg/l

**Table 1:** Basic data of the geothermal well

The well has a 200 meter long protective 26" casing against gas migration from an old gas storage layer, installed before rig up. In the 12 ¼" section deviation is build up in order to get a large intersection with the producing Malm formation. The annuli are fully cemented, just the 13 3/8" casing annulus is not cemented to surface and the casing needed to be set under pretension. The 9 5/8" liner has an overlap of 108 meters with the previous string. The 8 ½" open hole intersects the producing formation with a temperature of 83°C.

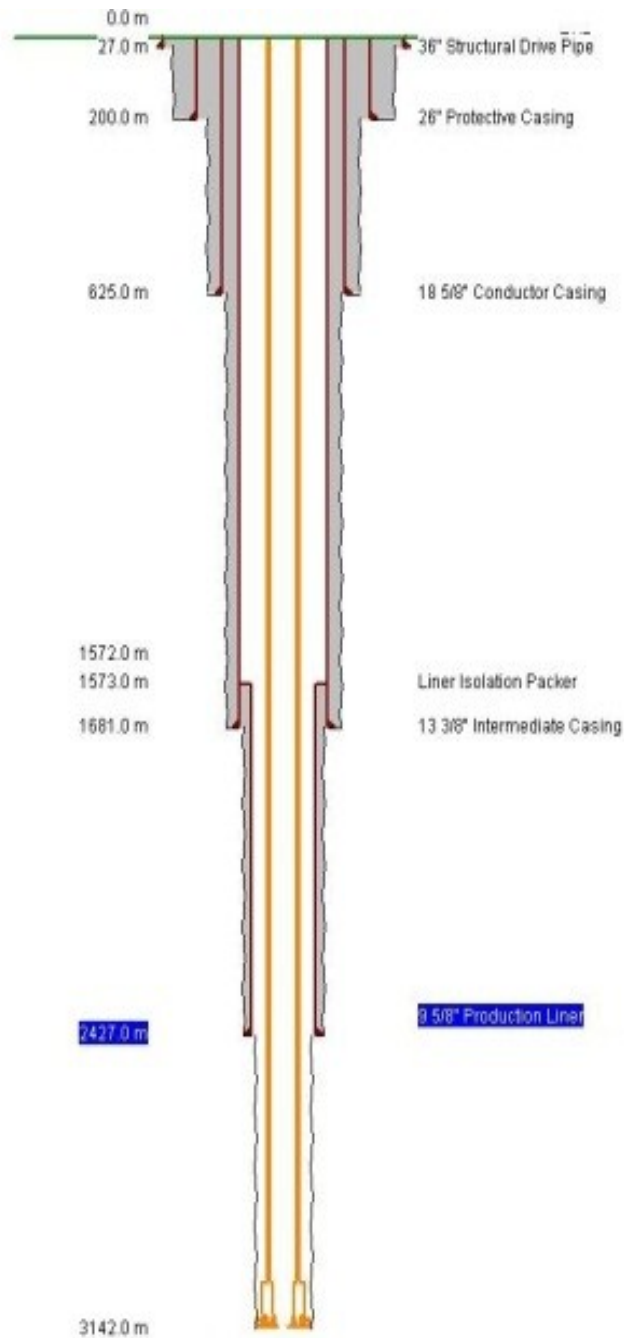


**Fig.14:** Wellbore schematics, reconstructed with the numerical simulator

The stratigraphy faced during drilling is typical for the foothills of the Alps and are similar in Bavaria and Austria, though the formation names as well as exact depths and thicknesses of layers are different. No report about the thermal properties of the given formations was available. Therefore values used for the simulation were taken from literature.

The thermal values for the uppermost layer were assumed to be those of average surface gravel. For the properties of the Malm formation the arithmetic average was calculated for the values of limestone and dolomite.

Formation Name	Lithology	Thermal conductivity, k [W·K <sup>-1</sup> ·m <sup>-1</sup> ]	Heat capacity, c <sub>p</sub> [J·kg <sup>-1</sup> ·K <sup>-1</sup> ]	Comment
Mittelmiozän	Clay, Silt, Sand; loose	1,8	1298	Value for "gravel"
Untermiozän (Karpát)	Marl to gravel sand; loose	1,6	1281	Value for "Silty sand"
Untermiozän (Ottomány)	Sand and Marl; loose to middle dense	2	1252	Value for "Sand"
Untermiozän (Oberes Eger, Aquitan)	Sandstone and Marl changing	1,8	913	Value for "Sandstone"
Oberoligozän (Unteres Eger/Chatt)	Fine- and medium sand ("Chatt-sand"); fine and medium-dense clay marl	1,2	921	Value for "Siltstone"
Unteroligozän/Oberozän	Marl, limestone, schist	2,5	1214	Value for "Limestone"
Oberkreide	Marl, sandstone	1,8	913	Value for "Sandstone"
Unterkreide	Limestone	2,5	1214	Value for "Limestone"
Malm	Limestone, dolomite	2,5	1865	Calc. mix "limestone - dolomite"

**Table 2:** Physical properties of the formations drilled <sup>[15], [34]</sup>

The geology data further indicated that some thin layers may cause loss of drilling fluid. Nevertheless, since no severe losses were observed during the actual drilling operation this information was neglected. Only the operations in the Malm formation itself caused total fluid loss, which will also be described later.

The temperature gradient is said to be 30°C per 1000 meters. Nevertheless, available temperature data from several sources was observed closely to get an exact reproduction of the temperature profile.

The average surface temperature was calculated with a regionally valid formula for temperatures in 0,2 meters beneath top ground surface and depending on the geographical height: <sup>[20]</sup>

$$T_0 = 12,43 - 0,0053 \cdot h$$

**Equation 4**

With an elevation of 507,4 meters over mean-sea-level the yearly average resulted in 9,7°C.

As there was no data indicating large shallow aquifers, the formula given by Carslaw and Jaeger was used for close to surface depth distribution  $T_{(z,t)}$ : [23]

$$T_{(z,t)} = T_{(0)} - \tau \cdot z + A_0 \cdot \exp\left(-z \sqrt{\frac{\omega}{2\alpha}}\right) \cdot \sin\left(\omega t - z \sqrt{\frac{\omega}{2\alpha}}\right), \quad \omega = \frac{2 \cdot \pi}{P} = \frac{2 \cdot \pi}{31,536 \cdot 10^6 \text{s/year}}$$

**Equation 5:**

T = Surface temperature gradient [K/m]

A<sub>0</sub> = Average temperature amplitude [K]

α = Thermal diffusivity [m<sup>2</sup>/s]

P = Interval [31,536 · 10<sup>6</sup>s]

The values found with literature data are 0,064 °C/m for the surface temperature gradient ,T, a maximum average temperature amplitude, A<sub>0</sub>, in Bavaria of 10°C and an average thermal diffusivity, α, of 0,6 ·10<sup>-6</sup> m<sup>2</sup>/s of the surface clay-soil. The start of the drilling operation was in November, so a time, t, of 260 days (22,464 ·10<sup>6</sup> seconds) within the years period was used of seconds was used.

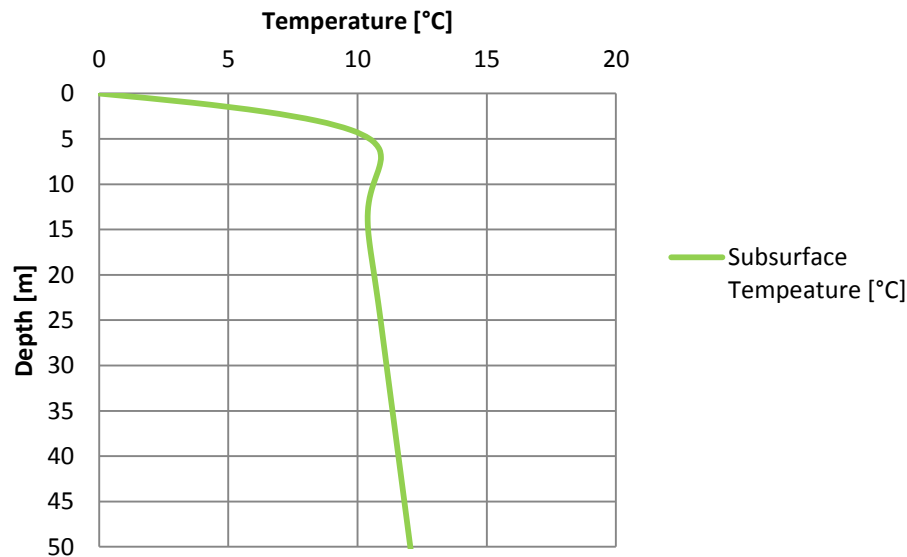


**Fig.15:** Temperature distribution in the close subsurface

The dampening effect due to the soil's heat capacity can be nicely observed in the curves peak. The observed curve nicely correlates with the temperature data and curves found in the folder of the Bayerisches Landesamt für Wasserwirtschaft <sup>[35]</sup>. There it is indicated that the impact of annual temperature fluctuations reaches a depth of about 20 meters and then continues with a static gradient of 3°C per 100 meters.

Further temperature gradient data from different sources were used and linear lines were approximated between them. <sup>[20], [36], [37]</sup>

On DrillTec's rigs besides the daily reports, the project sensor data is stored and available, describing the in- and outflow temperature, the ROP, the bit position, the total MD, the pump pressure, the torque, the trip-tank volume, the flow-rate in and the out every ten seconds. With this data, in conjunction with daily reports and further project information, an exact description of the drilling process was possible. The operations were simulated and then further analysed.

Temperature development during drilling process

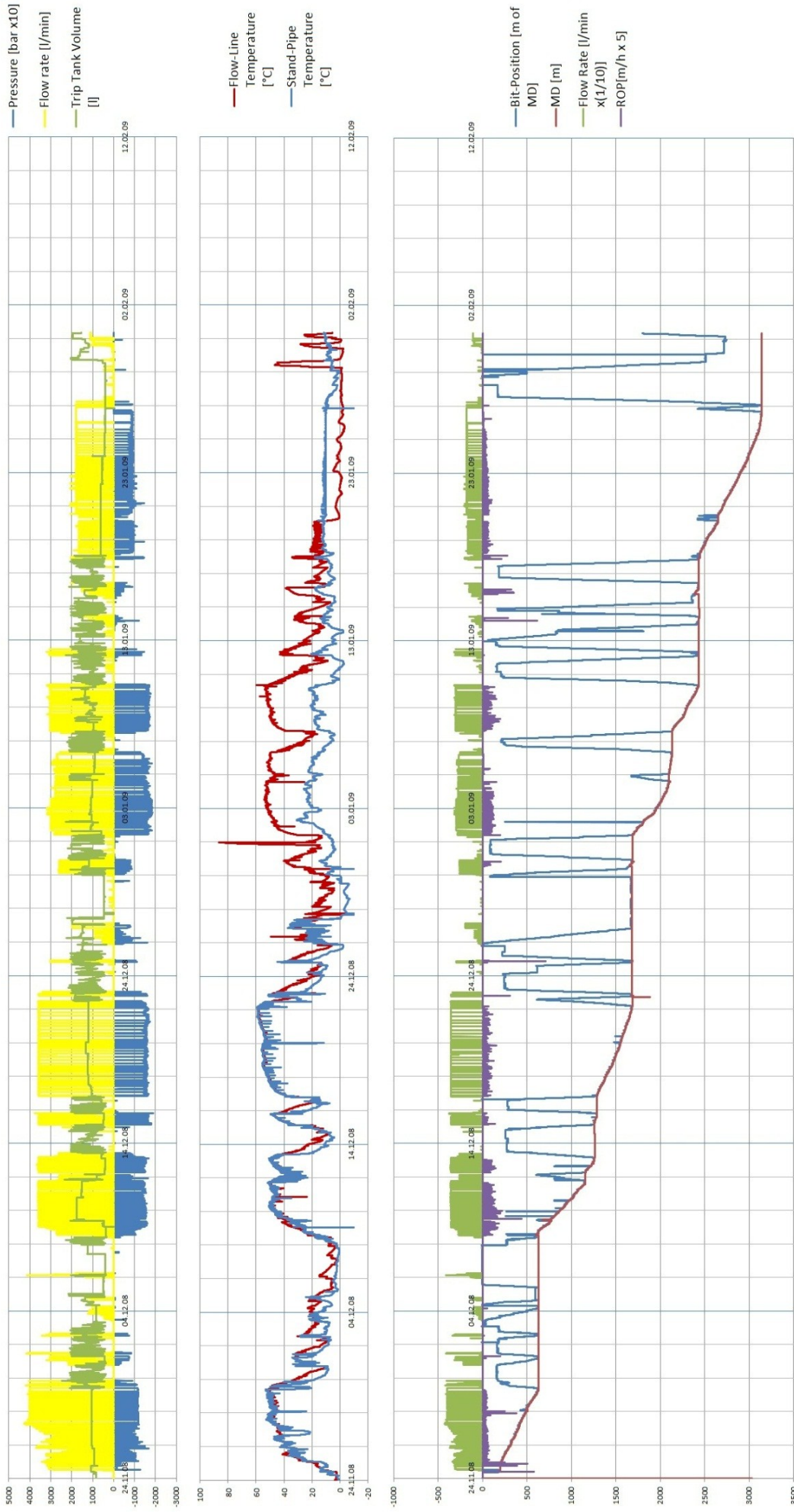


**Fig.16:** Diagrams of the sensor-data from the drilling operations. The lowermost represents the time vs. depth data with the according bit position. Flow rate and ROP were also integrated as this is important for temperature analysis. In the second graph the inflow and outflow temperatures are shown. The uppermost graphs shows the processed data of pressure and flow-rate data with the trip tank volume with time

The temperature data gathered must be read with care, as the observing sensors are only reading representative values when circulation is established. If no circulation is present a somewhat atmospheric temperature can be observed. Furthermore it must be taken into account that the drilling operation was conducted in winter, which lead to fast cooling of the mud as soon as circulation was ceased. Nevertheless, when taking a close look at the data one can observe typical drilling conditions, which are important for the down-hole temperature development and commonly observed in the fields:

- The flow-rate was the highest in the larger first section and then decreased continuously from section to section.
- The ROP is much more depending on formation type than on depth. (It is varying from 6,62 m/h, 13,1 m/h, 4,2 m/h, last section 5,4 m/h).
- The pumping pressure on the other hand is continuously increasing with each section. An exception is the last section in the Malm formation. This is due to the fact that total mud-losses are present there.
- The mud temperature is increasing with circulation time and tends to reach equilibrium especially during the long drilling operations. The dynamic equilibrium is reached in a matter of hours to a day.
- The average equilibrium temperature at the flow-line is slightly increasing from section to section. Though, circulation temperatures are surprisingly high in the first sections. This can be explained by the friction heat generated due to large hydraulic power input and will be discussed later.
- The marginal difference in flow-line temperature and standpipe-temperature indicates the little cooling effect in the mud tanks. The much larger differences in the later sections are due to an increased mud tank capacity and probably also due to the lower average air temperatures in January.
- As with many geothermal wells in the Malm formation mud-losses are present. For this well complete losses were observed. Water from nearby wells was pumped as drilling fluid. Consequently the temperature sensor at the flow-line shows the ambience temperature during this section. The sensor at the standpipe shows the temperature of the water from the nearby wells used.

Using a numerical simulation programe the information and data was processed in order to get an estimate for the temperature development down-hole. Thereby a reasonable accuracy of a maximum of 3°C deviation from sensor data during circulation could be reached. Following graphs show the down-hole temperature profiles at the end of each construction operation in a chronological order:



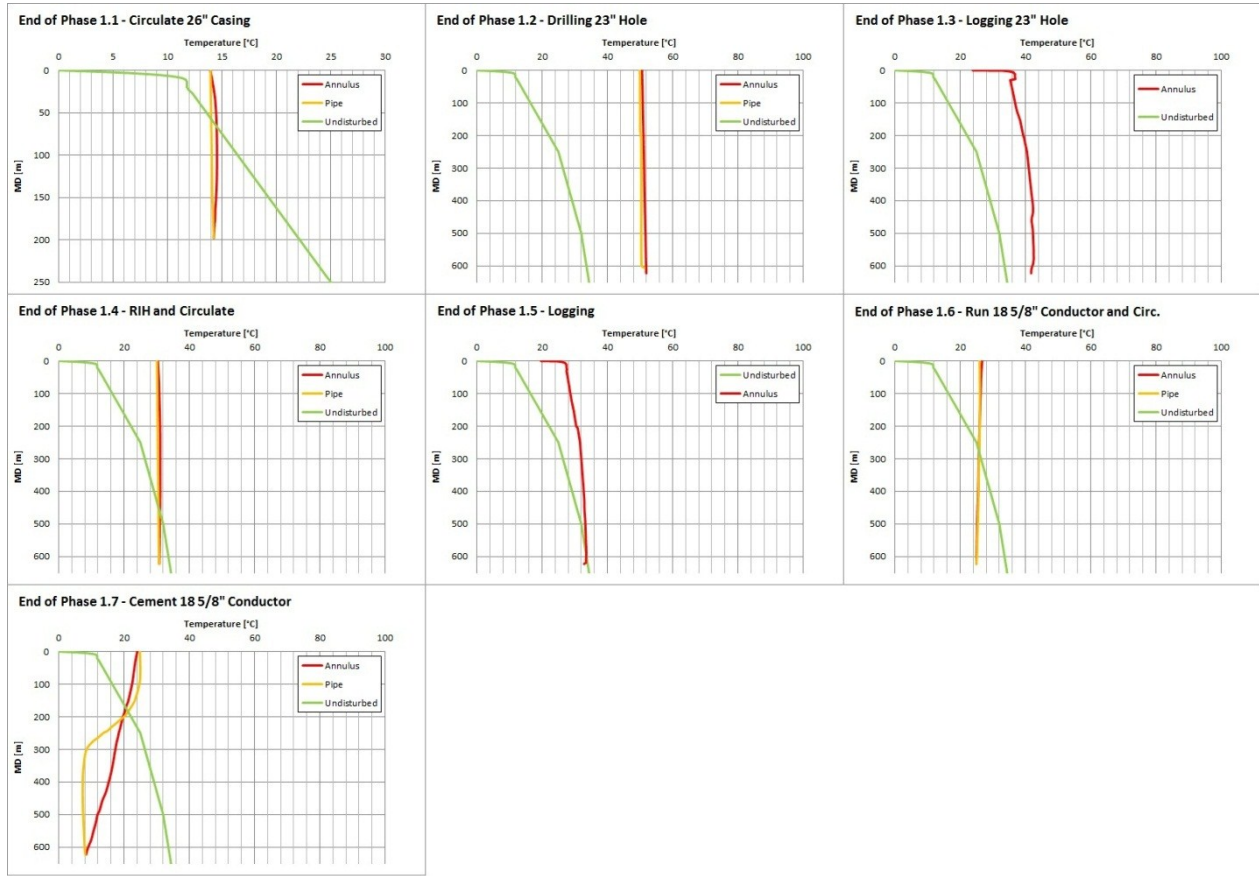


**Fig.17:** Diagrams of the down-hole temperature situation while constructing the 23” section

The construction work of the deep drilling operations start with the 23” section with a short circulation period in the 26” casing string already in place. A very typical profile can be observed during this operation, with a cooling action of the drilling mud in the lower formations and a heating in the upper ones.

At the end of the 23” hole construction an almost constant temperature profile of around 52°C develops. This temperature is larger than the geothermal gradient would predict at any depth. Nevertheless, sensor data approves the accuracy of the simulation data. Heat generated by fluid and mechanical friction is responsible for the unexpectedly high temperatures. The large diameter annulus offers relatively large fluid volumes per length, thus minimizing the cooling effect of the surrounding formation. Furthermore, the relatively short section will result in a minimum of mud volume present in the system and a maximum of pumping cycles of mud through the system, thus resulting in a fast heating. When calculating the energy balance (see 2.4) these observations in the surface section seem logical, though they are neglected in the literature due to their little impact on the drilling process.

During the subsequent logging operations with a single shot the temperature tends to return to the static profile. The latter circulating operations casing are performed with much lower flow-rates, thus generating far less friction and are not reaching any temperature balance due to short duration.

The pumping of the relatively cold cement will result in a cooling, especially at the casing shoe where most cement passes by. Nevertheless, subsequent hydration heat will cause heating, which is not presented here.

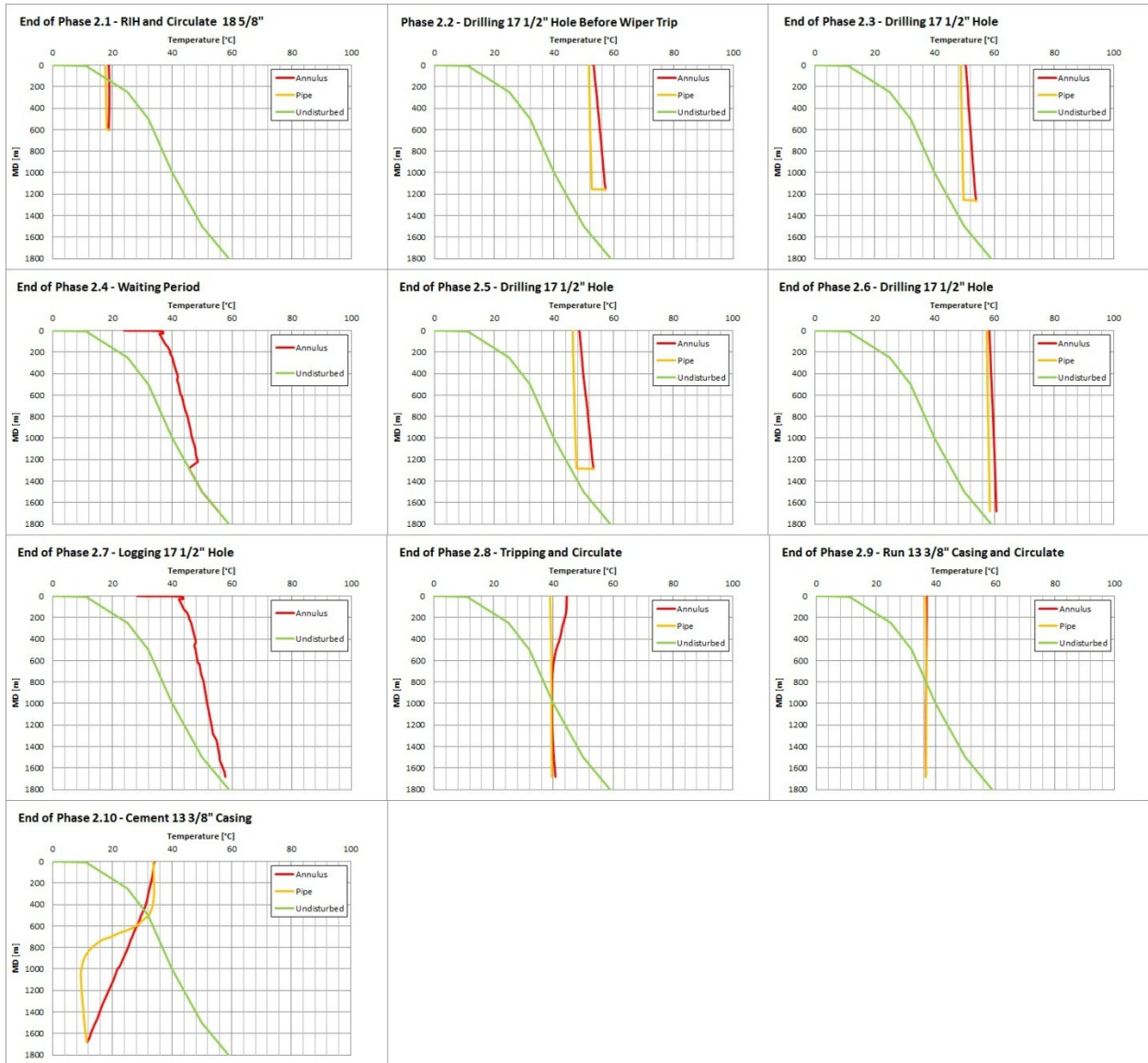


**Fig.18:** Diagrams of the down-hole temperature situation while constructing the 17 1/2" section

In the 17 1/2" section a dynamic equilibrium is reached again at relatively high temperatures, which can be attributed to continuous energy input. The high temperature increase at the bit can be nicely observed in the earlier drilling operations of the section, where a bit with a very low nozzle-area has been used.

In phase 2.6 it appears that a heat balance was established at a maximum of around 60°C due to a long continuous circulation interval of six days.

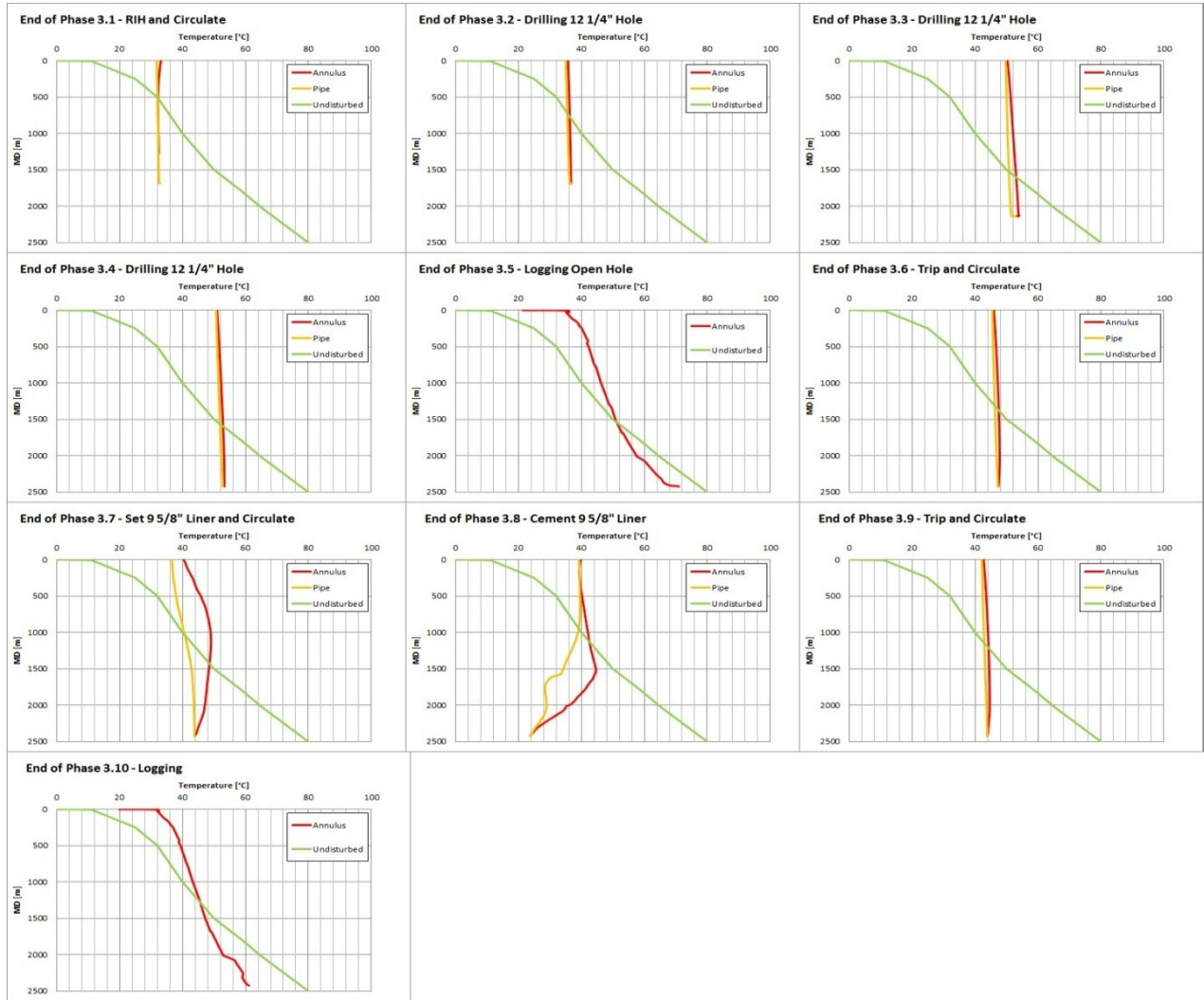


**Fig.19:** Diagrams of the down-hole temperature situation while constructing the 12 ¼” section

In the 12 ¼” section the temperature profiles during circulation and drilling operations represent the typical action of cooling the formation at bottom hole and heating the formation in the upper parts. Smaller diameters and longer distances (thus longer circulation cycles) increase the interaction between formation and drilling mud, resulting in a stronger effect of formation properties and relatively less heating.

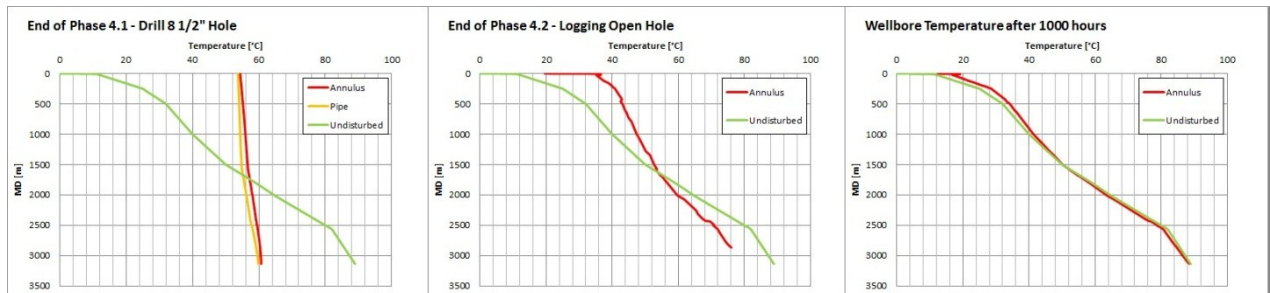


**Fig.20:** Diagrams of the down-hole temperature situation while constructing the 8 ½” section open hole

In the 8 ½" section the temperature profiles depend largely on formation properties and the geothermal gradient. The last diagram shows the temperature distribution of the annulus after an inactive time of almost 42 days (1000 hours). As can be seen there is still a slight difference between the annular temperature and the undisturbed formation temperature.

## 2.2 Analytical description of a geothermal well

As a matter of fact sophisticated simulation software is not always available when planning a well. Especially geothermal projects are often conducted by operators, not related to the petroleum industry. Often the engaged consulting companies don't use the expensive industry simulators. Analytical models may be a cheap alternative.

The analytical models used in this study were those created by Hasan and Kabir (1994) <sup>[2]</sup> and by Karstad (1999) <sup>[38]</sup>. The latter one represents an enhancement and includes also the input energy by pumping and rotation. These models seem to be the most up-to date for describing the wellbore heat transfer problem.

### 2.2.1 Description of the analytical model

Analytical models describe the behaviour of a counter-current heat exchanger with a moving outer boundary. As a first step an energy balance over a differential element of annulus is established. The energy enters and leaves the volume element by two sources, namely heat convection from mud flow and heat conduction from the formation.

The radial heat conducted from the formation ( $q_f$ ) towards the wellbore surface/casing can be expressed by the one-dimensional radial form of Fourier's law. When neglecting potential or kinetic energy effects and phase changes the heat transfer can be expressed according to Ramey (1962) with <sup>[36]</sup>:

$$q_f = \frac{2\pi k_f}{f(t_D)} (T_f - T_{wb}) dz$$

#### **Equation 6:**

$q_f$  = Energy flow [J]

$k_f$  = Formation conductivity [W/(m.K)]

$f(t_D)$  = Dimensionless time function

The dimensionless time function,  $f(t_D)$ , stated here depends on the formation-borehole heat transfer boundary conditions. Generally in a wellbore neither the heat flux nor the temperature at the wellbore remain constant. So the function describes the changes of the transient heat flow from the formation to the wellbore with time. Different solutions exist in the literature to find expressions for the dimensionless time function. The solution used in these models is an algebraic approximation:

$$f(t_D) = (1,1281\sqrt{t_D})(1 - 0,3\sqrt{t_D}) \quad \text{if } 10^{-10} \leq t_D \leq 1,5$$

$$f(t_D) = (0,4063 + 0,5 \cdot \ln(t_D)) \left(1 + \frac{0,6}{t_D}\right) \quad \text{if } t_D > 1,5$$

With

$$t_D = \frac{\alpha_h \cdot t}{r_w^2} \quad \alpha_h = \frac{k_f}{\rho_f \cdot c_f}$$

**Equation 7:**

$t$  = actual time [s]

$t_D$  = Dimensionless time

$r_w$  = Wellbore radius [m]

$c_f$  = Formation specific heat capacity [J/(kg.K)]

$\rho_f$  = Formation density [kg/m<sup>3</sup>]

The dimensionless time function shows a somewhat logarithmic behaviour. In the first long time interval the values are smaller than 1, thus increasing the theoretical heat flow. After sufficient time values for the function get larger than 1, thus decreasing the resulting energy flow. (value reaches 1 at about 156 hours circulation in drilling operation 1.2)

Further the heat transfer from the wellbore wall/casing to the annulus fluid depends on the overall heat transfer coefficient.

$$q = \frac{2\pi r_c U_a}{w} (T_{wb} - T_a) dz$$

**Equation 8:**

$w$  = Flow rate [m<sup>3</sup>/s]

$U_a$  = Overall heat transfer coefficient

$r_c$  = Casing radius [m]

The overall heat transfer coefficient,  $U_a$ , depends on the resistance to heat flow through annular fluid, casing metal and the cement and is also described by various authors.

The two equations can be combined, as they represent the same amount of heat energy flowing. Similarly an energy balance is conducted for the differential drill-string element, involving an overall heat transfer coefficient of the drill-pipe.

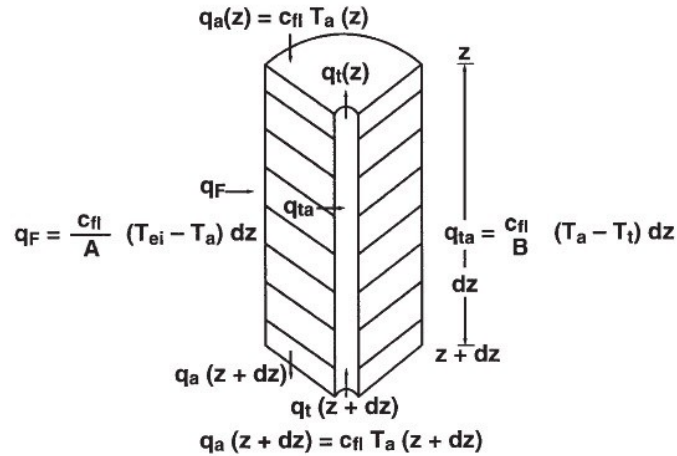


**Fig.21:** Schematic of heat balance for tubular and formation <sup>[2]</sup>

The energy balances can be combined, leading to a second-order linear differential equation. With the appropriate boundary conditions (fluid temperature and inlet temperature at zero depth are equal, same temperature at bottom hole in drill-pipe and annulus) the relationship can be reduced to two simple equations for the annulus and the drill-pipe.

$$T_{drill\ string}(z, t) = \alpha \cdot e^{\lambda_1 \cdot z} + \beta \cdot e^{\lambda_2 \cdot z} + g_g \cdot z + B \cdot g_g + T_{sf}$$

$$T_{annulus}(z, t) = (1 + \lambda_1 \cdot B) \cdot \alpha \cdot e^{\lambda_1 \cdot z} + (1 + \lambda_2 \cdot B) \cdot \beta \cdot e^{\lambda_2 \cdot z} + g_g \cdot z + T_{sf}$$

**Equation 9,**

with  $\lambda_1$ ,  $\lambda_2$ ,  $\alpha$ , and  $\beta$  are constants depending on the boundary conditions.  $A$  and  $B$  are parameters, which describe the formation and fluid properties and thus the heat flow. <sup>[2],[3]</sup>

The analytical model has a basic disadvantage over numerical models for simulation as it can only be used with the actually measured data. Prediction of temperature development is not possible, as the mud inlet temperature is an essential input. Energy stored in the mud from earlier circulation cycles is not considered, unless the actual mud inlet temperature is used. Also temperature changes caused by latent, potential and kinetic energy effects or viscous and friction forces are neglected.

Actually, the used analytical model is only proper for deriving the profile of a circulation operation and not for a drilling operation. The input parameters like well-depth, circulation time overall heat transfer coefficient, fluid properties, formation properties and inlet temperature are assumed to be constant and static. The dimensionless time function determines the amount of heat flow depending on the circulation time input. Thus, in a continuous drilling operation the final depth will be reached at the end of the circulation time, resulting in a wrong heat transfer assumption.

Nevertheless, the dimensionless time function has a logarithmic shape (mentioned before), so the error will minimize with long circulation time and a slow drilling process.

When using the analytical method to describe the drilling operation 1.2 the following shortcomings can be observed. For the input parameters average values (pump rate, circulation rate) as well as weighted averages (formation properties) were used.

In figure 22 the initial mud temperature was used constantly as the inlet temperature for the analytical models, resulting in their severe error. Consequently, an actual and exact input of the mud inlet temperature is mandatory.

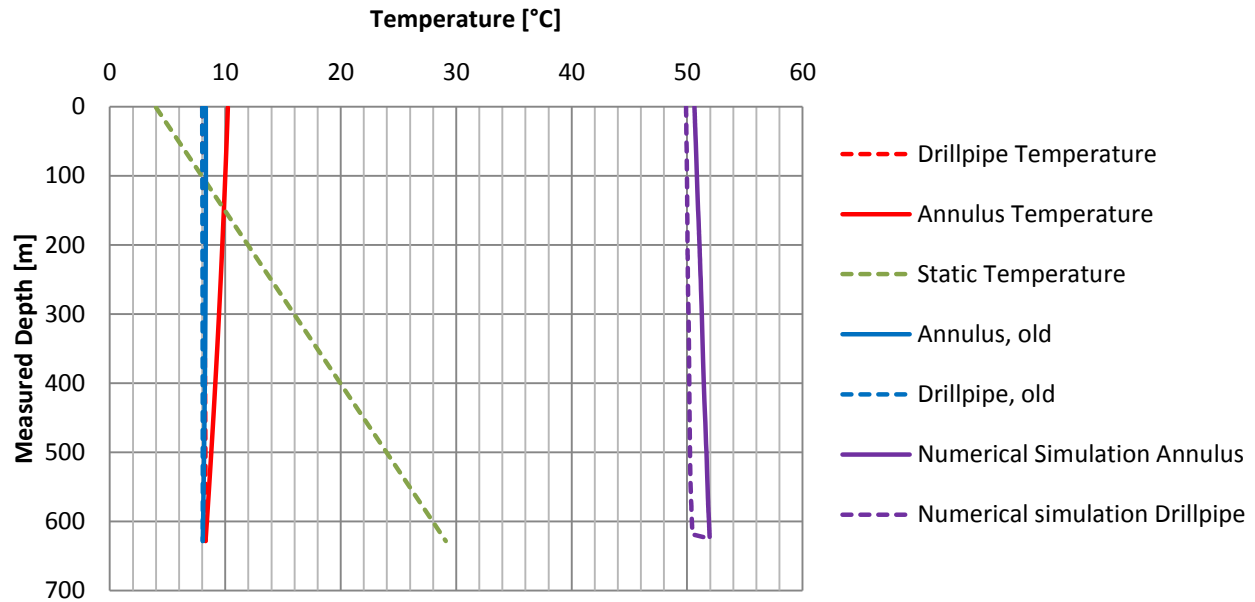


**Fig.22:** Comparison of analytical method and numerical simulation results

The numerical simulator calculates the energy balance for the small volume elements for the whole operation and consequently gives a reasonable output for the temperature profile at the end of the long drilling interval. The increased energy in the system with time is considered here naturally.

When comparing the analytical models with and without energy input from hydraulic and rotation a further detail can be observed. While the model neglecting energy input gets almost a straight line with drill-pipe and annulus having the same temperature, the model including energy input still has a curvy shape, causing a higher annular temperature.

When using the correct and actual mud inlet temperature as an input, the modified analytic model becomes somewhat useful for temperature prediction. The model including the energy input practically shows same flow-line temperature as the sensor or the numerical simulator.

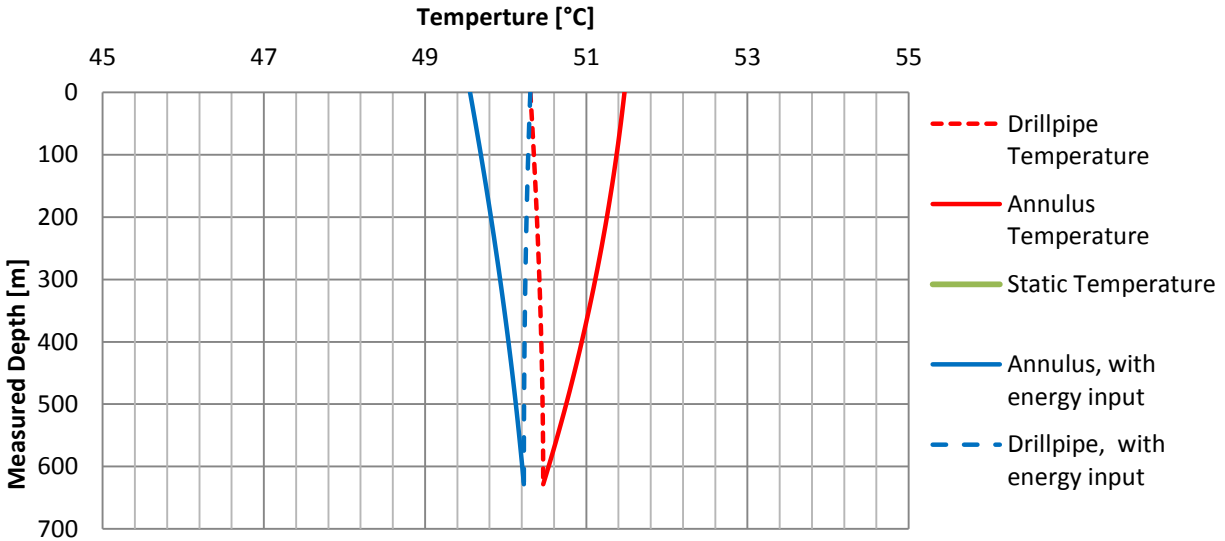


**Fig.23:** Comparison of results of analytical method with and without energy input

Nevertheless, in the analytical model the energy input is assumed to be constantly distributed over the whole profile, while the numerical simulator clearly indicates the source of the maximum heat generation: The pressure losses at the BHA. In the presented case of a shallow, vertical hole-section with high flow-rates and relatively small nozzle area the mentioned difference in distribution of input energy between the model and simulator is most evident.

Due to the relatively long time of operation (105 hours) and the rather slow average ROP (3,5 m/h), the error caused by the assumption of being at final depth already in the beginning of the operation is relatively low, as can be observed from the good correlation of flow-line temperatures.

The model neglecting the energy input from rotation and hydraulics once more proves insufficient. As can be seen it indicates lower flow-line temperatures than mud inlet temperatures. When neglecting the energy input and noticing that temperatures are far greater than static formation temperatures this result seems very logical, but wrong though.

Unfortunately the used numerical simulator did not allow for showing the temperature development with time of any drilling operations. Consequently the development of the annular temperature profile for the operation 1.2 shown in the following diagram was developed with the analytical method:



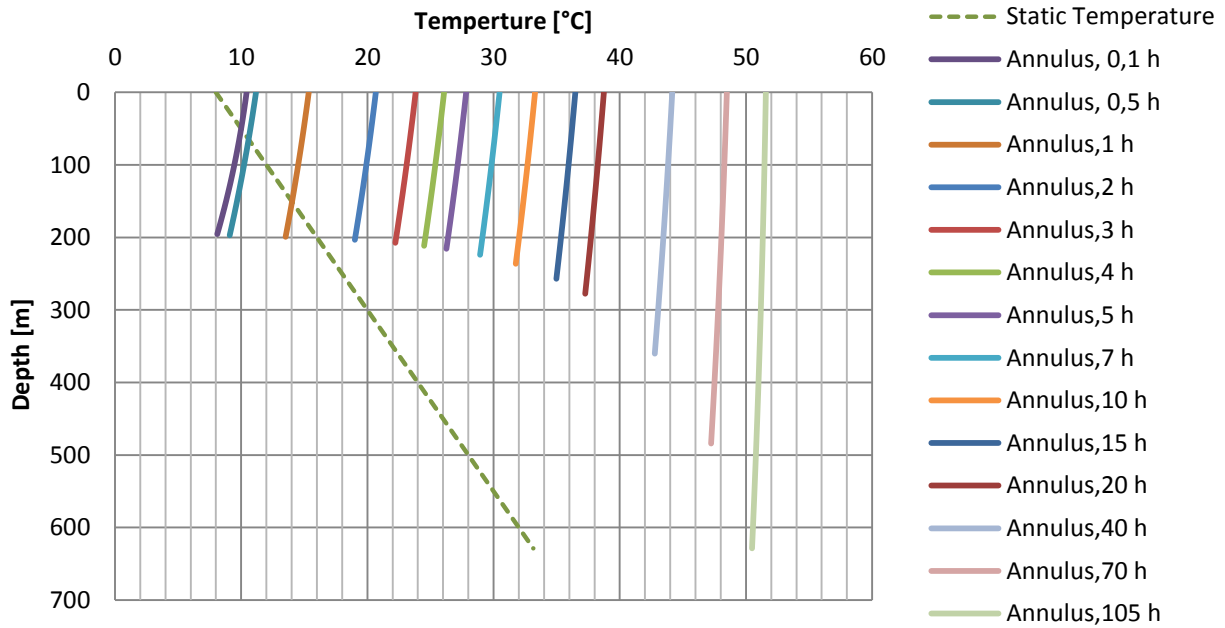


**Fig.24:** Down-hole temperature development in annulus according the analytical method

Similar to the numerical simulator the annular profile-lines are not curvy and almost vertical at the end, thus indicating the relatively little impact of heat flux through the formation. This is expected for the large flow-rates, the large diameter and the shallow well. As the mud inlet temperature increases, so does the temperature profile.

Due to the relatively larger heat losses with increased temperature difference between mud and formation, the increase of down-hole temperature is getting slower with time. As can be observed, the flow-line sensor data in figure 25 correlates good with the temperatures predicted. The observed kinks in the sensor data are caused adding cooler mud into the system.

The practically straight line for a time of 0,1 hours, when the new cool mud actually did not pass a single circulation cycle is a further shortcoming of the analytical model, which can only see the energy transfer as a whole, which will not be right for these short times.

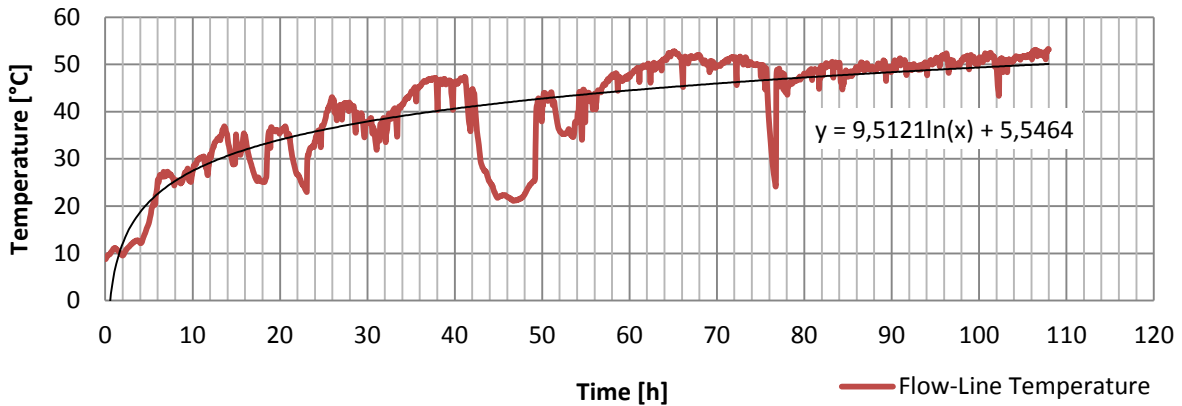


**Fig.25:** Sensor data at flow-line from drilling operation 1.2

Also the mud tank temperature development proves to be very important for the whole drilling process. The higher the heat difference down-hole gets, the higher gets the heat exchange with the formation. As the flowing fluid gains heat, also the tank fluids temperature increases and further heat exchange at the surface grows. The heat in the tank increases until the temperature approaches a steady value, when the heat gained from the circulating fluid from the formation equals the heat lost in the ambient air.

The overall heat transfer coefficient was calculated by comparing the difference of energy input and output at the flow-line and standpipe for the different drilling operations and was found to be around 62 W/K. The initial mud temperature and the actual mud temperature necessary were found from the sensor data. An interesting analytical model describing the temperature development in the mud tank is presented by Hasan, A.R.<sup>[34]</sup>. When comparing the model with the actually measured data, a good correlation can be observed. Nevertheless, one has to consider the continuous addition of drilling mud, especially for the shallow sections, which will deviate the actual mud temperature. Therefore in this picture drilling operation 3.9 was used for comparison, as in this section almost nothing was added to the mud.

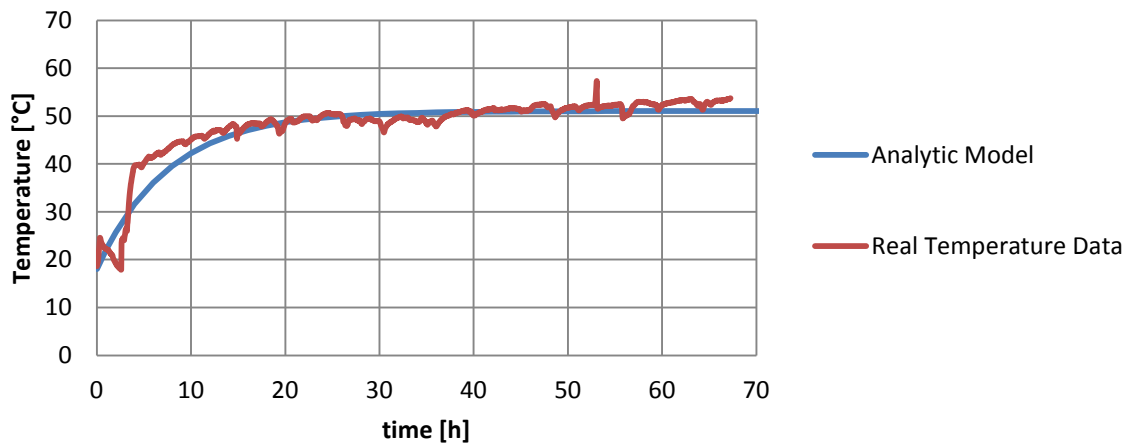


**Fig.26:** Comparison of measured data and analytic tank model for drilling operation

The model indicates further, that the tank's heat transfer parameters have a marginal effect on long term temperature development compared to flow rate and heat capacity of the fluid - similar to the sub-surface observations. The surface area has the biggest impact on the heat loss, while the tank volume is relatively unimportant. Wind can further increase the energy exchange at the surface, which is not included in the analytical model.<sup>[37]</sup>

## 2.3 Parameters affecting the temperature profile

After verifying the output of the numerical simulator with the actual sensor data the next step was to evaluate the influence of the different drilling parameters on the temperature development during drilling.

To get a first guess on the impact of the different drilling parameters the analytical temperature model was used for a parameter study.

### 2.3.1 Parameter study with the analytical temperature simulator

For the study of the impact of the different parameter a sensibility analysis was conducted. The observation that the sensibility of one specific parameter depends on the actual well layout and the range of the other parameters seems logical, thus important.

For a first comparison the drilling phase 1.2 was analysed after one hour of operation. The inlet temperature was 14,5°C at this time. For comparison the flow-line values were chosen to be displayed, as they proved to be predicted most accurately in comparison with the numerical model (mentioned before).

Percent Deviation	-20%	-10%	0% [20,79°C]	10%	20%
Surface temperature	-2,072%	-1,036%	0,00%	1,036%	2,072%
Temperature gradient formation	-10,989%	-5,495%	0,00%	5,495%	10,989%
Final depth	-14,519%	-7,321%	0,00%	7,329%	14,570%
Drillstem outer Diameter	1,570%	0,774%	0,00%	-0,752%	-1,482%
Hole diameter	-5,626%	-2,662%	0,00%	2,388%	4,525%
Actual mud inlet temperature	-6,459%	-3,229%	0,00%	3,229%	6,459%
Time of circulation	1,927%	0,919%	0,00%	-0,845%	-1,626%
Circulation rate	3,847%	2,035%	0,00%	-2,102%	-4,183%
Mud specific heat	3,847%	2,035%	0,00%	-2,102%	-4,183%
Annulus overall heat transfer coeff	-1,842%	-0,833%	0,00%	0,700%	1,295%
DP overall heat transfer coeff	1,570%	0,774%	0,00%	-0,752%	-1,482%
Formation specific heat capacity	-1,995%	-0,934%	0,00%	0,832%	1,580%
Formation density	-1,995%	-0,934%	0,00%	0,832%	1,580%
Formation thermal conductivity	-2,203%	-1,031%	0,00%	0,916%	1,738%
Rotation energy input	-0,014%	-0,007%	0,00%	0,007%	0,014%
Pumping energy input	-0,466%	-0,233%	0,00%	0,233%	0,466%

**Table 3:** Impact of the different parameters in drilling operation 3.4 at 1 hour of drilling

In the beginning of the circulation period the difference between mud and formation temperature is still large, thus causing more efficient heat transfer. Many of the observed

deviations of the flow-line temperature seem marginal though. Nevertheless, the calculated change of temperature has to be seen as a continuous one. When considering a mud cycle duration of less than one hour and a duration of drilling of many hours, the presented differences seem more significant. In the observed papers deriving the model it was argued that the equations give a close estimate on the actual down-hole temperatures. Thus, the results were used as an indication for first order and second order effects.

After one hour of circulation the well geometry depending properties (final depth, annular diameter), the actual formation temperature (geothermal gradient) as well as the mud properties (mud inlet temperature, circulation rate, mud specific heat) have a dominating influence on the temperature development.

The formation properties (thermal conductivity, specific heat capacity, overall heat transfer coefficient) which actually define the amount of heat that can be conducted through the rock, are comparatively small. This is no big surprise, because convection is much more efficient in energy transport than conduction.

Of course over longer circulation periods the parameters' significance is changing in various ways, though depending on each other. For a closer observation the parameter study was conducted again at a circulation time of 105 hours, which represents the end of the drilling operation. The mud inlet temperature here was close to flow-line temperature, namely 51,12°C.

Percent Deviation	-20%	-10%	0% [52,3°C]	10%	20%
Surface temperature	-0,262%	-0,131%	0,00%	0,131%	0,262%
Temperature gradient formation	-1,554%	-0,777%	0,00%	0,777%	1,554%
Final depth	-1,329%	-0,728%	0,00%	0,844%	1,789%
Drillstem outer Diameter	0,025%	0,013%	0,00%	-0,013%	-0,025%
Hole diameter	-0,055%	-0,027%	0,00%	0,026%	0,050%
Actual mud inlet temperature	-17,868%	-8,934%	0,00%	8,934%	17,868%
Time of circulation	0,028%	0,013%	0,00%	-0,011%	-0,021%
Circulation rate	0,419%	0,195%	0,00%	-0,170%	-0,318%
Mud specific heat	0,419%	0,195%	0,00%	-0,170%	-0,318%
Annulus overall heat transfer coeff	-0,005%	-0,002%	0,00%	0,002%	0,003%
DP overall heat transfer coeff	0,025%	0,013%	0,00%	-0,013%	-0,025%
Formation specific heat capacity	-0,026%	-0,013%	0,00%	0,012%	0,023%
Formation density	-0,026%	-0,013%	0,00%	0,012%	0,023%
Formation thermal conductivity	-0,049%	-0,023%	0,00%	0,021%	0,041%
Rotation energy input	-0,010%	-0,005%	0,00%	0,005%	0,010%
Pumping energy input	-0,306%	-0,153%	0,00%	0,153%	0,306%

**Table 4:** Impact of the different parameters in drilling operation 3.4 at the end of the operation

The temperature difference between flow-line and inlet is very small, thus causing very little heat flux. The dynamic temperature equilibrium is practically reached here. As can be observed almost all parameters lose their impact for further temperature development.

Only the mud circulation properties, namely the inlet temperature, have still some significance. The inlet temperature is of basic importance for long circulation operations and even gained importance. The mud heat capacity and rate decreased by the factor 10.

The impact of the heat transfer properties, however, decreased by a factor 100. Also the hole diameter did so. Therefore it can be concluded that the properties supporting the heat transfer in the formation are more important to determine the early, transient stage of the temperature development. After the equilibrium is reached with sufficient circulation time they practically lose their impact.

From the mathematical point of view this is logical, as the time function becomes larger and is therefore reducing the heat flux between mud and formation. Further also the mud inlet temperature increases considerably with time, which causes a smaller temperature differential between mud and formation temperature and thus also a decreased heat exchange.

From the physical point of view it correlates to the idea that the radius of the temperature disturbance through the formation increases with time. Thus, the energy transfer from / to the formation reduces until steady state conditions are reached, which causes less energy exchange with the drilling mud. The circulation properties like inlet temperature, mud capacity and flow rate determine, how much heat energy is actually transferred and at which temperature the system equilibrates, and therefore stay important.

Generally it can be stated that in deeper, small diameter wells the formation properties show a greater effect on the temperature development. In shallow wells dynamic equilibrium is approached much faster, and the effects of heat flux from the formations are minimal due to shallower depths.

For a further evaluation of the impact of the actual operational parameters given, the numerical simulator was used again. At first some drilling parameters were evaluated, which are important for well planning phase. The latter parameters may be changed to some extend during the hole construction on the well-site.

### 2.3.2 Influence of static temperature profile

Often the static temperature profile of a formation is simply described by a temperature gradient, which is approximated by a linear line between surface and TVD. The following graph shows the impact of such a simplification:

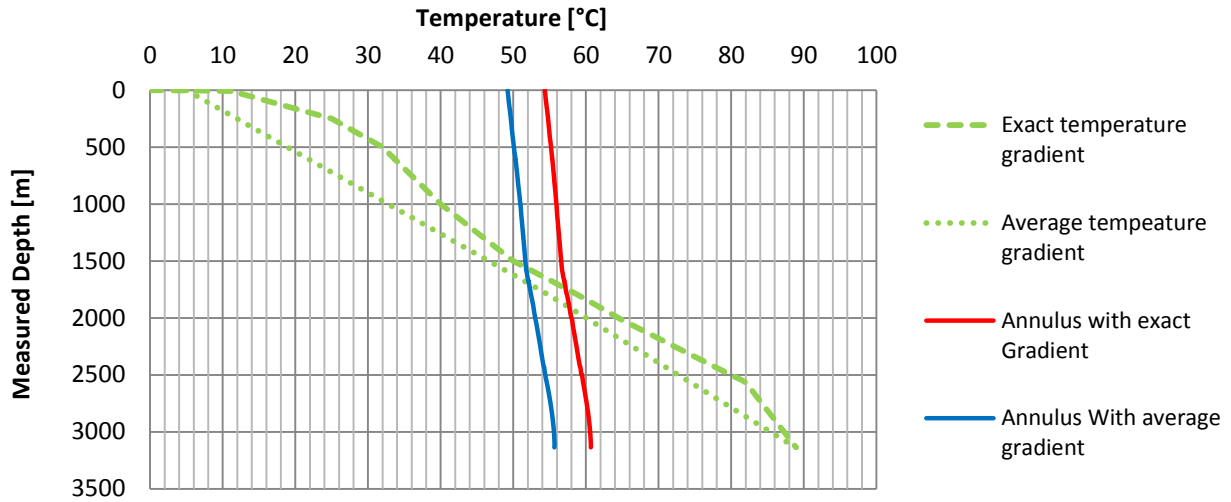


**Fig.27:** Profiles for exact and linear gradient

	With exact gradient	With linear gradient
Flow-line Temperature [°C]	54,33	49,21
Bottom hole Temperature [°C]	60,67	55,65

**Table 5:** Results for exact and linear gradient

Obviously the larger temperatures found in the upper horizons have a relatively large impact on the temperature profile. When offset well data is available, one should pay close attention to the exact static profile. In formations with predominantly conductive heat transfer a linear approximation of the temperature gradient may be justified, while such an assumption will cause significant errors in convective profiles. This may be essential in geothermal wells with fractured reservoirs such as in Turkey or Italy. <sup>[16]; [21]</sup>

Another interesting comparison is that of the effect of different geothermal gradients besides each other. The following graphs show the simulated wells with the actual lithology but with various temperature gradients. A linear gradient of 28°C/km (leading to a BHT of 80°C), one linear gradient of 38°C/km (120°C BHT), one linear gradient of 48°C/km (150°C BHT) and one linear gradient of 56°C/km (175°C BHT).

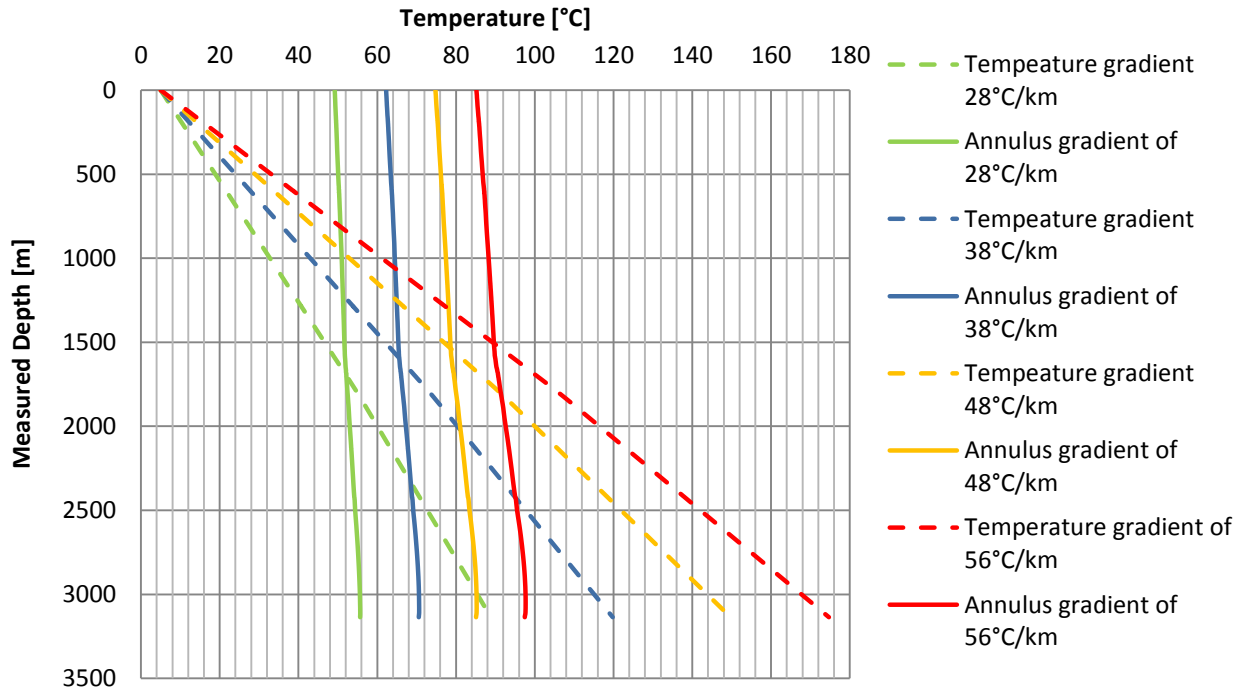


**Fig.28:** Profiles for different temperature gradients

	BHT of 86°C	BHT of 120°C	BHT of 150°C	BHT of 175°C
Flow-line Temperature [°C]	49,21	62,25	74,78	85,19
Bottom hole Temperature [°C]	55,65	70,55	85,09	97,46

**Table 6:** Results for various temperature gradients

As can be observed the temperature increases continuously, but with decreasing intensity, when increasing the temperature gradient. For the given well profile at the highest gradient only the last section would reach a surface temperature greater than 80°C (85,19°C), which would result in issues regarding rig modifications.

Here it should be noted, that this relatively low temperatures at the high adjacent formation temperatures are observed due to the sufficient cooling in the large diameter flow volume. A smaller annulus with same flow velocity is relatively more depending on the formation temperature. Though, geothermal wells are less sensitive to high temperatures due to the obligatory large diameters.

### 2.3.3 Influence of lithology information

Material properties from the down-hole formations like the specific heat capacity or the thermal conductivity of rock are hardly available. For this study average values from the literature were considered and led to sufficient results. Nevertheless, when comparing the standard values from the software with the values used during simulation the following can be found:

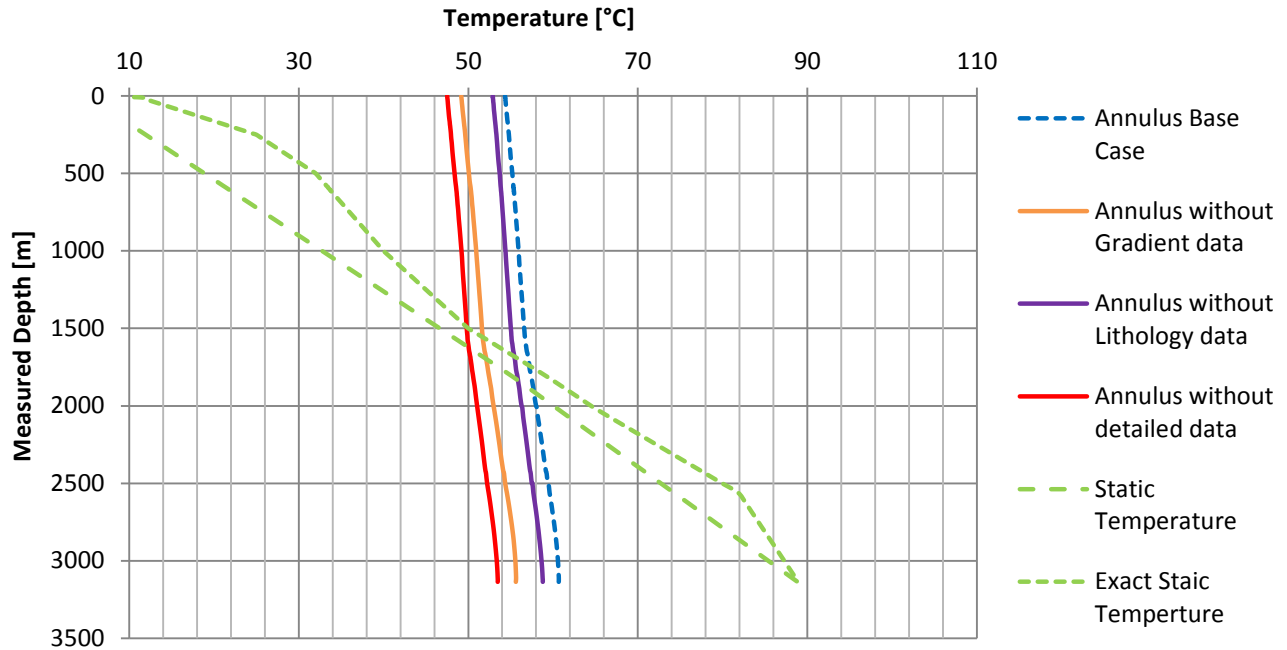


**Fig.29:** Temperature profiles depending on temperature and rock properties

	With detailed Lithology	With average Lithology
Flow-line Temperature [°C]	54,33	52,17
Bottom hole Temperature [°C]	60,68	58,79

**Table 7:** Results for different well-paths

The average lithology suggested by the software has a capacity of 1676 J/(kg·K) and a thermal conductivity of 1,75 W/(m·K). Although it is often hard to observe formation properties in advance, an optimal research might be advisable when temperature problems are a concern.



### 2.3.4 Influence of the well profile

Before starting the drilling process it might be interesting to evaluate the effect of the wellbore profile on the drilling process. Therefore three wells with the same measured depth but different profiles were simulated under the same geological conditions:

- A totally vertical well
- A J-shaped wellbore profile
- A S-shaped wellbore profile
- A build and hold wellbore profile

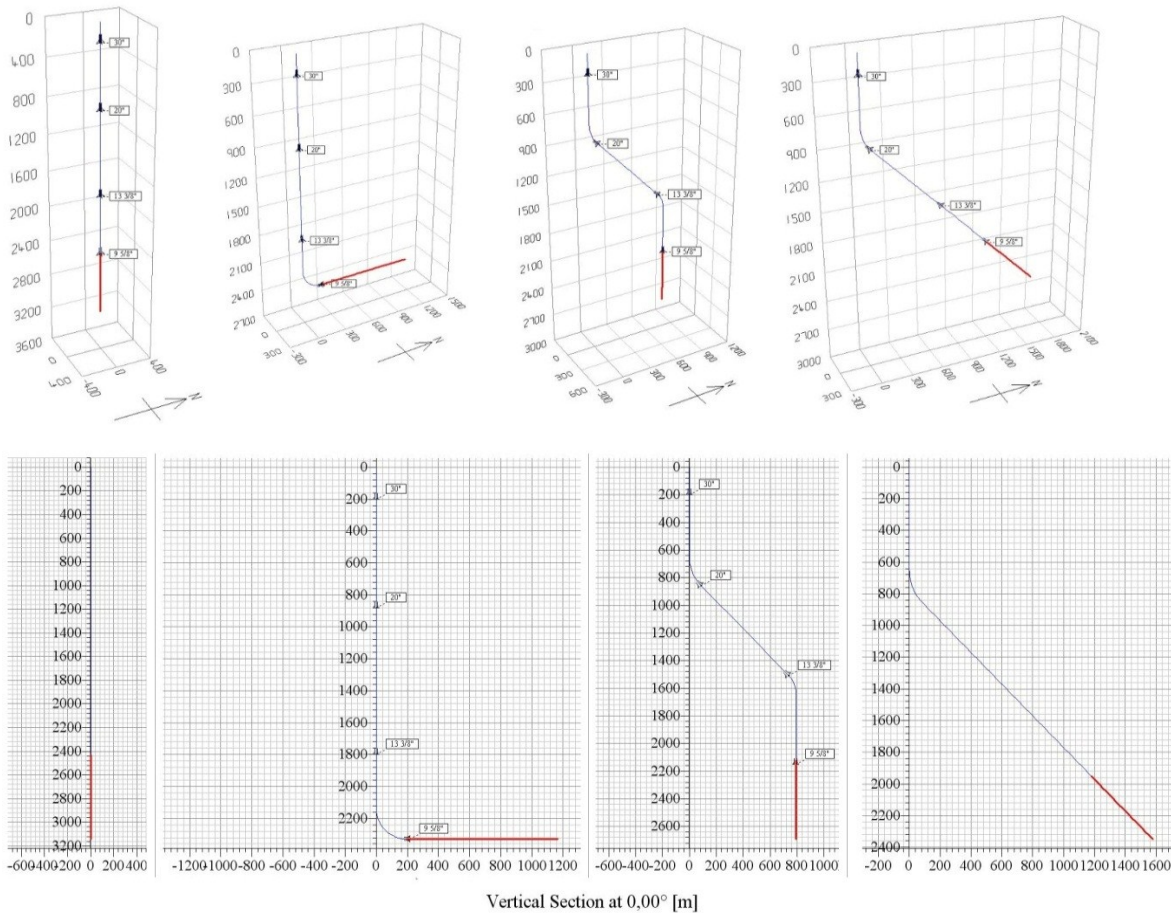


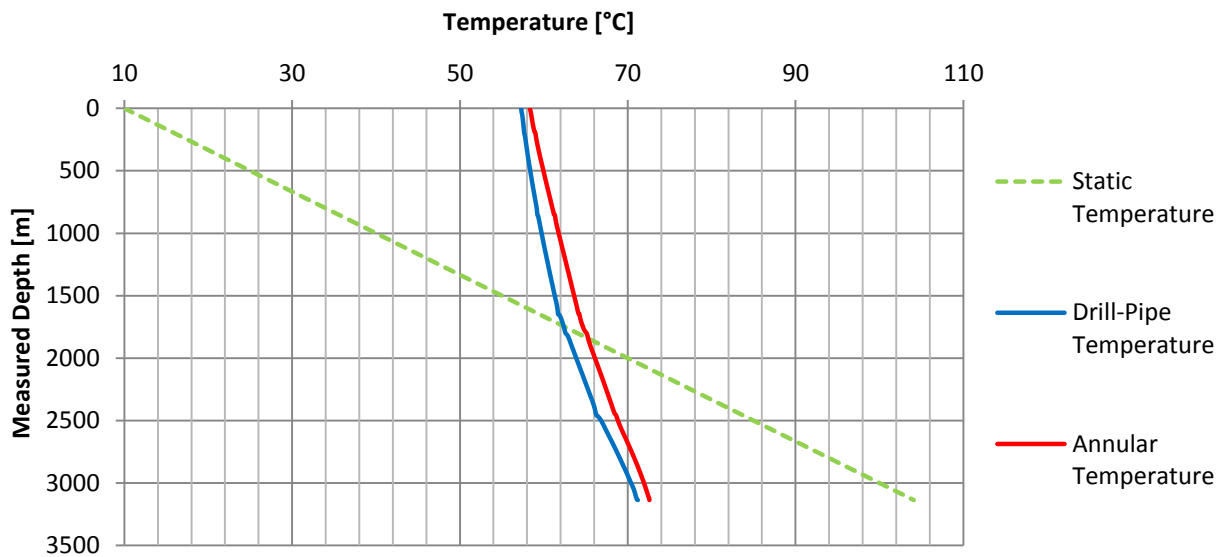
**Fig.30:** Wellbore trajectories and vertical section of simulated wells: vertical well (left), J-shaped, S-shaped, build and hold profile

Operation parameters, times and sequence as well as temperature gradient and casing setting depths were adopted from the analysed geothermal well. They were assumed to be equal for all well-paths, although small changes were conducted with the operational times and the bottom-hole assemblies used. Namely extra trips for every build or drop sections were considered and the concerned ROPs were reduced by 10 percent. Pressure drops due to different BHAs as well as the geological details were neglected.

	vertical well	J-shaped	S-shaped	build and hold
<b>1<sup>st</sup> section [m]</b>	200 MD / 200 TVD	200 MD / 200 TVD	200 MD / 200 TVD	200 MD / 200 TVD
<b>2<sup>nd</sup> section [m]</b>	878 MD / 878 TVD	878 MD / 878 TVD	878 MD / 855 TVD	878 MD / 856 TVD
<b>3<sup>rd</sup> section [m]</b>	1800 MD / 1800 TVD	1800 MD / 1800 TVD	1800 MD / 1507 TVD	1800 MD / 1507 TVD
<b>4<sup>th</sup> section [m]</b>	2460 MD / 2460 TVD	2460 MD / 2329 TVD	2460 MD / 2452 TVD	2460 MD / 1974 TVD
<b>5<sup>th</sup> section [m]</b>	3142 MD / 3142 TVD	3142 MD / 2329 TVD	3142 MD / 2692 TVD	3142 MD / 2456 TVD
<b>Build rate [°/30m]</b>	-	8,85	1 <sup>st</sup> : 5,9 2 <sup>nd</sup> : 8,56	5,9
<b>KOP</b>	-	KOP : 2135 MD	KOP 1 : 650 MD KOP 1 : 1800 MD	KOP : 650 MD
<b>Max inclination [°]</b>	0	90	45	45

**Table 8:** Input trajectories

For detailed analysis the last section of the well was chosen, as the differences are most evident in that phase.



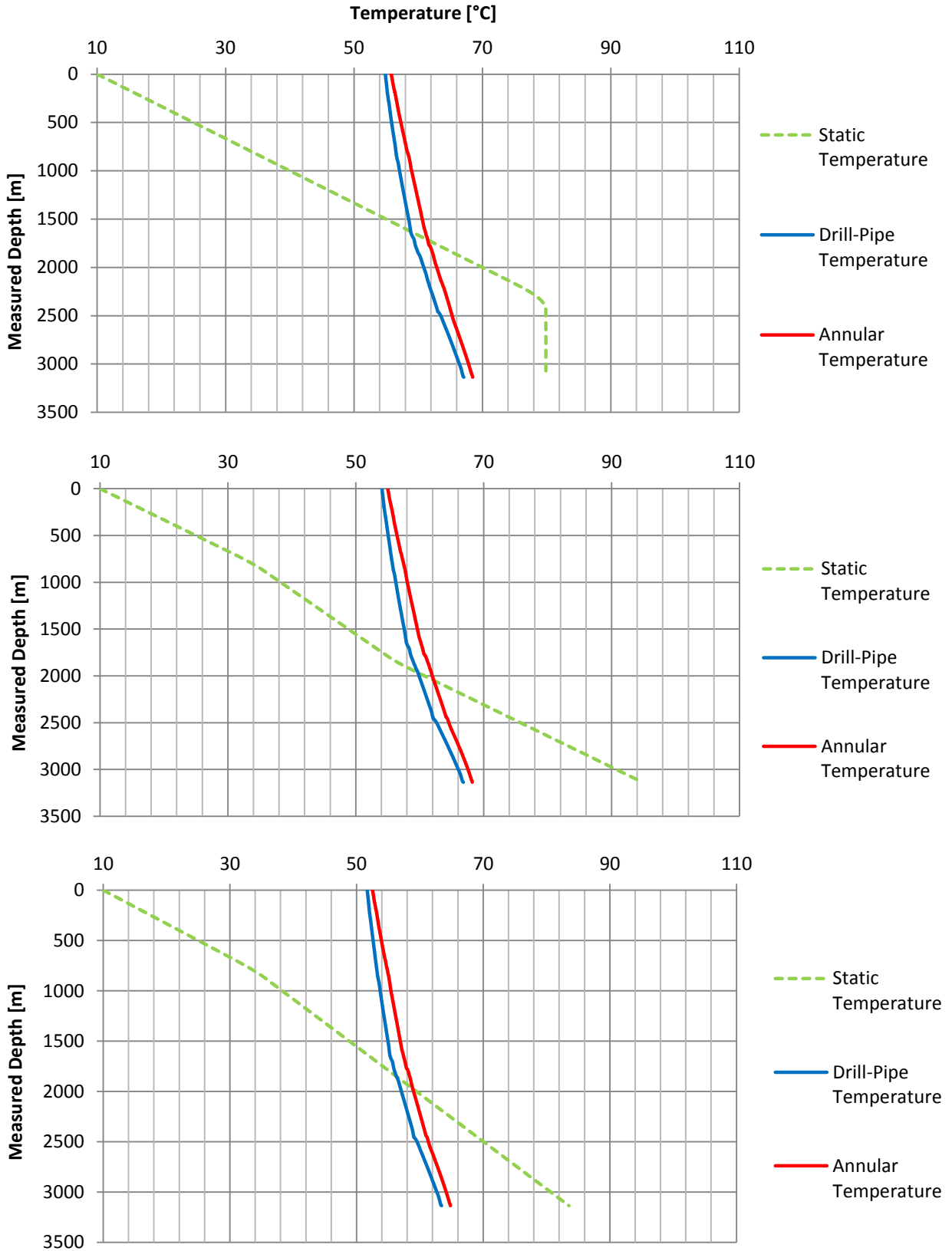


Fig.31: Temperature profiles of various well-paths

	Vertical well	J-shaped	S-shaped	build and hold
Flow-line Temperature [°C]	58,35	55,81	55	52,54
Bottom hole Temperature [°C]	72,58	68,49	68,21	64,82
Max. Static Temperature [°C]	104,09	79,89	94,84	83,54

**Table 9:** Results for different well-paths

Here the different temperature of the adjacent formation has a dominating effect on the profile. The vertical well reaches the greatest depth and has consequently the highest outflow and bottom-hole temperatures of all wells.

The J-shaped well reaches the shallowest TVD, but suffers from the second highest bottom-hole temperatures and flow-line temperatures. This is logical, when thinking about the mud passing the high fraction of thousand meters horizontal section through the vertically deepest part of the well. The maximum static temperature might not be that high, but has more contact area for a heat transfer.

Thus, when dimensioning tools simply according to the static down-hole temperature it has to be kept in mind that the drilling mud gets close to the static temperature by the effect of a long horizontal section in the end alone. Further heating effects like hydraulic or friction heat may cause dynamic temperatures larger than the static ones, as indicated in some case studies.<sup>[17]</sup>

Generally the temperature differences presented here are marginal, which is a consequence of the average gradient and depth of the well analysed. Nevertheless, the small differences observed may become important in deeper wells or with higher gradients.

### 2.3.5 Influence of the wellbore geometry

Wellbore geometry has an impact on the down-hole heat flux, as it determines the area available for heat transfer.

The base case, represented by the given geothermal well, was therefore modified. Three derivations have been analysed in order to get an estimate for the effect on temperature development. In the first derivation the last section's diameter was increased from 8 ½" to 9 ½", which would represent a low clearance solution.

The second derivation involves a low clearance programme from bottom to top, with the bottom diameter of the base case. Therefore the Conductor casing was assumed to have 20" instead of 18 5/8". (20" Hole --> 16" casing --> 14,75" open hole --> 11,825" casing --> 10,625" open hole --> 9,625" casing --> 8,5" open hole).

In the third derivation on the contrary the 23" section was held constant and a low clearance solution was further extended downwards, resulting in a 12 ¼" open hole section. (23" Hole --> 18 5/8" casing --> 17,5" open hole --> 16" casing --> 14,75" open hole --> 13 3/8" casing --> 12,25" open hole)

The flow-rates in the casings were adopted to reach the same annular flow velocities as in the base case. Like this the time involved for heat exchange is the same for all fluid elements and the temperature differences are deviating due to geometry only. For the first two sections reduced rates have been used, which were calculated by a minimum annular flow-rate of 0,61m/s (120 ft/s). Thus, larger annuli cause higher pumping rates.

	1 <sup>st</sup> Section	2 <sup>nd</sup> Section	3 <sup>rd</sup> Section	4 <sup>th</sup> Section
Flow Velocity [m/s]	0,26	0,41	0,79	1,24
Base Case [l/min]	4000	3500	3000	1775
Derivate 1 [l/min]	4000	3500	3000	2451
Derivate 2 [l/min]	2976	2396	2108	1775
Derivate 3 [l/min]	4000	3500	4619	4698

**Table 10:** Pumping rates for the different derivations

The following graph shows the results of the derivatives simulation:

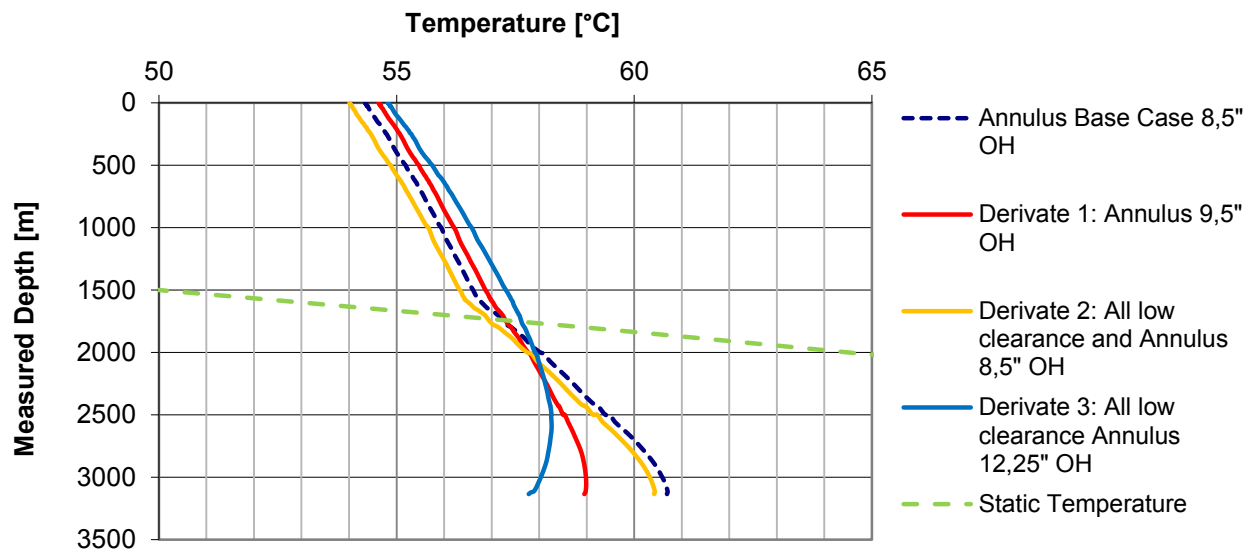


**Fig.32:** Annular temperature profiles for various well-geometries

	Base Case	Derivate 1:	Derivate 2:	Derivate 3:
Flow-line Temperature [°C]	54,34	54,62	54,01	54,82
Bottom hole Temperature [°C]	60,69	58,95	60,42	57,78
Max. Dynamic Temperature [°C]	60,7	58,99	60,43	58,26

**Table 11:** Results for different well-paths

The temperatures at the flow-line are practically the same for all cases. The notable difference that can be achieved here is a variation of the down-hole circulating temperatures. Increasing the diameter of the last section will reduce the bottom-hole temperature by almost 2°C.

It can be nicely seen, that a smaller annulus will increase the heat flux and thus increase the temperature at the lowermost parts. The low clearance solution with the lowest diameters (derivate 2) shows almost the same temperature profile as the base case. The slightly smaller temperatures comes from the more efficient cooling at shallow diameters.

The large diameters with their comparatively large flowing volumes on the contrary reduce the down-hole temperatures most efficiently. More heat is brought from the lower formations and more is absorbed in to the upper ones, thus causing almost no change of flow-line temperature.

### 2.3.6 Influence of tubular size

During the construction process of the well DrillTec used 5" drill-pipes. Larger drill-pipes may suffer from less friction losses inside and increased annular flow-velocity, but on the other side the annular volume is reduced, thus causing more formation exposure per differential volume. As can be seen the effects in both ways are marginal and negligible.

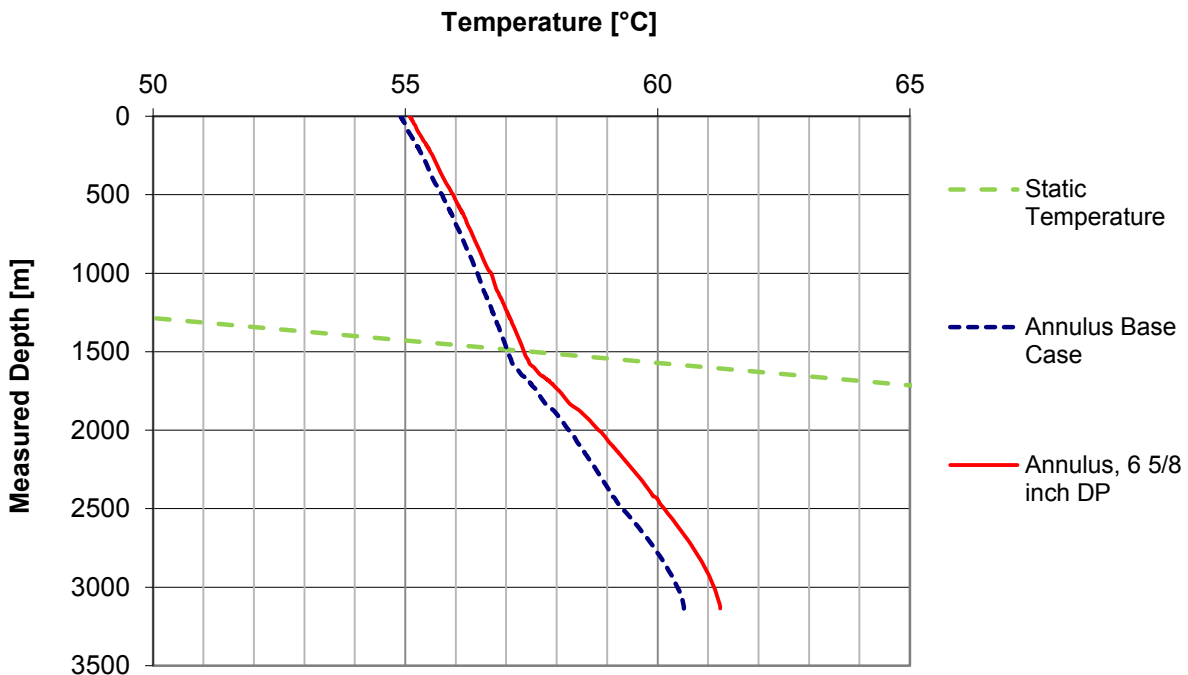
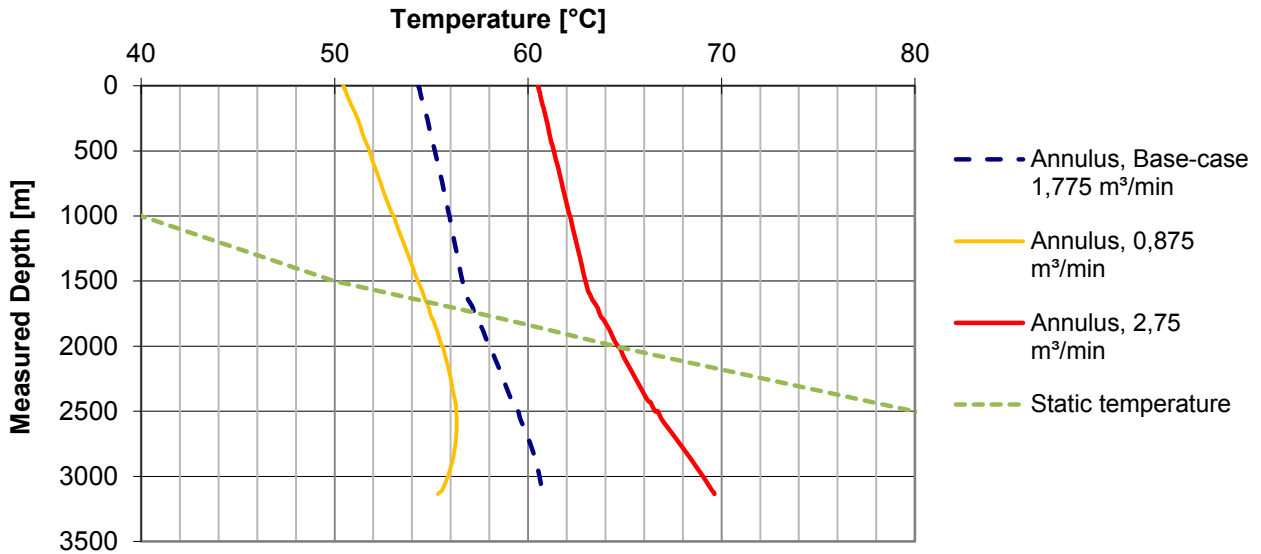


Fig.33: Temperature profiles different pipe diameters

### 2.3.7 Influence of flow rate

The flow-rate has various effects on the temperature profile. On one hand, it reduces the heat transfer efficiency with the formation, similar to a diameter reduction. This is due to the shorter time available for the fluid volume to interact with the formation. On the other hand fluid friction losses are increased, thereby generating more heat. Thus, the actual impact is depending very much on the well depth. For the analysed well the flow-rate increase and decrease of 50 percent compared to the base case was simulated for the last section.



**Fig.34:** Temperature profiles of different flow-rates

	Base Case: 1,775 m <sup>3</sup> /min	Flow-rate: 0,875 m <sup>3</sup> /min	Flow-rate: 2,75 m <sup>3</sup> /min
Flow-line Temperature [°C]	54,34	50,45	60,52
Bottom hole Temperature [°C]	60,69	55,34	69,63
Max. Dynamic Temperature [°C]	60,7	56,31	69,63

**Table 12:** Results for different well-paths

Pumping energy input and the according transformation to heat is an important temperature driver, causing a large increase of dynamic equilibrium temperature for the whole profile with time.

At higher flow-rates the temperature profile tends to get closer to a straight line, due to the minimized time for heat exchange with the formation. At lower rates, on the contrary, the profile has a more curvy shape, depending on the adjacent formation temperature.

The increased friction heat generated and more efficient heat flux with smaller diameters can be observed in the deeper part of the annulus by a kink in the profile at 1648 meters MD. At that depth the liner overlaps and the diameter increases from 12 ¼" to 17 ½". As the casing

diameter gets bigger less fluid friction is generated and relatively less surface is available for heat transfer, thus resulting in a steeper profile.

To avoid misleading it should be mentioned, that an increased flow-rate for a well like the simulated one will result in an increased cooling of the bottom hole, at least in the beginning. More flow-rate brings more “cooling” down, but more “heating” upwards. As the presented graphs show the temperature profile in the end of the long operation, the friction heat accumulation already heated up the whole system. Thus, when considering a constant mud inlet temperature an increased circulation rate will cool down the formation in the lower sections.

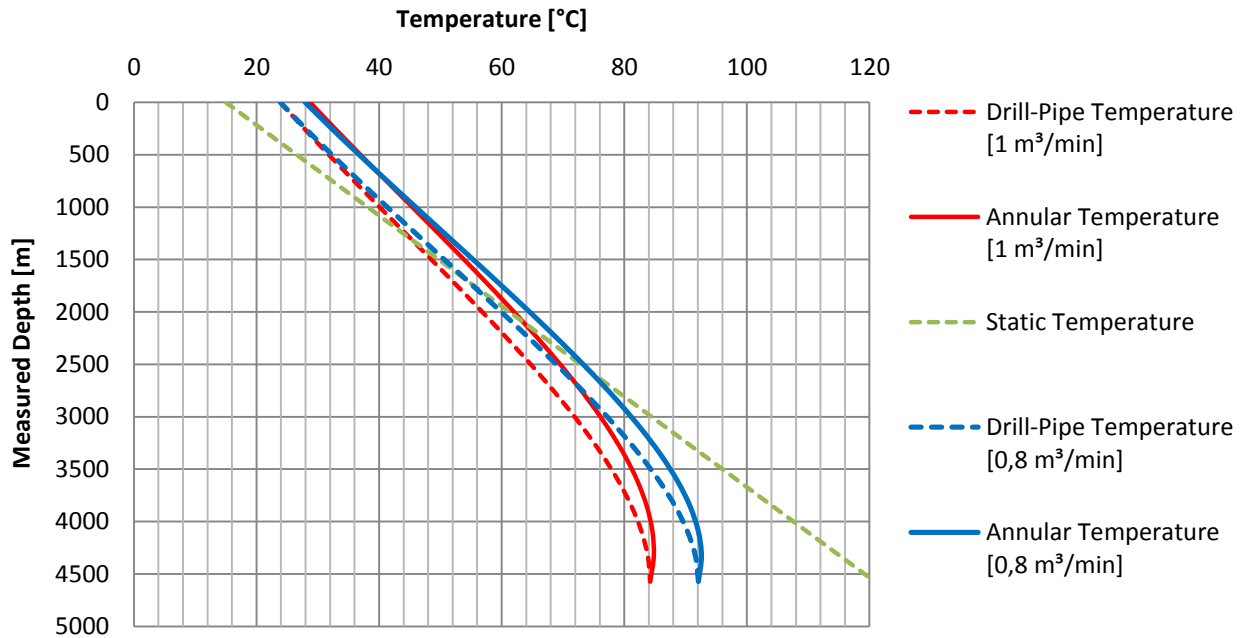


**Fig.35:** Temperature profiles of different flow-rates in a deep well

### 2.3.8 Influence of fluid type

The specific heat of a drilling mud is depending mainly on the base fluid, which is for oil based mud about half that of the water based one. Mud additives are said to have generally a negligible impact on the heat capacity, though weighting additives should be considered in the calculation. <sup>[52]</sup> Actually the heat capacity decreases with increasing pressure and increasing with temperature (for relevant pressure ranges at  $T > 40^{\circ}\text{C}$ ), but these effects are comparatively small. <sup>[38]</sup>

For simulating the following temperature profiles two muds have been used with the assumption of same rheological properties and density. One mud was water based with a specific heat capacity of 4 kJ/kg/K and one oil based with 2,5 kJ/kg/K.



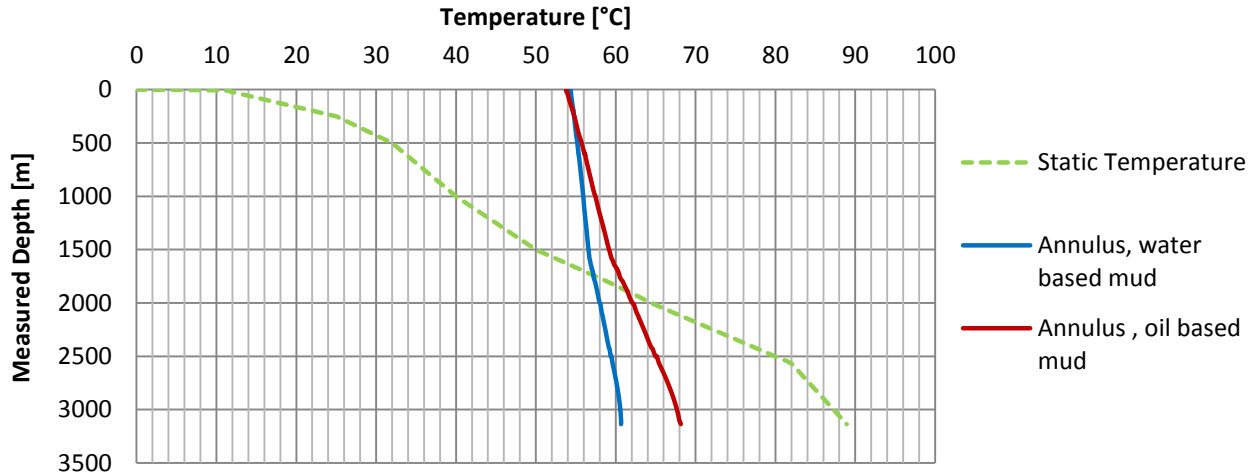


**Fig.36:** Temperature profiles for water-based and oil-based mud

	Water Based Mud	Oil Based Mud
Flow-line Temperature [°C]	54,34	53,81
Bottom hole Temperature [°C]	60,69	68,14
Max. Dynamic Temperature [°C]	60,7	68,14

**Table 13:** Results for different well-paths

The reduction of the muds heat capacity is causing a stronger dependency on the rock temperature. Consequently less heat is absorbed by the mud down-hole, resulting in less efficient cooling of the formation. On the contrary the gained temperature is also lost faster when flowing through the cooler formations in the upper sections.

For drilling operations the usage of water based mud has the advantage of decreasing the bottom hole temperatures, which is positive for the down-hole equipment. On the other hand more heat is brought to the surface which may lead to problems with the surface equipment.

### 2.3.9 Influence of nozzle size

The large pressure differences across the nozzle of the bits cause an accordingly large temperature increase in the circulating fluid. The following formula can be used to express the temperature differential: <sup>[32]</sup>

$$\Delta T = \frac{\Delta P}{\rho_{Mud} \cdot c_p} = \frac{61 \cdot 10^5 Pa}{1120 \frac{kg}{m^3} \cdot 4181 \frac{J}{kg \cdot K}} = 1,3K$$

**Equation 10**

As can be seen in the formula, the temperature increase is directly proportional to the pressure losses and is in the range of some degrees. Furthermore it is indirectly proportional to the heat capacity and density of mud (see above). The result presented in this example-calculation represent 50% of the pressure input of the first drilling operation 1.2 and the result show to be close to this one from the energy balance mentioned later (2,3°C for 122 bar pressure input).

Increasing the bit nozzle sizes will consequently reduce the heat generation and thus the actual dynamic temperature equilibrium. The following picture shows the simulation of the base case with a PDC bit with a nozzle area of 2,806 cm<sup>2</sup> (7x9/32" nozzles) case compared with 7 x 10/32" nozzles (3,46cm<sup>2</sup>) and 5 x 9/32" nozzles (2cm<sup>2</sup>).

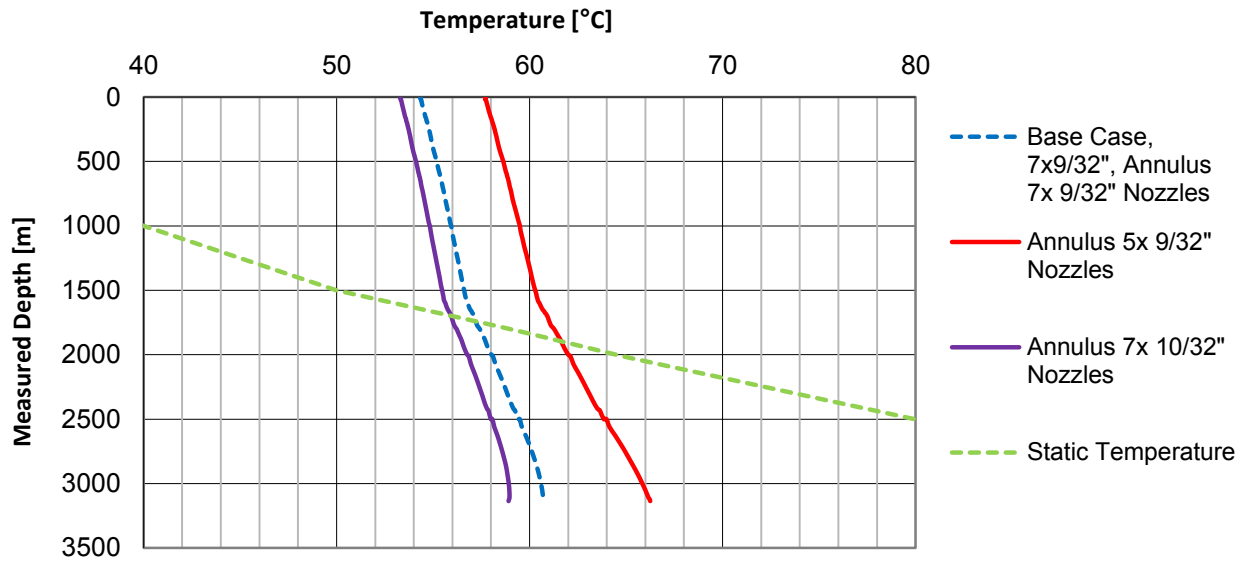


**Fig.37:** Temperature profiles for different nozzle sizes

	7x9/32" nozzles [Base Case]	7 x 10/32" nozzles	5 x 9/32" nozzles
Flow-line Temperature [°C]	54,34	53,3	57,69
Bottom hole Temperature [°C]	60,69	58,91	66,25
Max. Dynamic Temperature [°C]	60,7	58,96	66,25

**Table 14:** Results for different nozzle sizes

It can be observed, that a reduction of the nozzle size has thereby a higher effect on increasing the final temperature profile than vice versa. This seems logical, when considering the standard pressure loss formula over the bit, which indicates a quadratic relation to nozzle diameter.

This observation, that pressure losses at the BHA can have such an impact on the temperature profile in this well must be seen relatively to the number cycles the mud is exposed to. In deep wells the number of cycles will be smaller, thus causing less heating of the profile over time. Nevertheless, when close temperature margins are reached at the BHA the effect of pressure losses must be considered.

### 2.3.10 Influence of surface cooling equipment and riser

Eventually a mud cooler or a mud-chiller is installed when excessive temperatures are expected. These cooling devices can be installed to process mud from the mud pits or suction tank onwards with a rate multiple times of the actual pumping rate down the drill pipe. Mud coolers offer benefits from an HSE standpoint of view as they achieve sufficient cooling of the mud present at the surface. Nevertheless, for cooling the down-hole system the efficiency is depending on the well layout and operating parameters. The devices can cool down the overall system with a big, but also with no effect.

To demonstrate the effect of cooling devices on the wellbore here the analytical model was chosen. This is because the possible comparison with a deeper well seems reasonable.

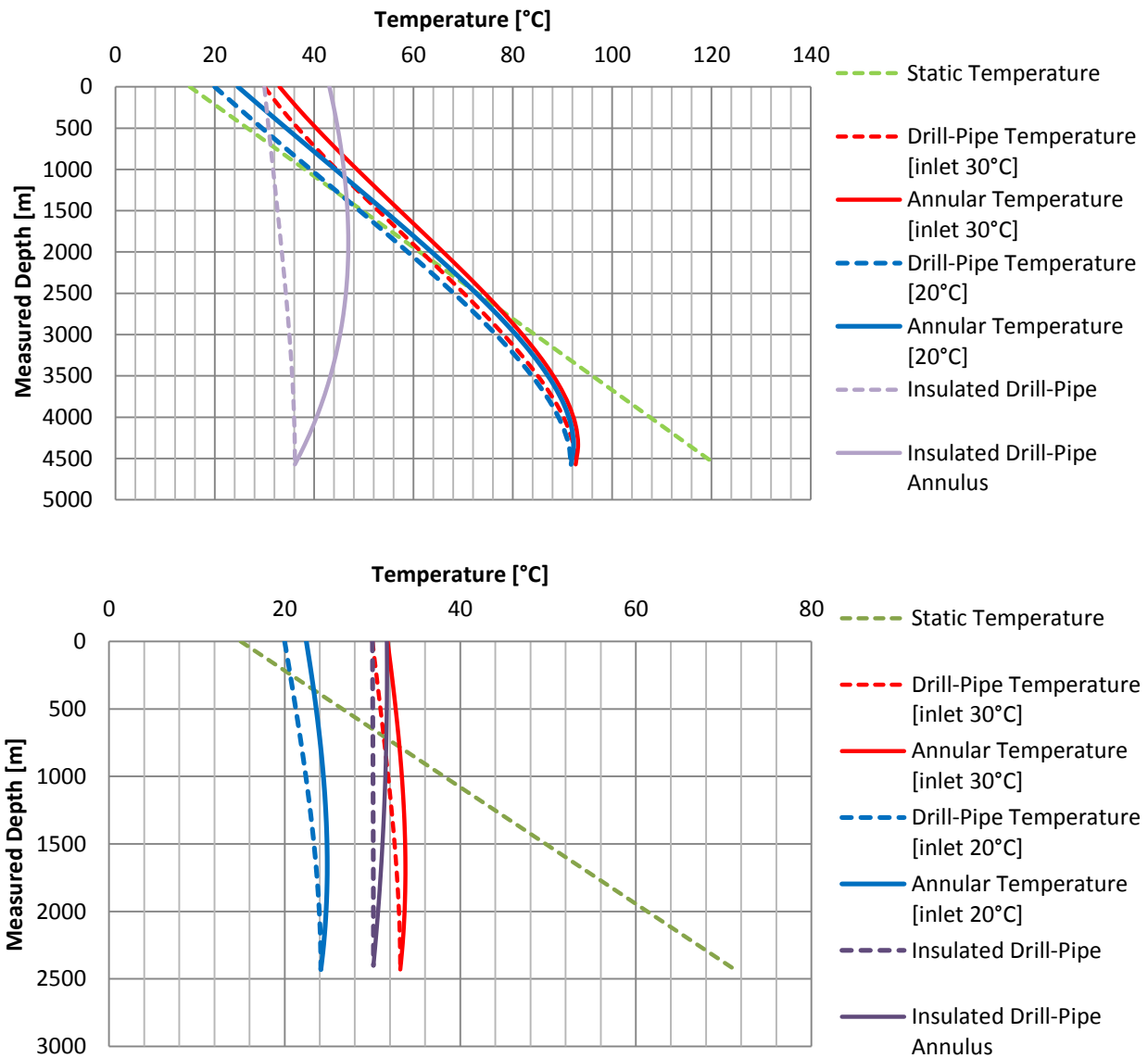


**Fig.38:** Comparison of mud inlet Temperatures for a deep well given in a paper <sup>[2]</sup> (upper), and for the shallower drilling operation 3.2 (lower)

In the graphs the deep well represented the standard case for the development of the analytical model. To obtain the graph the inlet temperature was simply reduced by 10°C. The same was done for drilling operation 3.4, from the comparatively short well of this study. The different impact of a different mud inlet temperature on the temperature profile is evident.

It can be concluded, that cooling systems will have especially a great effect on the wellbore temperature profile for shallow and large diameter wells. Geothermal well construction in hot areas will profit largely from coolers, as the mud inlet temperature is a dominating factor. The effect on the consequent heating due to the rigs energy input will be nullified and further also the formation can be cooled more efficiently. A real benefit for tool and material lifetime can be achieved.

For deep wells facing high bottom-hole temperatures, however, a practical effect for down-hole temperatures is not obtained necessarily by mud coolers. Nevertheless, a profit for surface equipment and HSE will always be given. The application of mud coolers is depending strongly on company policy. While some companies relate the usage with the occurrence of hammering effects of mud pumps, other ones define maximum flow-line temperatures. Due to the limited demand in Europe these systems are not widely available, though they are not really expensive.

The third line couple show the temperature profile when using insulated drill-pipes. This is a rather rare approach, which was only used for extremely high-temperature geothermal wells. Nevertheless, a beneficial effect for cooling can be clearly observed, especially for deeper wells. [39], [68]

In offshore applications the presence of a riser has a similar cooling effect due to the cold water surrounding the annular mud column. The actual depth of the water, current and temperature profile have an important impact on cooling. Also the presence of insulation material or a riser booster pump can have an impact on the circulating temperature profile. [47]

### 2.3.11 Influence of surface conditions and tank capacity

As the simulated geothermal well was drilled in winter simulation temperatures around zero degrees were assumed. To estimate the impact of the weather conditions the same well was assumed to be drilled in summer with a surrounding temperature of 25°C. To get a complete idea about the impact of surface weather conditions a further comparison with a constant wind of 20 km/h was added. As a third guess for the impact of the surface heat exchange the tank capacity was doubled compared to the base case from 120m<sup>3</sup> in three tanks to 243m<sup>3</sup> in six tanks. All of this was then compared to a profile with a profile, where a mud-cooler causes a constant inlet temperature of 25°C.

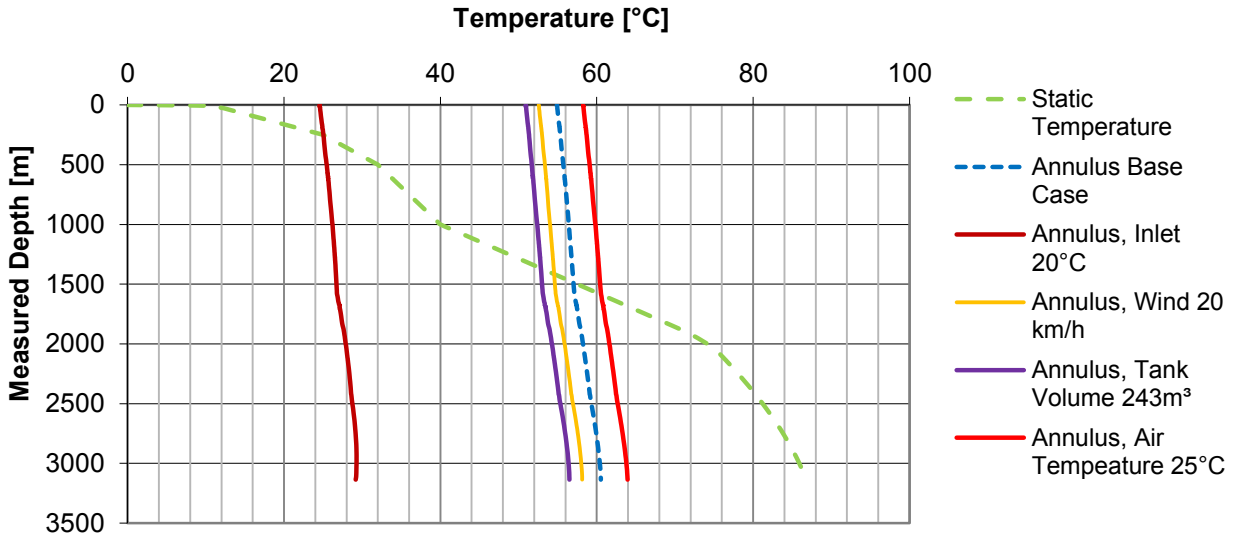


**Fig.39:** Temperature profiles different surface conditions

	Base Case	Mud Cooler with 20°C Inlet	Constant Wind 20 km/h	Double Tank Volume 243m <sup>3</sup>	Air Temperature 25°C
Flow-line Temperature [°C]	54,34	24,55	52,58	50,92	58,26
Bottom hole Temperature [°C]	60,69	31,17	58,15	56,50	63,94
Max. Dynamic Temperature [°C]	60,7	31,28	58,13	56,52	63,95

**Table 15:** Results for different surface conditions

In this graph the action of the mud-cooler is determined with the numerical simulation, and gives the same beneficial result. The influence of surface heat exchange between mud and air at the tanks has a relatively small impact. A 100% increase of tank volume only cause a decrease of 4°C in mud temperature. Similar level of impact can be stated for the temperature conditions in summer.

Some wells, especially off-shore, have closed tank types. This may be good for HSE but will be a disadvantage, as by far most of the temperature exchange happens towards the exposed air.

### 2.3.12 Conclusion

By re-simulating the typical geothermal well in Germany a quick over-view about the impact of the drilling process properties on the temperature profile was tried to be gained. Therefore the input parameters of the proved model were altered in a reasonable way. The following absolute impact of the single parameters could be observed:

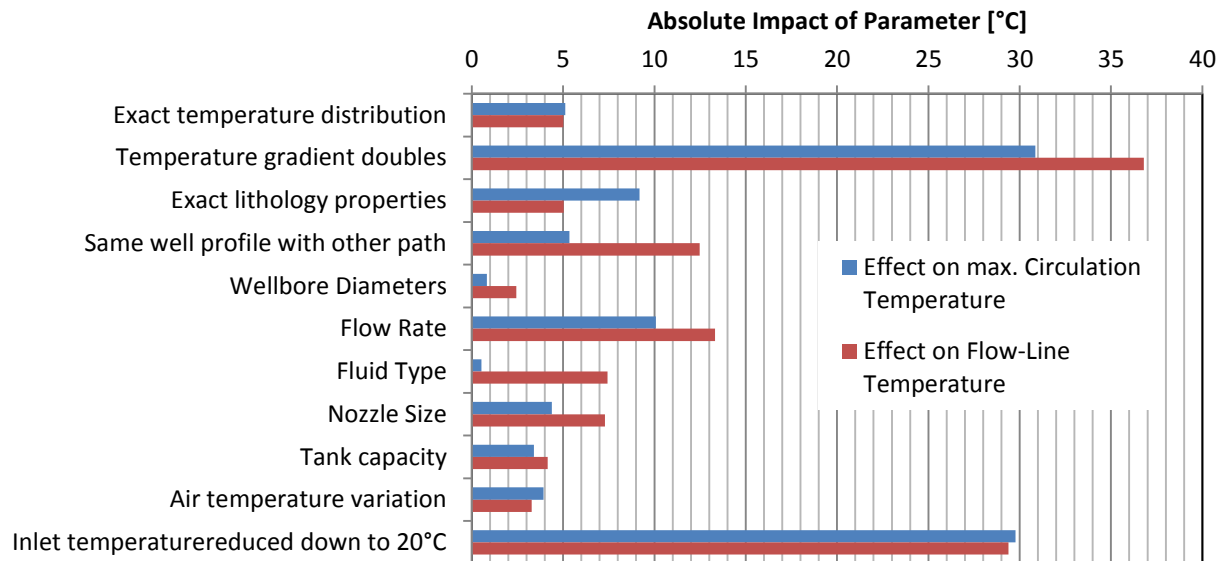


**Fig.40:** Possibility of temperature changes

The observation of this graph is in good accordance with the observations from the parameter study conducted with the analytical model: When the equilibrium conditions are approached, as it is the case for the given well, the mud-inlet temperature is clearly a first order effect with a major impact. The bigger impact of the temperature gradient resulted simply from the much larger assumption of doubling the gradient.

Compared to the parameter study of the analytical model, one can also observe the importance of exact inputs on well profile, temperature gradient variations and lithology.

Generally, the analytical method proves somewhat inappropriate to actually simulate the temperature development for the comparatively shallow well. Most models do not include the energy input caused by hydraulic and rotational energy, thus causing mistake. The here presented models include it, however, it is not capable of predicting the circulation temperature development with time. Thus actual sensor data input is obligatory.

Regarding the band-width of possible operation temperatures by deviation of a single parameter, the following figure gives a clue. The blue and the green line here present the base case flow-line and maximum circulation temperature.

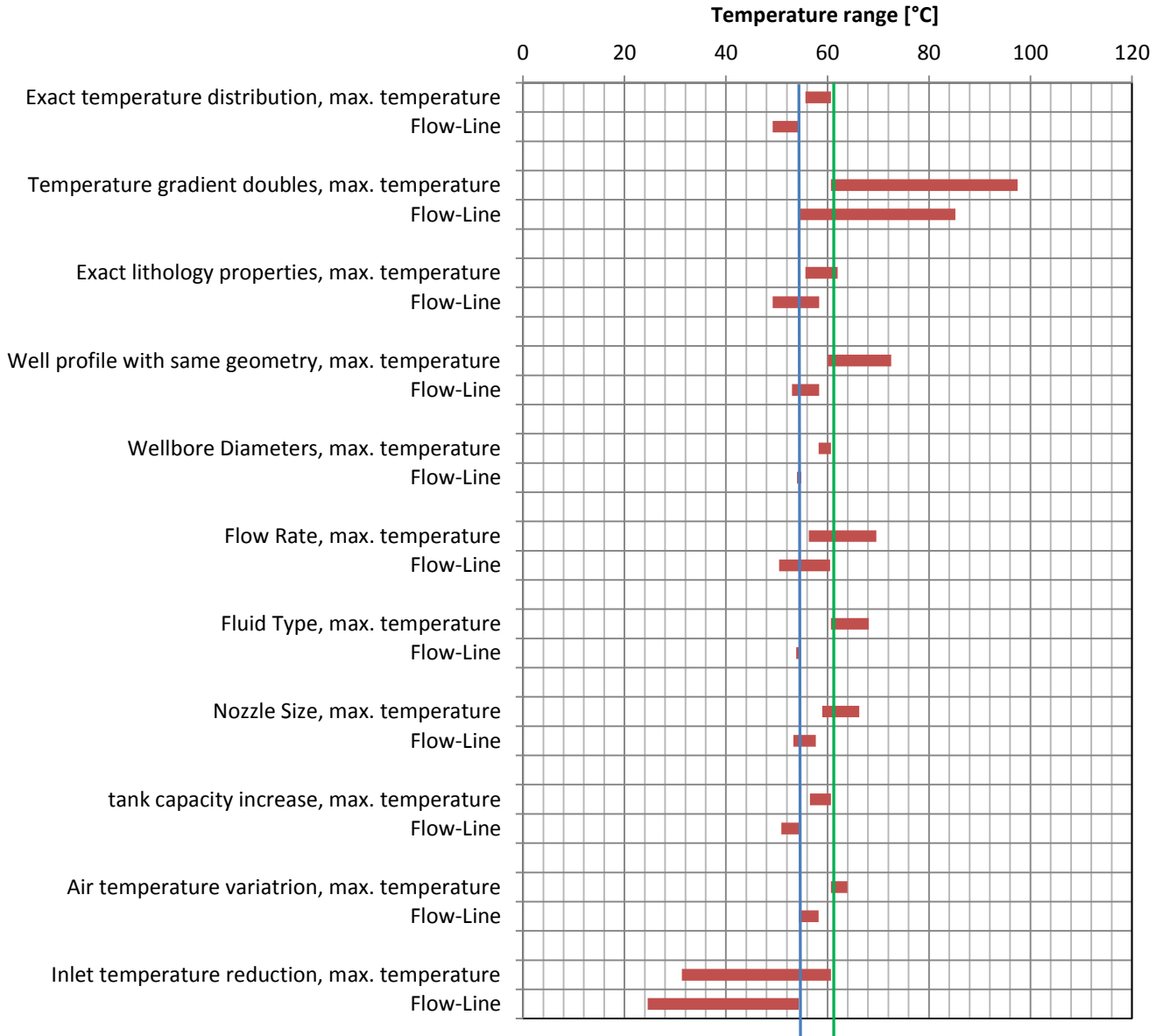


**Fig.41:** Temperature ranges when changing specific properties

Obviously, the shown deviations are not representative for all wells. Nevertheless, this study had a certain attention towards the temperature development of geothermal wells. Thus, for similar wells a quick, facile estimate for the consequences of parameter alteration can be made.

Generally speaking, the deeper the well gets, the more important the interaction between formation and fluid becomes. Shallow, large diameter wells (<2500m MD, >12 ¼" diameter) are rather independent from down-hole temperature conditions and depend much more on the energy input from the rig, due to the short circulation cycles. Bottom-hole temperature and surface temperature are very close, due to the minimal heat exchange with the formation. Steady state conditions are approached very fast, if no disturbing additives would be added. Thus, the actual mud inlet temperature is soon the dominating factor for controlling the

temperature of the whole well profile. The temperature profile is almost a straight line when equilibrium is reached. If a mud system is already heated up above static conditions, the highest temperature is reached directly behind the bit.

The deeper a well gets, the more important becomes the heat flux between formation and drilling mud. The smaller diameters result in a larger surface area per volume of mud. Also the circulation intervals are much longer, thus offering enough time for energy exchange. Consequently also cooling of the formation happens much slower and steady state conditions are approached rather slow. Thus, the well stays much longer in transient conditions and the different operating parameters have a larger impact on the temperature profile. The difference between bottom-hole temperature and surface temperature is large. The present inlet temperature has not necessarily a great impact on the actual bottom-hole temperature. Also the energy input generated from the rig has hardly any impact over time. Still, when equipment limits are narrow the continuous heating at the BHA due to pressure losses should be considered.

The practical temperature equilibrium between heat input from the formation and heat output at the surface, however, will be reached in a matter of hours (shallow wells) to days (deep wells). Then the temperature difference between mud and the formation is small and hardly any flux will occur. The final profile is depending on how much heat energy can be absorbed from the formation and how much can be given to the ambient air. The initial conditions of mud temperature have a little effect over time.

For further study the development of a proved simulation of a deep (e.g. HP/HT) well would be of interest for the exact comparison of changing properties. While the geothermal wells with a similar geometry should show similar tendencies, deep wells probably have significant differences in their temperature profile development with time.



## 2.4 Analysis of the drilling system energy balance

According to the first law of thermodynamics the energy is only transformed into other states, but never generated or erased. The internal energy of a system equals to the heat supplied by the system minus the work done by the system. Therefore the well should be seen as an open system with a continuous exchange of energy only at the wellhead. A theoretical volume element with a large radius should be defined, to allow no energy transfer within the formation but only at the top of the well.

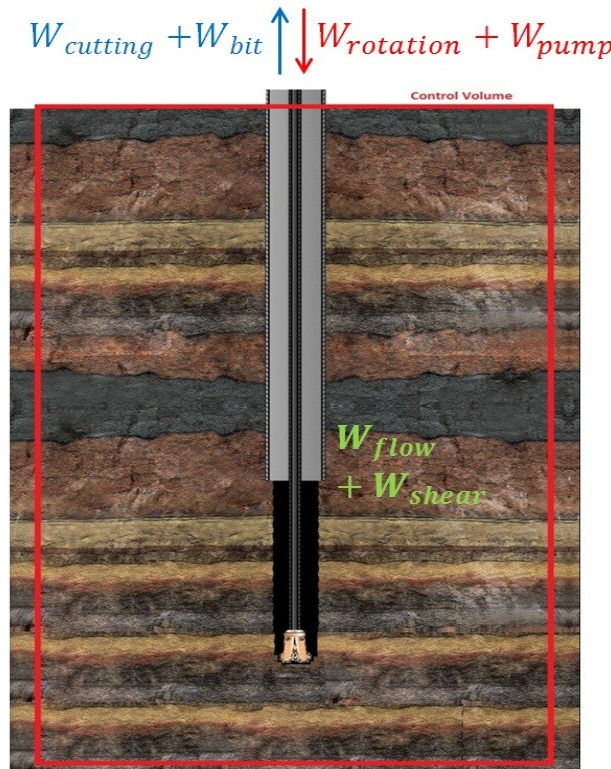


**Fig.42:** Control Volume of the well

The energy accumulated in the system at the moment of observation is the thermal energy in the rock as well as the potential, kinetic and internal energy of the fluid circulating. Internal energy may consist of thermal, intermolecular, chemical and nuclear energy. When neglecting chemical and nuclear energy as well as latent, potential and kinetic energy effects (phase change, position of fluid in gravitational field, spiral fluid flow due to string rotation and density change) the change in energy accumulation conforms to the change of the fluid thermal energy.

During circulation of the drilling mud an equal mass flow is assumed, without losses or gains, thus neglecting additional cuttings. This is justified due to the marginal mass of cuttings compared to fluid flow. With these assumptions the amount of energy into and out of the control volume depends only on flowing fluid velocity and thermal energy. The energy transfer from the surrounding formation is neglected due to the large radius of the control volume. It could not be stated in general anyway. The change of energy inside the control volume depends on the input and output into and from the control volume. Hereby simply the work added into

the system is added while the work performed by the system is subtracted. The input into the system can be described by the net energy input from rotation and pumping. The rate of change in energy per unit of time can be given as:

$$\Delta W_{Volume} = (W_{rotation} + W_{pump}) - (W_{bit} + W_{cutting} + W_{flow} + W_{shear})$$

$$\rightarrow \Delta W_{Heat} = (W_{flow} + W_{shear}) = (W_{rotation} + W_{pump}) - (W_{cutting} + W_{bit})$$

### Equation 11

As mentioned above the continuous input power from rotation and pump is important and causes a general heating of the circulating mud system. On the contrary the system contributes mechanical work to the surrounding by the cutting action of the bit and by lifting the cuttings. The work to overcome normal and shear stresses in the fluid is not available to perform mechanical work. Thus, due to the frictional forces these components of work input are transferred into thermal energy down-hole.

The continuous input of pumping and rotation work by the rig is therefore responsible for the surprisingly high temperatures observed during the analysed drilling operation. The actual energy balance can be represented with the operational data from the drilling operation 1.2, which showed the most surprisingly high temperatures. <sup>[3], [17]</sup>

<b>Standpipe pressure:</b>	122	bar
<b>Flow rate:</b>	4000	l/min
<b>Surface Torque:</b>	5,6	kNm
<b>String RPM:</b>	105,5	min <sup>-1</sup>
<b>Hole Size:</b>	23	in
<b>ROP:</b>	3,33	m/h

**Table 16:** Sensor parameters at the end of drilling operation 1.2

### 2.4.1 Hydraulic power input

The hydraulic energy input can be basically estimated by the hydraulic energy input of the pump. Therefore the differential pressure between the standpipe and the bell nipple should be multiplied with the flow rate:

$$W_{pump} = Flowrate \cdot Pressure = \frac{4000 \left(\frac{l}{min}\right) \cdot 122 (bar) \cdot 10^6 \left(\frac{Pa}{bar}\right)}{1000 \left(\frac{l}{m^3}\right) \cdot 60 \frac{s}{min}} = 813.333,33 \left(\frac{J}{s} = W\right)$$

### Equation 12

## 2.4.2 Mechanical power input

The mechanical energy input can be estimated from the energy input at the top drive. The torque generated there in connection with the RPM is responsible for the cutting action of the bit as well as for some heat generation by friction. The API Bulletin 1981 states the calculation for the rotational energy input:<sup>[23]</sup>

$$W_{rotation} = \frac{Torque \cdot Rotation}{5250} = \frac{5600(Nm) \cdot 0,7375621 \left(\frac{lb-ft}{Nm}\right) \cdot 105,5 \left(\frac{1}{min}\right)}{5250} = 83hp \equiv 61.893,34 (W)$$

### Equation 13

## 2.4.3 Mechanical power output of the drill-bit

The mechanical work done by the system is represented by the digging action of the bit. Various papers indicate the high complexity of the drill bit efficiency estimation. The section of concern was drilled with a Roller Cone bit which means that the efficiency given in the literature lies between 20-30%. An estimate of 25 % was used for the calculation.<sup>[93]</sup> It is assumed, that no torque is lost in the drill-string, thus the rotation power is fully transferred from the Top Drive. The power consumed by the drill-bit can then be simply written as:

$$W_{bit} = W_{rotation} \cdot eff_{Bit} = 61.893,34 (W) \cdot 0,25 = 15.473,34 (W)$$

### Equation 14

## 2.4.4 Power for cuttings transport

To calculate the amount of work related to cuttings transport,  $W_{CT}$ , a hole cleaning efficiency of 100% was assumed. The well is assumed to be vertical, so the energy required for lifting the cuttings is simply the potential energy.

$$Cuttings Volume = ROP \cdot hole cross. = 3,33 \left(\frac{m}{h}\right) \cdot \frac{(23 (in) \cdot 0,0254 \frac{m}{in})^2}{4} \cdot PI = 1,093 \left(\frac{m^3}{h}\right)$$

### Equation 15

The last section drilled was a limestone section and an average density of 2600 kg/m<sup>3</sup> was assumed. The required work for the cuttings transport is therefore:

$$W_{cutting} = (Cuttings Volume \cdot \rho_{Rock}) \cdot MD \cdot g$$

$$W_{cutting} = 1,093 \left(\frac{m^3}{h}\right) \cdot 2600 \left(\frac{kg}{m^3}\right) \cdot 9,81 \left(\frac{kg \cdot m}{s^2}\right) \cdot 3143 \left(\frac{Joul}{s}\right) = 24.322,8 (W)$$

### Equation 16

As can be seen the work from cuttings transport is small:

Input	kW	%
Hydraulic power input:	813,3	92,9
Mechanical power input:	61,9	7,1
<b>Total power input:</b>	<b>875,2</b>	<b>100,0</b>
Output		
Power output by the bit:	15,5	1,8
Power for cuttings transport:	24,3	2,8
<b>Total power output:</b>	<b>39,8</b>	<b>4,5</b>
<b>Remaining power for heat generation:</b>	<b>835,4</b>	<b>95,5</b>

**Table 17:** Comparison of input and output power distribution of a well

According to the results by far the largest amount of energy put into the system is converted into heat. This observation is in accordance with the literature, where it is assumed that 99% of the power input is transferred into heat.<sup>[23]</sup>

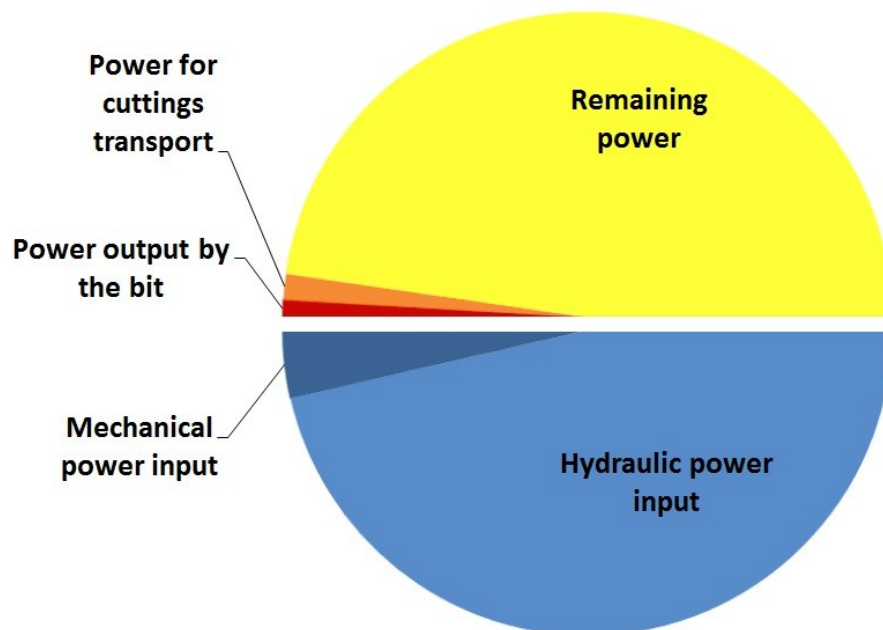


**Fig.43:** Energy balance in the well

The calculation shows, that 835,4 kW are remaining in the energy balance, which will be transferred into heat energy. During drilling the first section 287m<sup>3</sup> (163m<sup>3</sup> down-hole and 123m<sup>3</sup> on surface) of mud with a density of 1050 kg/m<sup>3</sup> were used. When taking into account a specific heat capacity of 4181 J/(kg.K) this energy would suffice to increase the mud temperature by 2,4°C per hour. Considering the fact that the drilling operation under

observation took 105 hours the surprisingly high fluid temperature above geothermal conditions can be explained.

As mentioned above, parts of this generated energy will be lost towards the cooler formation, especially when the actual temperature difference between mud and formation gets larger. This can be observed by the faster increase of flow-line temperature in the beginning of the circulation and a slow increase to more or less constant state after sufficient time. The observation of the first section drilled is thus beneficial, as the comparatively large diameter and shallow depth conditions will minimize formation effects in heat flow. The pump power input on the contrary needed to be at a maximum for proper cutting removal at the large annular cross-section.

### 3. Impact on materials & equipment

Proper design of the tools and materials used in high temperature drilling applications is essential to avoid excessive wear and malfunction of the components or expensive failures. A detailed examination of the expected surface and down-hole temperatures should be conducted, when the tools limits may be reached.

As observed during this study the drilling mud's temperature decline throughout the surface equipment is minimal. If no risk shall be taken the selection of the appropriate equipment should be conducted according to the maximum expected flow-line temperature.

For the down-hole equipment however, the temperature will alternate between dynamic and static gradient. A close look must be taken on the temperature development with time in order to decide, how long the equipment can withstand the temperatures during the operation of interest. For logging operations as an example the time for reaching temperature limits down-hole is essential to plan the operation. For LWD/MWD tools the dynamic down-hole temperature may be acceptable, but static temperatures may be not.

The actual tool selection with temperatures and the risk taken hereby is depending on gathered know-how as well as company policy.

The subsequent chapter represent an overview of literature and company know-how gathered during the thesis research.

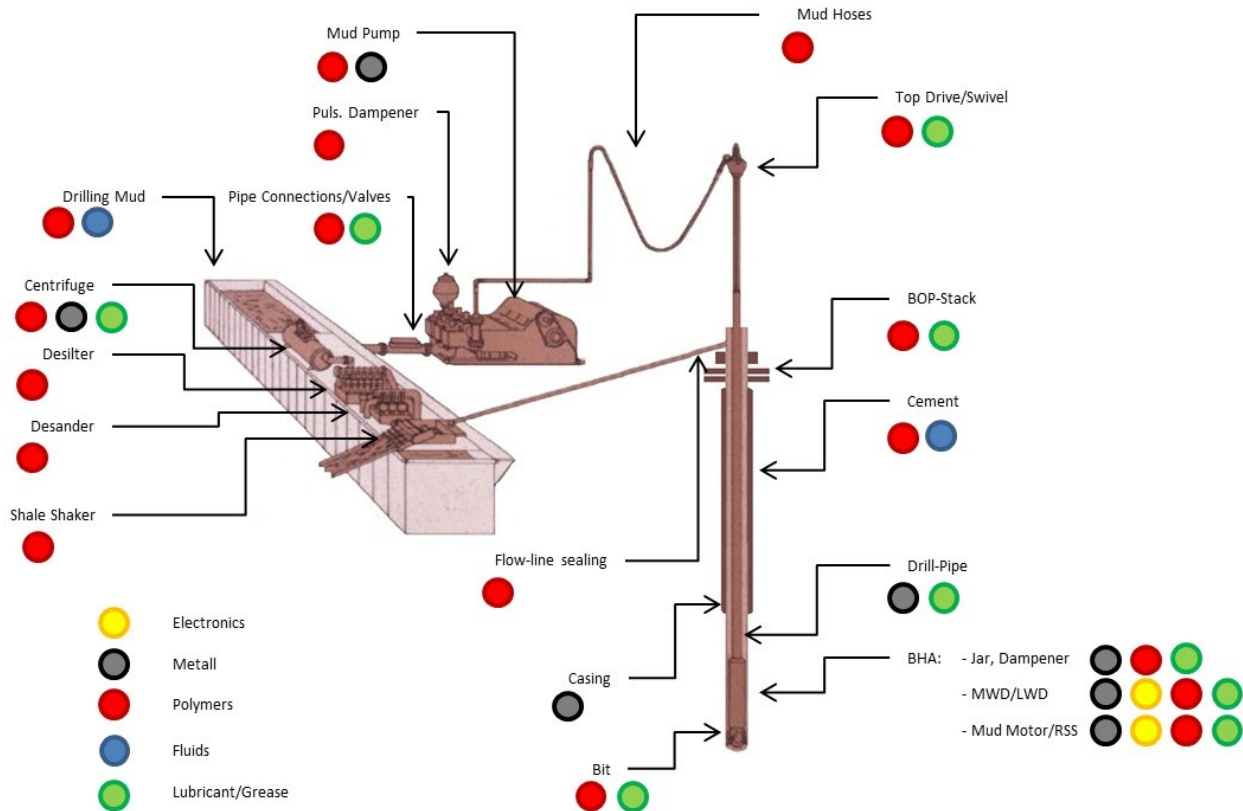


**Fig.44:** Components causing concerns at high temperatures

### 3.1 Metallurgy

Metal components and tools are omnipresent during the hole construction process. Although it is not really a limiting factor regarding high temperature operations, some effects should be kept in mind. Consequences for the drilling equipment and procedures depend mainly on reduced yield strength, the thermal expansion and the increased rate of corrosion. Generally, in shallow normal-pressured wells, temperature will typically have a secondary effect on tubular design. At the presence of high temperatures, on the other hand, it can be one of the governing criteria in the design.

#### 3.1.1 Reduced yield strength

The reduced yield stress mainly implies considerations in the layout of the drill-string and the casing. Basically an increased temperature facilitates the gliding action between the atoms in the metals lattice structure, thus causing a reduction in yield strength or Young's Modulus. Thereby the alloying compounds, lattice structure and heat treatment are of importance. Thus even the same steel with different heat treatment has different properties. Also the toughness is changing.<sup>[71]</sup>

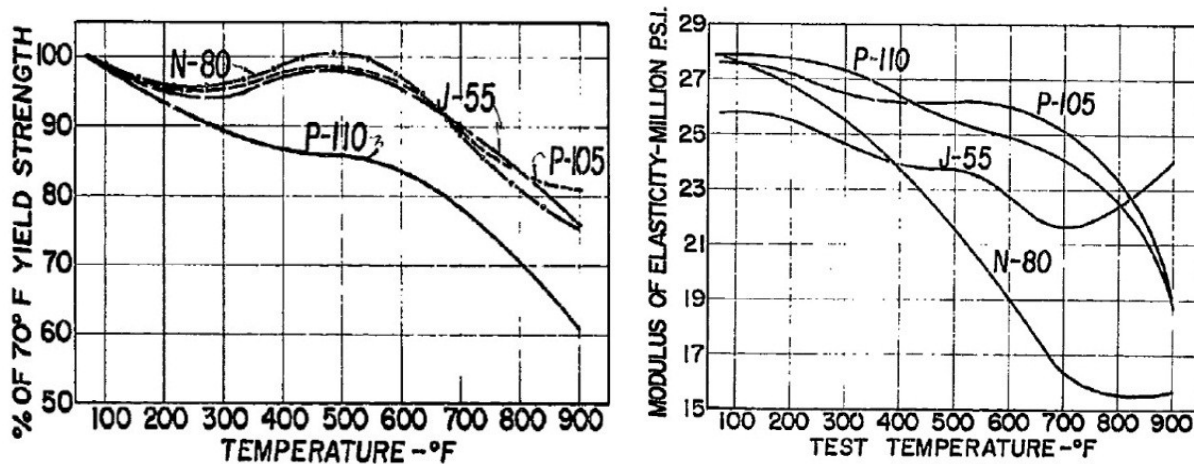
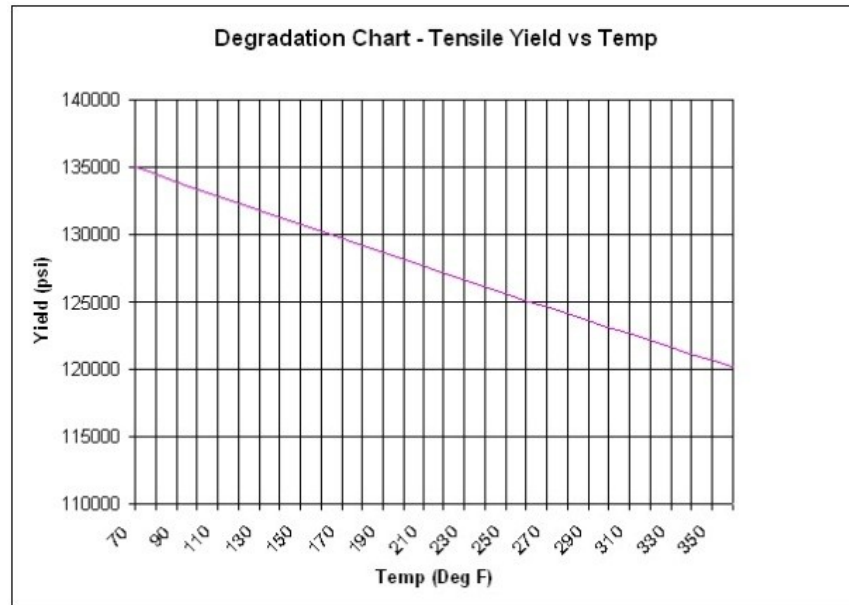


Fig.45: Yield Strength and Modulus of Elasticity vs. Temperature<sup>[71]</sup>

Manufacturing standards for tubular equipment are regulated in API specification 7 and 5D&L, but these specifications are given at room temperature. Therefore, for accurate operation, providers of the tubular equipment should be asked to provide specifications for larger temperature ranges and appropriate correction. These correction factors should then additionally to the safety factors.<sup>[97]</sup>



**Fig.46:** Degradation Chart of a Vallourec & Mannesmann S 135 6 3/8" drill pipe

In this example we can see that a temperature increase of 167°C ( $\Delta T_{\text{C}} = \Delta T_{\text{F}}/1,8 = 300^{\circ}\text{F}/1,8$ ) results in a decline of the yield strength of 11%. Thus, especially for deep wells with high tension and torque margins this consideration is important. Burst strength, collapse resistance, tensile strength and triaxial ratings will be influenced by temperature variations, as in all equations yield strength is an important factor.

The reduction in yield strength applies actually to all down-hole components. For example the relatively thin housing of the mud-motor must be engineered carefully. Nevertheless, for well planning applications the tools are specified by the provider and care must be taken for a proper selection of equipment.

The usage of a metallurgical alternative to steel pipes, like titanium or aluminium, raises the need for special consideration. Titanium pipes show similar properties to steel regarding temperature, though they have an improved corrosion resistance also for HT applications. Aluminium drill-pipes have the advantage of less weight, a longer fatigue life and also more corrosion resistance towards  $\text{H}_2\text{S}$  and  $\text{CO}_2$ . Nevertheless, most aluminium pipes are very sensitive to temperature. Plastic deformation, creep or phase transition, which doesn't cause problems with steel or titanium pipes, can get problematic. With a growth in temperature the material properties are noticeably reduced. Depending on the exact aluminium alloy, some aluminium pipes are even not recommended for use at temperatures greater than 110°C (1953T1 alloy). Thereby also the exposure time to temperature is an important factor. For string-design the observed yield point tested after 500 hours of operation is used. Thus, design with aluminium tubular must be conducted carefully at high temperature conditions. <sup>[48], [50]</sup>



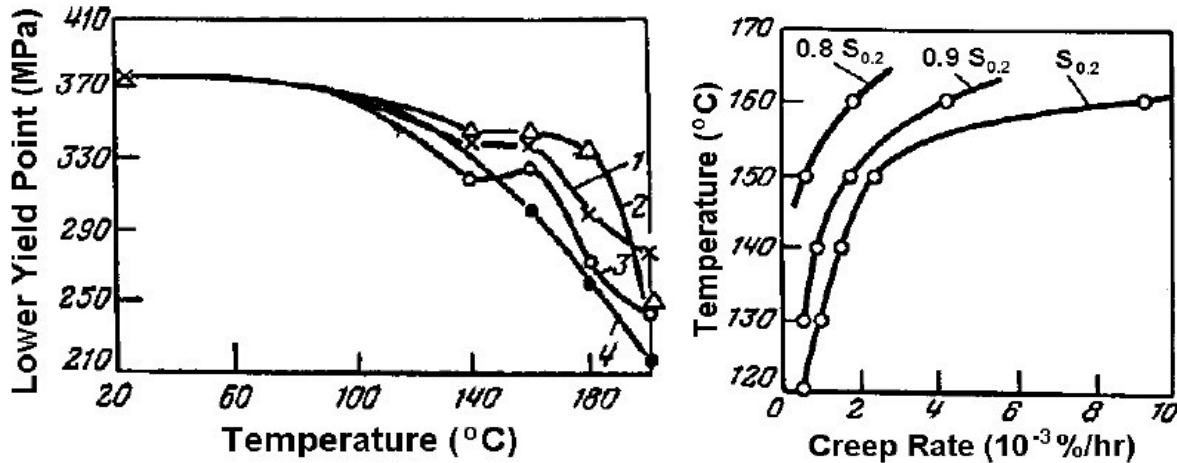


**Fig.47:** Aluminum D16T alloy: Yield Point vs. temperature at different exposure times (left), creep vs. temperature at different exposure stress ranges (right) <sup>[50]</sup>

### 3.1.2 Thermal expansion

During various temperature conditions faced, tubular will undergo a certain change in length, which can be simply determined by the thermal expansion coefficient of steel ( $\alpha = 11 - 13 \cdot 10^{-6}/K$ ):

$$\Delta L = \alpha \cdot L \cdot \Delta T$$

#### Equation 17:

L = Length of string [m]

$\alpha$  = Linear thermal expansion coefficient [1/K]

$\Delta T$  = Temperature difference [K]

To quickly show the impact of length elongation on drill-pipe a simple calculation was performed with the well data observed from a deeper well, presented before for the determination of the analytical temperature model. The following table compares the deviation of length of the longest drill-string at surface conditions, dynamic circulation and a static profile:

Length of Drillstring	4572 m
$\Delta L$ with static gradient	4,36 m
$\Delta L$ with dynamic gradient	3,88 m

**Table 18:** Elongation for different temperature profiles

As can be seen under normal conditions the difference in elongation between the static and dynamic gradient is not too high, even for deep wells. This comes from the fact, that the upper part of the dynamic gradient is warmer than the formation and the lower part is cooler, thus the compared elongation effects somewhat cancel out. When the difference between the static and

the dynamic profile increases, for example with the usage of mud coolers, the differences in tubular length will be accordingly higher and should be considered.

While elongation in drill-pipes is more an issue for a correct determination of the measured depth, the effect may cause serious problems for the casing, when not handled properly. Several problems are possible such as compression/tension failure in cemented pipe, radial expansion and cement damage or buckling.

Tubing and casing undergo repeated fluctuations in axial stresses, which are mainly driven by temperature dependent elongation and contraction when drilling subsequent sections, cementing, shutting in, producing or injecting. These stresses cannot be avoided. However, when facing higher temperatures these effects gain more importance. Thermal expansion occurs under flowing conditions and may reduce stresses, while the stresses may increase when static conditions approach. Stress fluctuation in the order of 100 MPa (15 000 psi) are typical. <sup>[72]</sup>

Buckling is a serious issue and causes problems in casing stability, subsequent drilling operations or early burst failures during production. The buckling caused by thermal stresses is different from buckling from applied loads. A slow deformation into the deformed shape occurs rather than a catastrophic failure. The type of buckling occurring depends in pressure differentials, unsupported length and temperature change. The thermal stress can be calculated with:

$$\sigma_t = \alpha \cdot E \cdot \Delta T$$

**Equation 18:**

$\sigma_t$  = Thermal stress [m]

E = Young's modulus [GPa]

Where the thermal stress  $\sigma_t$  is directly proportional to the change in temperature,  $\Delta T$ , the Young's modulus (E= 200 GPa) and the linear thermal expansion coefficient of steel ( $\alpha = 11 -13 \cdot 10^{-6}/K$ ). Like this, an stress increase of around 2,5 MPa/°C can be observed. When taking a K-55 casing with a yield strength of 55 000 psi (3 792 MPa) as an example, a temperature differential of 149°C is sufficient to reach the yield strength. Between static and production temperature in the upper parts of the string such a temperature differential may occur.

Consequently, especially for geothermal wells, casings are cemented completely bottom up. The cement offers support for the casing, but also restricts it's movement by shear bond strength and resistance of embedded collars. Nevertheless, experience showed that with a bad steel selection casing failure can occur also when cemented. The thermal stress in a casing that is cemented solidly is described by the equation:

$$\sigma_t = \alpha_{casing} \cdot E_{casing} \cdot \Delta T_{casing} - \alpha_{cement} \cdot E_{cement} \cdot \Delta T_{cement}$$

$$\sigma_t = \alpha_{casing} \cdot E_{casing} \cdot \Delta T_{casing} - \alpha_{cement} \cdot E_{cement} \cdot \Delta T_{csh} \cdot \frac{C_{cement}}{C_{steel}}$$

**Equation 19**

For a cement heat capacity  $c_{steel}$  of 0,837 J/(g.K) and a steel capacity of 0,49 J/(g.K) the same calculation as above yields an allowable temperature differential of 282°C for K-55. <sup>[62]</sup>

Thus the selection of the proper steel grade is essential, as it determines how much temperature induced stress can be absorbed. The “stress resistance ratio” can be simply calculated by:

$$R_{ST} = \frac{\text{Yield Strength}}{\text{Youngh's Modulus}}$$

**Equation 20:**

$R_{ST}$  = Stress resistance ratio []

Temperature [°C]	P-110 [reference]	P-105	N-80	K-55
205	1	0.966	0,916	0,916
232	1	1.037	0,972	0,614
260	1	1.05	1,038	0,633
350	1	1,042	1,183	0,696

**Table 19:** Stress resistance ratio for some common steel grades with P-110 as reference <sup>[62]</sup>

The table shows, that above 260°C the N-80 alloy is preferable to compensate for temperature induced stresses. At lower temperatures it can be seen that P-110 shows a bit better properties. Still, using P-110 or P-105 has a disadvantage regarding corrosion and economics. Research shows that the stress material failure is same for both, tension and compression. Thus the API values can also be used for buckling prediction.

Accurate knowledge of the cement set temperature is mandatory, because at this temperature the casing becomes constrained. Further derivations from this temperature will cause the according stress.

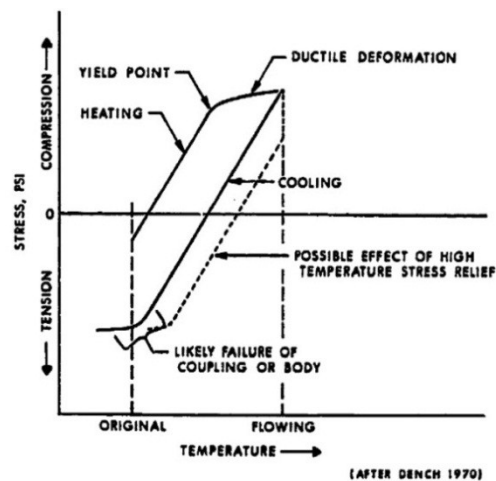


**Fig.48:** Thermal stresses in cemented casing <sup>[73]</sup>

This figure shows how stress can increase with temperature rise until the yield point is exceeded. Continued heating causes steel deformation in compression. On cooling, stresses return on a parallel path last zero stress, into tension loading. As can be seen in such a situation tensile stress limits may be exceeded before original temperatures are reached.

Generally the weakest point of the casing is at the couplings. If tapered API Round thread couplings are installed the joint may fail first, as such couplings are 20-35% weaker than the pipe body. Special premium connections like buttress, VAM, X-Line and Hydrill threads give increased coupling strength to minimize failures when temperatures exceed 121°C. However, usage must be evaluated critically due to their increased price. <sup>[62], [44]</sup>

Fatigue errors will be caused by cyclic loads. Especially at the couplings the casing can get torn after repeated compression, tension cycles. Corrosion fatigue further reduces the amount of cycles needed to tear to roughly the half. <sup>[62]</sup>

Furthermore for casing and coupling design also other factors, like high pressure (typically > 5,000 psi), sour environment, gas production, usage as a high-pressure gas lift or steam well and large doglegs, must be seen in combination. <sup>[44]</sup> As directional drilling is popular, also for geothermal drilling projects, the stresses caused by the build rate must be added to the stresses caused by temperature. For a pipe with a bent of 0,16° and a temperature difference of 80°C a compression stress of 30 000 psi from temperature and 10 000 psi from the bent can be observed, which illustrates the critical issue. <sup>[62]</sup>

Besides the thermal elongation also a radial increase in diameter will be caused. This can have negative effects on cement bound quality. Studies for steam injection wells showed, that an increase of 0,2-0,3% of diameter is a reasonable value for temperature differentials of around 200°C. <sup>[74]</sup> Thus, diameter variations may be only an issue for extremely hot geothermal wells.

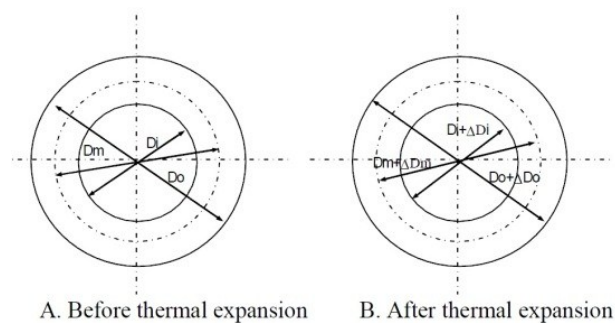


**Fig.49:** Casing cross-section before and after thermal expansion <sup>[74]</sup>

Often inappropriate cementing jobs allow for buckling. Support can be critical through lost circulations zones, poor displacement of thickened mud or failures of stage cementing tools from heat. Slotted liners may also buckle if movement is restrained by sand or shale sloughing in the unsupported areas. <sup>[73]</sup>

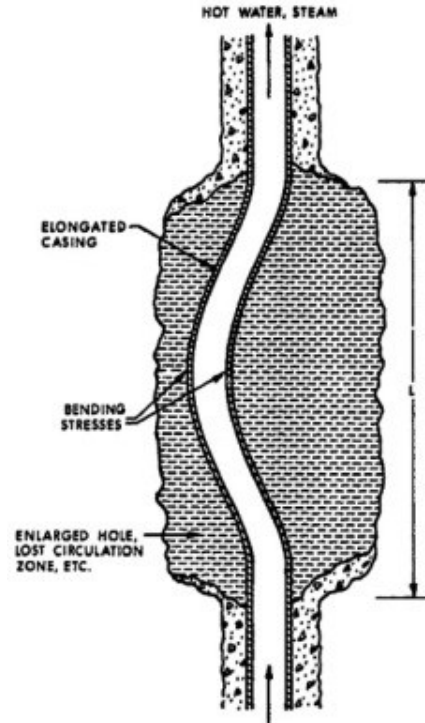


**Fig.50:** Casing buckling with heating and elongation <sup>[73]</sup>

For a simple understanding the resulting buckling can be estimated with Euler's formula. <sup>[94]</sup> Nevertheless, the triaxial design criteria is recommended to account for large temperature effects, especially for combined burst and compression loading. For high burst loads (i.e., high tangential stress and moderate compression), a burst failure can occur at a differential pressure less than the API burst pressure.

For high compression and moderate collapse loads, the failure mode is permanent corkscrewing (i.e., plastic deformation because of helical buckling). The combination of a collapse load that causes reverse ballooning and high temperatures increases compression in the uncemented portion of the string. <sup>[44]</sup> Collaps can be a problem while drilling if severe losses are encounter, such as it is often the case in geothermal wells. <sup>[97]</sup>

When casing sections are left without cement support an appropriate pre-tensioning has to be conducted after the cement hardened. Thereby simply the expected stress is calculated according to the expected temperature profile and the transferred in an according length. The casing is then set under tension. The wellhead is also affected by the expansion of the tubular and the down-grading of pressure resistance.

Fluids present in the annuli may also cause problems. For instance, water at 25°C and a temperature increase of 1°C will produce a pressure increase of more than 5,5 bar in a rigid container. This increase in pressure will be moderated by the elasticity of casing and formation. Nevertheless, the increase in volume has been proven a serious design problem especially in offshore wells with sealed annuli.

For the surface equipment specifications are usually conducted according to EN or DIN norms, which means, that the tools are engineered for temperatures between  $-20^{\circ}\text{C}$  and  $+40^{\circ}\text{C}$ . Generally in mechanical engineering  $80^{\circ}\text{C}$  is a critical border in dimensioning and expansion effects may get a problem for tools fittings and seats. Pumps or centrifuges, for example, can cause problems. The distance between the bearings may not be sufficient for the axis elongation. The centrifuges capable of higher temperatures are usually made of high quality steel against corrosion. If the operating temperatures are out of this range, it is the responsibility of the operator to check up its working capability from the supplier. An additional price of about 20% is common for the modified surface installations, due to more expensive material and manufacturing costs.

mass increase  $\Delta m$

### 3.1.3 Corrosion

Exact predictions for corrosion rates with increased temperatures can hardly be made. This is due to the various interacting parameters of material (chemical composition, mechanical properties, grain structure, heat treatment, surface), medium (temperature, electrochemical conditions, oxygen, carbon dioxide ( $\text{CO}_2$ ), hydrogen sulphide ( $\text{H}_2\text{S}$ ), pH, brine, sand, bacteria, velocity, flow behaviour) and structure (geometry, mechanical load). In general it can be stated that corrosion problems increase with temperature, as can be conducted from the Arrhenius equation. The activation energy for reactions is decreased and therefore chemical reactions run faster resulting in more corrosion of the equipment. As a rule of thumb corrosion rates double with every  $31^{\circ}\text{C}$  increase of temperature. <sup>[97]</sup>

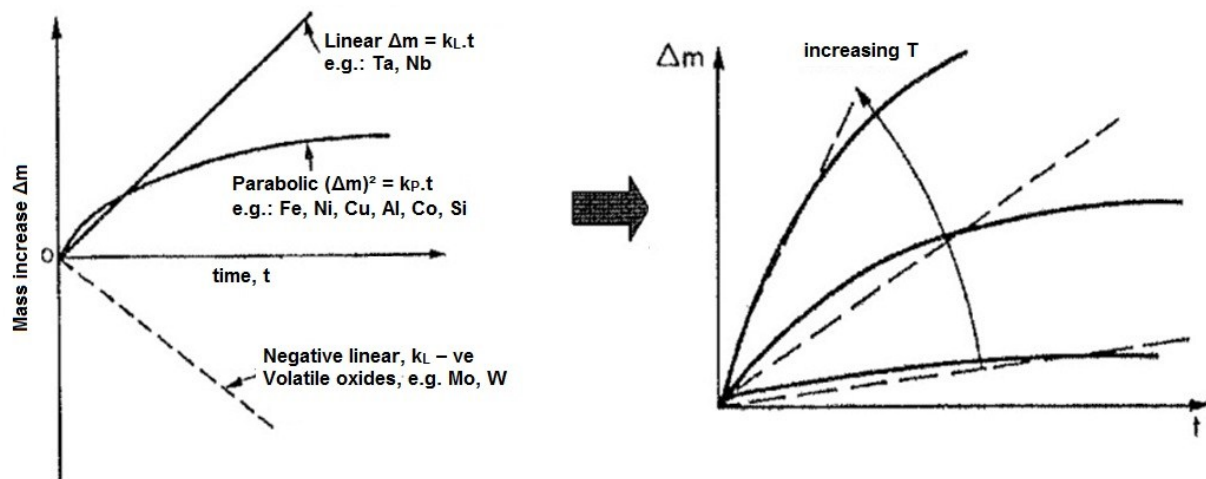


**Fig.51:** Rate of oxidation according to the Arrhenius-law <sup>[41]</sup>

Corrosion is a destruction of metal by direct chemical reaction or by an electrochemical reaction of metal with its environment. Chemical corrosion is the direct combination of metal with another material. It usually occurs at higher temperatures above  $260^{\circ}\text{C}$  ( $500^{\circ}\text{F}$ ) and is thus uncommon during normal drilling operations. The second, more common, type is the electrochemical corrosion which occurs at the solid/liquid interface. It arises in nearly every instance where water or brine contacts with metal equipment. <sup>[45]</sup>

The pH-value is one of the key parameters in understanding the mud chemistry and it plays a major role in controlling the corrosion problem. However, during the circulation the pH is varying, due to H<sub>2</sub>S or CO<sub>2</sub> from degraded additives and a changed ionic-equilibrium with temperature. Also its actual measurement is not easy due to the lack of a proper measurement technique and calibration standards for high temperatures.<sup>[45]</sup>

Generally, for higher temperatures problems with sulfide stress cracking are reduced. This temperature effect can be used to advantage in the design and completion of sour wells. The most serious conditions for corrosion with H<sub>2</sub>S are observed between 65 – 85°C in a well with condensing mist present. Above 65 – 70°C also salts (Chloride) cause corrosion, thus the overlapping area is critical. Chloride-Stress-Corrosion Cracking is getting a problem for drill-pipes, especially for austenitic stainless steels above 100°C. The hardness of steels is an important parameter for H<sub>2</sub>S corrosion. For N-80 casing steel for example the hardness should be below 22, so tempering and hardening has a bad effect when the hardness exceeds this. L-80 steel has the same steel properties but is developed especially for H<sub>2</sub>S environment.

At higher temperatures corrosion from acid carbon and H<sub>2</sub>S pitting can occur. The sources can be a sudden inflow of gas or a gradual degradation of lignosulfonate mud additive, caused by bacteria or high temperatures (>165°C). When extremely high temperatures are encountered lignosulfonate should be avoided. (>190°C). Further, during drilling oxygen is almost always present and causes significant corrosion in the form of clustered pitting, already at very low concentrations. Oxygen corrosion increases sharply with temperature and is influenced by salinity.<sup>[45], [46], [62], [75]</sup>

Titanium alloys have advantages in areas where traditional steel and aluminium alloys are suspected to corrosion. Changes of pH and oxygen content don't affect titan alloys. Care must be taken when they are used in contact with other steels, due to the low position in the galvanic series.<sup>[47]</sup>

Practical experience shows, that the surface equipment also suffers from the high temperature applications. The tempered mist leaving the mud at flow-line and tanks shows a somewhat negative effect on the surrounding tools. In many studies it is pointed out, that an increased awareness and education of field engineers for corrosion development and control would be beneficial. This obviously comes true for high temperature conditions, which are in either case more influenced by corrosion.

## 3.2 Polymers

Polymers encompass a large class of natural and synthetic materials with a very large variety of properties. This also indicates the broad field of usage in the well construction process, where fluid additives as well as tool components, seal, gaskets and housings consist of these materials. Depending on their particular chemical and physical properties polymers are sensitive to high temperatures and therefore a concern in HT-operations.

A polymer is basically a large molecule (macromolecule), composed of repeating structural units (monomers). These subunits are typically connected by covalent chemical bonds. Each of the monomers which link to form the polymer is usually made of carbon, hydrogen, oxygen and/or silicon. The large polymer chains are entangled towards each other and thus form a heterogeneous material. The physical properties of the polymers are depending strongly on the macro- and microscopic structure of the polymer chains. Depending on the chains total length and arborisation, the different monomers present and their arrangement as well as the chemistry of the monomers, the movement of the long chains is tolerated or hindered. Reducing the chain's mobility causes increasing strength, toughness, impact resistance, viscosity as well as glass transition temperature ( $T_g$ ), melting ( $T_m$ ) and boiling temperatures. Also the flow resistance in its melt state tends to increase with molecule length. Further the thermal and UV-radiation stability of elastomers and their oxidative and chemical stability with other media are set.

According to DIN 7724 polymer materials can be divided into four groups regarding to their shear modulus behaviour with temperature: Thermoplastics, thermoplastic elastomers, elastomers and thermosetting plastics.

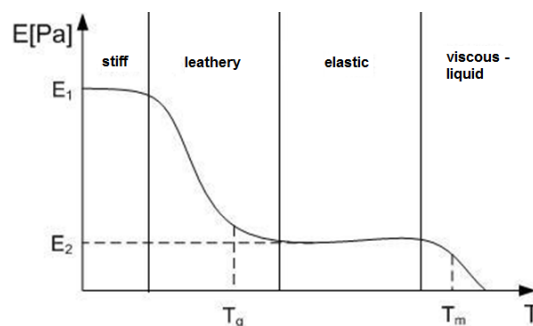


**Fig.52:** Definition of the Rubber plateau <sup>[65]</sup>

As can be seen in the figure the different polymers have very different properties depending on the given temperature range. In temperature area I the polymer-molecules are in a glassy state with little movement of the polymer chains towards each other. Thermoplastics and thermosetting plastics are in this state during their application ( $T_g \gg 0^\circ\text{C}$ ).

Area II is very sensitive to temperature and an increase leads to increasing molecule movement. This in turn causes a smooth decrease of viscosity in the order of many magnitudes, without a distinct change in the material's structure. Consequently the solid like mechanical properties



alter towards elastic properties and a softening of the material. The inflection point is referred to as glass transition temperature ( $T_g$ ).

Area III is between the glass transition temperature,  $T_g$ , and the melting temperature,  $T_m$ . This region is called the rubber plateau and the stiffness remains close to constant. The polymers show entropic-elastic behaviour with a low shear modulus. The chains are very flexible, but due to chemical and physical interaction yielding is restricted. Elastomers and thermoplastic elastomers are in this state during their application. ( $T_g < 0^\circ\text{C}$ ).

In area IV the melting temperature  $T_m$  is reached. Viscous yielding occurs in thermoplastics and thermoplastic elastomers. They can be reshaped and then cooled again to glassy state. Elastomers on the contrary start to degenerate.

A thermosetting plastic is polymer material that irreversibly hardens after manufacturing and has a hard, brittle character thereafter. It has an energy-elastic behaviour and degenerates at high temperatures.

Most of the used polymers for tools and equipment are elastomers. They have their application temperature between the glass transition temperature and the melting temperature. In this range they are viscoelastic, which means partially elastic and partially viscous. In viscous mechanisms applied energy is not stored by the deformation but transferred into heat. Again, the movement of the polymer chains in the heterogeneous bulk is important for the given properties. Thus material parameters generally depend largely on temperature present and the speed of the deformation. The young's modulus lies between 0,1 – 100 MPa.

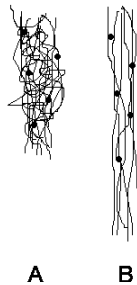


**Fig.53:** Polymer network arrangement in elastomers <sup>[76]</sup>

Elastomers are produced from rubber. Rubber in turn is produced from latex from source trees, for natural rubber, and from polymerization of different monomers, for synthetic one.

For manufacturing the elastomer, one or more rubber types and additives are mixed together according to a recipe. Hereby basic properties of the product are adjusted. Various additives are further added, such as filler material, softening agent or aging protection agent. Generally elastomer mixtures include at least seven ingredients. When optimizing the recipe for advanced mechanical properties, costs and processability, twelve or more ingredients are common. The mixture of the recipe is complex and always a compromise, due to the components interaction.

The next step is the molding process of the material by extrusion or calendar, where the elastomer is shaped. Often the products are further vulcanized, which modifies the polymer



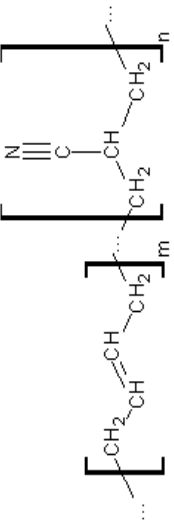
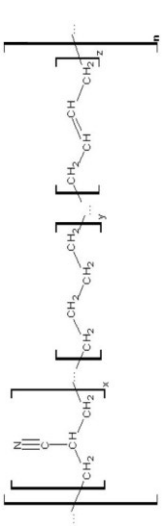
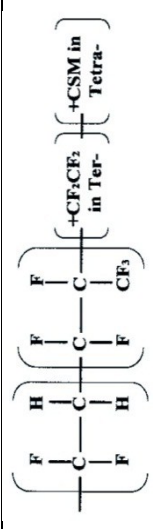
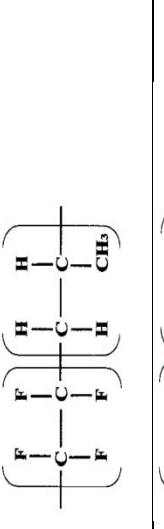
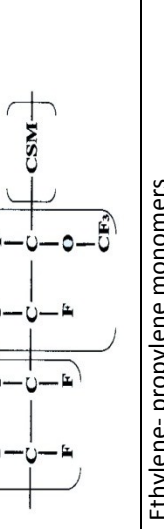
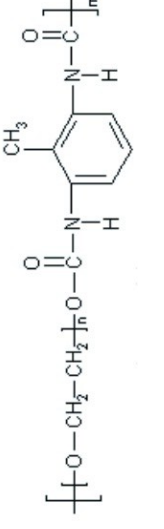
Name	Common Trade Name	Chemical Composition	Common use	General Limit [°C]	Price Factor
Nitrile Rubber (NBR)	-		Most common elastomer: Belts, hoses, O-rings, gaskets, oil seals, formed items like in mud motor, bit seals, BOP	100	1
Hydrated Nitrile Rubber (HNBR)	-		Belts, hoses, O-rings, gaskets, oil seals, formed items like in mud motor, bit seals, BOP	160	15
Fluoroelastomers (FKM)	Viton®, Dyneon™, Tecnoflon		O-rings, hoses, seals and linings	<260	20
Tetrafluoroethylene/ dipolymers, (TFE/P)	Aflas®		Cable isolation, seals	170 for steam 200 for oils	17
Perfluoroelastomer (FFKM)	Kalrez®		Seals and gaskets	275	n.a.
Ethylene propylene rubber (EPR)		Ethylene- propylene monomers	Hoses, seals and gaskets, limited due to little oil resistance	150	n.a.
Polyurethane			Various plastics, resins, thermoplastics, elastomers or thermosetting plastics: Seals, gaskets, expanding foam, fibres, coating composite materials, screens, hydrocylones	various <120	n.a.
Polyamide	Nylatron	Various polymers with an Amide-group	Various	<120	n.a.

Table 20:Frequent polymeric materials in the oilfield

The given table shows only a view elastomeric and a polymer compounds, which seemed to be of special importance for the actual study. On the complete well-site, however, many more types of polymers find employment.

It can be observed that elastomers and other polymer material are available over a broad temperature range, from below zero up to +327°C. Nevertheless, none of the materials comprises the whole range with acceptable properties. Thus, in practice a separation between normal and high-temperature components has to be established (in the field usually indicated by the color), which causes operational and logistic problems.

Beside the above mentioned products also composite materials find application, where elastomers are mixed with fabric, plastic or metal. [78], [79]

A completely different issue represent polymers as additives in cement or drilling muds. Components like cellulose, lignosulfonates or different saccharides find frequent utilization in fluid mixtures. Nevertheless, the many existing additives consist of different materials with different properties and cannot be summarized in general. The effect of polymers in the fluid and the temperature limits will be discussed in the next chapter.

### 3.2.1 Effects on drilling equipment

For drill string and the circulation system tools mostly elastomer components as well as various polyurethanes, Nylatron and Teflon are used due to their beneficial properties. For bits, mud-motor stators, jars, MWD/LWD tools, wire-line logging tools, BOPs, diverters, screens, hydrocyclones, pumps, various connections, hoses, top drives and so forth these components are important, due to the necessary sealing abilities. With temperature a deterioration of the properties can be observed. As an example the set resistance is shown, which describes ability of rubber to return to its original thickness after prolonged compressive stresses at a given temperature and deflection.

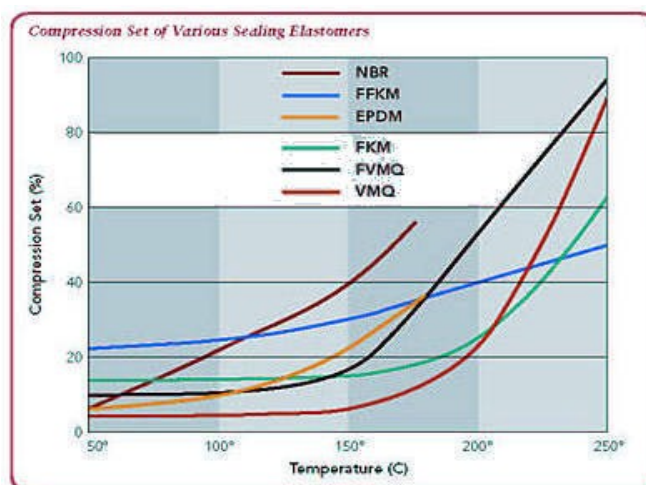


**Fig.56:** Temperature dependence of compression set [76]

The appropriate selection for a seal must be made according to the faced temperature during the usage as well as the maximum differential pressures and the fluids faced. The mechanical properties and the stability must be granted through all temperature fluctuations the component is confronted with. Degradation can generally not be avoided, as polymers represent consumption equipment. With time the elastomers generally become stiffer and porous, lose their elastic properties and become hard and brittle. This is especially the case at elevated temperatures. A combination of high temperatures and mechanical stresses causes swelling or shrinkage of the polymer element. This comes from the increased absorption of chemicals and fluids or an extraction of soluble ingredients. An optimisation regarding seal lifetime is always beneficial, if not mandatory for safety. <sup>[81], [82], [80], [83]</sup>

While static seals can be made out of elastomer materials as well as of polymers like Teflon, Urethane or even metal sealing components, dynamic seals represent a more delicate problem. Thus in down-hole motors or BOPs especially NBR or HNBR find application.

#### Drilling bits

For drilling bits temperature at bits is a concern for roller cone bits. Sealing of the bearing lubrication, the grease reservoir and the O-rings at the nozzles contain elastomers and are can be an issues at high temperatures. The temperature limits for standard roller cone bits are around 150°C (300°F), above that high temperature bits have to be used with the appropriate elastomer compounds.

The bit sealing assembly contains O-ring or, for newer equipment a shaped, bi-material sealing. For simple O-ring seals a polymer ring is fit in shaped glands in the axis where it is set. A bi-material seal ring consists of two parts, an energizer and a wearing resistant part. The purpose of the energiser is to push the wear resistant part with a certain force onto the moving shaft of the cone. The energizer is made out of a high entopic, softer elastomer to provide energization and pushing force. The wear resistant layer must resist dynamic wear for long running times. It is made out of very hard elastomere, polymere fabric or in newer developments also metal.



**Fig.57:** Cross-section of a modern bi-material seal <sup>[52]</sup>

Older roller-cone bits models comprised non-sealed bearings. They had no seals and the lubrication of the bearing was conducted simply by the drilling mud. This approach

resulted in a relatively short life due to the spalling and abrasive wear of the roller balls. Nevertheless, a non-sealed bit is independent from temperature as there are no polymer components existent. Therefore unsealed-bearing drill bits are often used in geothermal drilling, where well temperatures prevent the use of any seals. <sup>[51]</sup>

The roller cone bits lubrication system comprises several connection bores and a grease reservoir. The reservoir is engineered to provide sufficient lubricant storage, displacement of the lubricant to the bearings by a small overpressure, appropriate pressure equalisation with the exterior fluids and a capacity for volume expansion of the grease due to temperature. A sophisticated rubber design is a critical issue, especially at high temperatures.

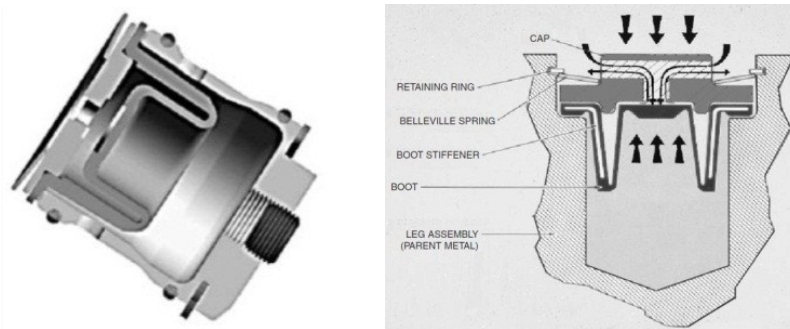


**Fig.58:** Typical roller cone bit lubrication reservoir <sup>[52]</sup>

The O-rings at the nozzle are not that critical for design, as they are static with no moving part around. They can be changed at the well-site.

Elastomers used for bit assemblies are HSN (Highly Saturated Nitrile) with an operation range of  $-40^{\circ}\text{C}$  to  $150^{\circ}\text{C}$  ( $-40^{\circ}\text{F}$  to  $300^{\circ}\text{F}$ ) and Viton (Fluorocarbon) with  $-29^{\circ}\text{C}$  to  $205^{\circ}\text{C}$  ( $-20^{\circ}\text{F}$  and  $400^{\circ}\text{F}$ ). For the total bit price, the high temperature components will only have a relatively minor influence on the price with an increase of about 5 – 10 % compared to the normal range bit.

#### Down-hole motors

For down-hole motors the presence of high temperatures is an important design consideration. The usage of positive displacement motors is very common and the large elastomeric compound in the stator can cause problems at higher temperatures. The stator provides a resistance to the fluid flow, thereby generating torque with the metal rotor. The stator is injection-moulded, with attention given to elastomer composition consistency, bond integrity and lobe profile accuracy. <sup>[77]</sup>

It is an important operational consideration that an increase in temperature can reduce the performance output of the motor, depending on elastomer type and composition. This is due to an increase in ductility of the elastomers, resulting in insufficient sealing of the cavities, fluid leaking and a decline in torque output. In the worst case, a complete wash-through (drilling fluid moves through the motor without rotating it) occurs and the motor stalls. In some cases the torque may not be sufficient for rotating PDC bits but for Roller Cone bits. In critical situations elastomer loading from flow rate and differential pressure should be minimized according to the temperature, in order to reduce the loss of life expectancy.

One important approach to reduce the negative impact of high temperature on elastomers is the introduction of *shaped stator housings* covered by a thin rubber or elastomer.

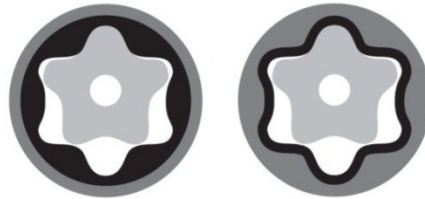


**Fig.59:** Comparison of two 5:6 stators: Full rubber (left), rubber coated (right) <sup>[77]</sup>

The reduced volume has several advantages. Firstly, the loads from the rotor are conducted to the metal of the stator housing instead of a rubber core. This prevents the rubber from strong deformation. Secondly, the thinner rubber will be less prone to induced friction from the rotor's churning action, which causes excessive heat development. This is especially a problem for two-phase drilling (air drilling), as the small heat capacity fluid cools less effectively. Rubber is a bad heat conductor and therefore the fully shaped rubber lips store much more heat than a thin rubber surface does. The developed heat is also dissipated much better by the metal.

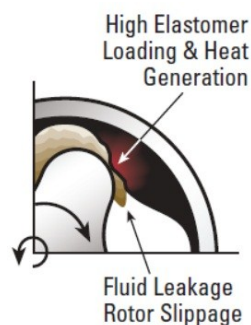


**Fig.60:** Problem areas for massive heat development in the stator rubber <sup>[77]</sup>

On one hand the movement of the rubber element is reduced, on the other one the metal housing takes the loads better, thereby increasing the torque output and preventing the rubber from deformation. Better temperature capabilities and a wider temperature spectrum for application are the consequence.

Nevertheless, the main reason for the usage of the full rubber stator is the much cheaper manufacturing price. Exact milling with tight tolerances is extremely difficult for long pieces and the prices of the component may be three to four times more expensive. Another disadvantage is that the shaped stators are more sensitive to stalling which causes rubber damages.

Finding an appropriate, temperature resistant binding element between the metal stator housing and the stator rubber is another issue. Rubber to metal binding is very difficult and it is more difficult to develop a proper glue than to manufacture the according rubber. Temperature cycling has a more deteriorating effect on the glue than on other components. A certain advantage can be seen with the shaped stator housing, as the glued surface area between rubber and metal stator is larger.

The *fit between the rotor and stator* is another essential temperature dependent parameter for maintaining efficiency and life expectancy of a mud motor. Temperature and drilling fluid type cause some swelling of the rubber elements and the correct fit has to be established according the operating conditions. On one hand a certain gap between rotor and stator is necessary to compensate for the rubber's volume expansion causing excessive pressure differentials, on the other hand a loose fit will result in a decline in efficiency.

Depending on company policy the correct fit can be accounted for with the availability of different rotor and stator sizes or by downgrading the motor by correction factors. For the first case manufacturers define certain ranges of operating temperatures applicable for the tools. Motors configured for high temperature applications will have a relatively loose fit between the rotor and stator. The reduced sealing capacity results in low running pressure and torque output at lower temperatures.

For bigger motors (8" through 11" diameter) the composition of the drilling fluid has the dominating influence, as big motors are usually not used in hot environments. For smaller motors (< 6/8" diameter) on the contrary, the temperature gets the important factor for the layout. The accurate fit for smaller motors is much more important than for big ones due to the smaller ratios and clearances. For a bigger motor a deviation of up to 1 mm in fit has a large influence but may be acceptable, for a smaller one the deviation must be much less in the range of +/- 0,2 mm.

Performance graphs of tools are usually recorded at surface conditions and with water as fluid, resulting in deviations to the down-hole conditions. As the tools are configured for down-hole conditions the maximum differential pressures and output characteristics can vary.

Suppliers of down-hole motors use *scaling factors or percentage ranges* as a guideline to define the tolerable differential pressure and flow rate according to the faced temperature. The following picture shows such a scaling factor diagram:

<b>Recommended Maximum Operating Differential Pressure for Elevated Downhole Temperature Applications</b>							
As a percentage of the operating differential for typical lower-temperature applications							
Motor Type	100 – 130° F	130 – 170° F	170 – 210° F	210 – 240° F	240 – 270° F	270 – 300° F	300 – 320° F
	38 – 54° C	54 – 77° C	77 – 99° C	99 – 116° C	116 – 132° C	132 – 149° C	149 – 160° C
Standard Service	100%	80%	65%				
Standard Service*		100%	100%	80%	65%	50%	
Special Service			100%	80%	65%	50%	
Special Service*				100%	80%	65%	50%

**Fig.61:** Scaling factors for down-hole motors <sup>[77]</sup>



It can be observed, that already below 77°C the full operation is impaired for standard motors. The scaling factors are thus used, to determine the maximum differential pressure or flow-rate of a specific motor configuration based on the given temperature. When not correctly fitted and down-rated for the faced temperatures an exponential decline of lifetime will be caused with all consequences. The down-hole operating hours for the drilling motor and tools must be adjusted accordingly for temperature. Also the decline of lifetime with the cyclic thermal load must be respected.

Several other components include elastomers, like various seals in Circulating Subs (a hydraulically actuated valve located at the top of the drilling motor to allow the drill string to fill when running in hole and drain when tripping out), Float Valves (run above the motor and prevents drilling fluid from flowing back into the motor and thereby keeping the cuttings out of the motor) the bearings, depending whether they are drilling fluid-lubricated or sealed oil-lubricated, in the transmission unit as well as in the electronics and steering systems for the more advanced RSS tools. However, these parts should be tuned accordingly by the provider and should not be of consideration in the direct drilling process.

The successful use of the elastomer component depends on its ability to maintain efficient and effective sealing with loads for sufficiently long periods of time. Nitrile elastomers (NBR) are used most frequently, due to the beneficial properties of chemical and abrasion resistance while maintaining acceptable mechanical properties (temperature range 98 -121°C). For higher temperatures HBNR rubber is used, which has a temperature range of 121 – 160°C.

For higher temperatures, up to 300°C, turbine motors can be used, as there are no dynamic seals causing temperature limits. The rotation of a turbo-drill is derived from the interaction of the drilling fluid and the multiple stages of turbine blades. The rotational speed and torque is directly related to the fluid velocity. Turbine motors offer higher rotation speeds and the flow can always be maintained, independent from the torque and bit RPM. The major disadvantages of this type of motors are the limited use of roller cone bits (high speeds), the requirement of large flow pumping volumes, the low efficiency, the low starting torque, the inability to obtain whether the motor is working efficiently, the motor's particle sensitivity and the length. Also a much higher price and limited availability represent a drawback. <sup>[84], [26]</sup>

#### Mud cleaning equipment

*Shale shaker* screens' clothing, bonding layers and bedding rubbers (stinger protectors) cause concerns for high temperature returns. The screen clothing can be made out of metal wires, synthetic polymer wires or molded-one-piece polymer cloth. The bonding layers are made of elastomers between the screens to keep them grounded. The single screens layers are further glued together with synthetic glue, which represents another weak point and must be engineered accordingly. The bedding rubbers avoid a metal to metal collision with the shaker frame.

Most commonly the polyurethane, fluoroelastomers (FKM, FFKM), NBR or NR are used. Standard screen cloths are capable for temperatures up to around 55°C. High temperature screens can be used until 110°C. Compared to the standard screens the high temperature versions are said to be about 20% more expensive.



**Fig.62:** Bed material probes (left) and stinger protector probes (right) with allowed temperatures

*Hydrocyclones* are stable to a temperature of around 80°C. The body consists usually of a polyurethane polymer, because it is comparatively resistant against wear from the accelerated sand and silt particles at a reasonable price. Above the temperature limit the polyurethane component will get flexible and can tend to change its shape with applied fluid loads. This will not only hinder the cyclone of working properly but may also be dangerous as the body can fall out of the holding clamp and hot mud will spill under pressure. As hazardous mud temperatures are usually reached only for deep sections, high temperature equipment is usually not installed. When the hole diameter is sufficiently small, cleaning is done by a combination of fine screens and centrifuges. High temperature rated hydrocyclones did not prove economical. Nevertheless, in high temperature geothermal drilling this approach can potentially cause problems.

*Centrifuges* are dimensioned according to general mechanical engineering for operation up to 80°C. Nevertheless, operating capabilities should be confirmed by the manufacturer, if a centrifuge is useful for higher temperatures than 40°C. Higher temperatures can result in design problems with axis elongation, seals and greases. Centrifuges capable of higher temperatures are usually made of high quality steel against

corrosion. An additional price of about 20% was assumed due to more expensive material plus more expensive manufacturing costs.

### Surface installations

For *mud pumps* temperature limits depend on the rubber parts of the seals and pistons. Depending on the material used the standard temperature limit is around 80°C. Furthermore, at temperatures over 66°C (150°F) critical suction problems can occur. The increased vapor pressure with temperature can cause a boiling of the mud, thus decreasing pump efficiency as well as causing additional wear (vapor pressure of water: 2,3 kPa at 20°C and 47,3 kPa at 80°C). A properly designed pre-charge pump is mandatory. Many mud pumps rated for high temperatures also often have heat exchangers installed on the liner back wash, in order to minimize heat damage of liner and piston and increase lifetime.

The heat generated by the pump from hydraulic energy was discussed in the previous chapter. When assuming a pumping efficiency of 0,9 the waste heat generated here can be calculated with:

$$dT = \frac{P_s * (1 - \mu)}{c_p * q * \rho} = \frac{441 \text{ kW} * (1 - 0,9)}{4,181 \text{ kJ/kg.K} * 0,033 \text{ m}^3/\text{s} * 0,998 \text{ kg/m}^3} = 0,32^\circ\text{C}$$

#### **Equation 21:**

dT= Temperature rise in the pump [K]

q = Volume flow [m<sup>3</sup>/s]

P<sub>s</sub> = Brake power [kW]

c<sub>p</sub> = Mud heat capacity [kJ/kg.K]

The maximum output capability of one single mud pump available on the rig side was assumed. Further the total amount of pressure loss at the surface pipe installations was measured to be around 5 bar. With the formulas from the last chapter a temperature increase of the mud of 0,1°C is caused. As can be seen the heat developed on the surface is marginal and amounts to around 0,4°C, neglecting heat losses from pipes.

Pulsation dampeners also contain elastomers within the in the pressured housig. Temperature limits are generally also around 80°C

*BOPs* will probably represent the most important concern for safety, when dealing with high temperatures. It has been argued in the literature, that the actual temperature limit at the elastomer compounds will hardly ever be reached, especially and obviously during the BOP operation. Nevertheless, the proper function of this equipment is mandatory and the limits are taken serious through the industry.

The exact mixture of the elastomeric compound of the BOP depends on the type, the pressure rating, the chemical environment and the faced temperature. Generally natural rubber (NR) is used for water based drilling muds, having a temperature limit of around 100°C. For oil based muds, due to swelling of NR, nitrile rubber elastomers (NBR) have to be used. Here the usual temperature limit lies at around 82°C. For high temperature equipment BOP elastomers are a considerable price driver, as the price is usually doubled. Of course also the according valves have to be modified according to the operation environment.

*Surface Valves*, like butterfly-valves, ball-valves or gate-valves, contain various rubber elements such as NR, NBR, Nylatron or Viton. Usual temperature ranges are 120°C, but this is very dependent on the type of components. They are regulated by various API specifications (API 6A). Generally, for valves temperature resistant greases are the bigger cost driver.<sup>[81]</sup>

Due to the high pressures present in *mud hoses*, they are usually made out of a multi-layered polymer-fabric compound. NB-Rubber is frequently used as the core material. The manufacturing is demanding, thus resulting in high prices. Temperature limitations are around 85-100°C for standard hoses.

#### Rig components

Further analysis for *DrillTec GUT GmbH's rigs* was conducted to find temperature sensitive points in the circulating system. Generally the layout of the rigs is conducted for a maximum surface temperature of 80°C. When facing higher flow-line temperatures many elastomeric components suffer from faster degradation and need to be revised more frequently. The investigated components (see subsequent table) have different temperature limits, thus improvement and cost estimate should be based on the knowledge of the exact potential flow-line temperature with an additional safety margin.

Nevertheless, most components have a fairly small impact on the overall cost of a drilling operation. Most seals are mass-produced goods, thus having hardly value themselves, but rather causing an additional logistic and engineering effort.

The total value of the rig's equipment, which can be reasonably influenced by temperature limitations, is roughly 250 000 Euros. This amount is only reached, when temperatures of up to 107°C would be observed, which should be avoided anyway. The following diagram shows the different cost drivers arranged by importance:

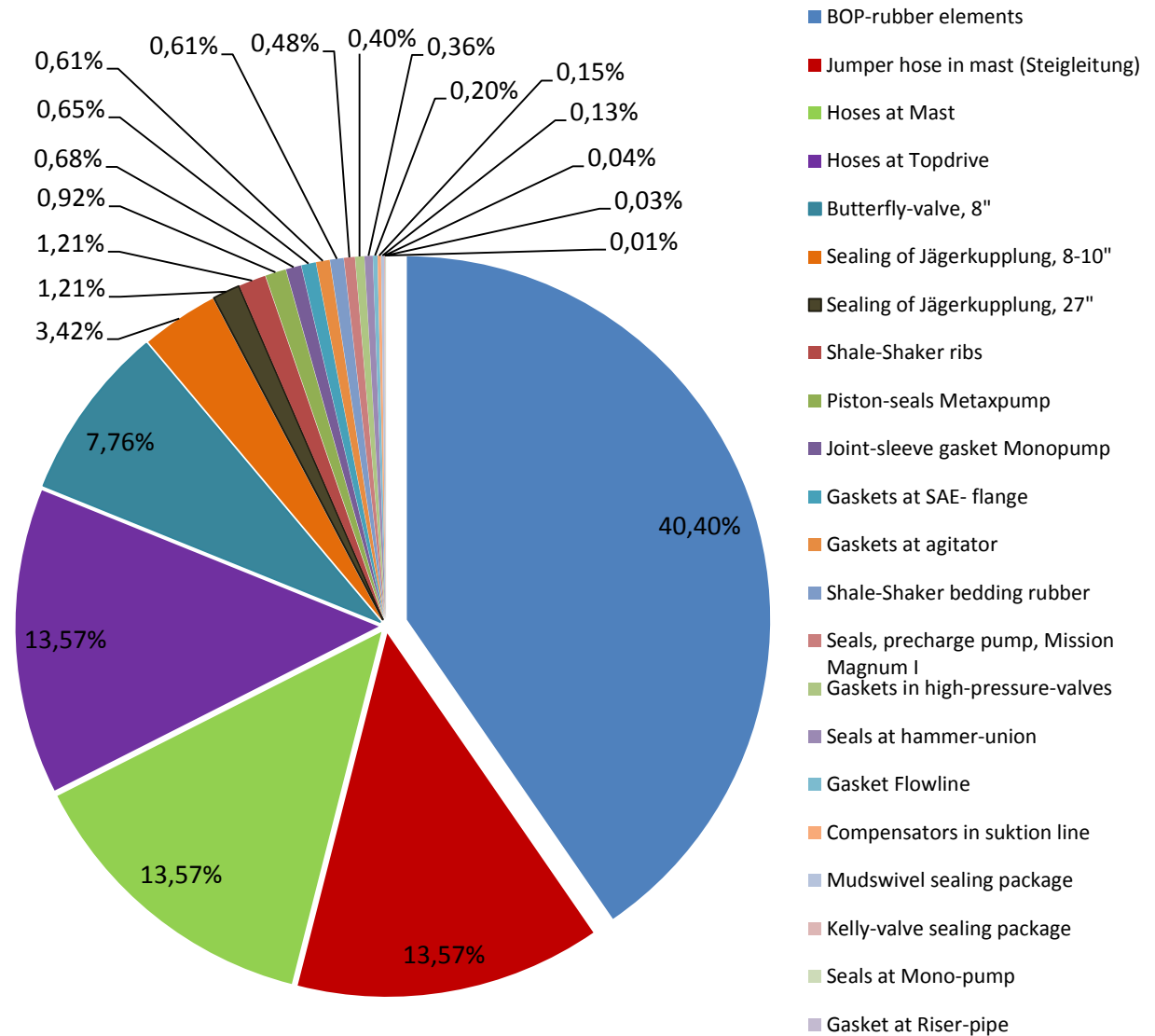


**Fig.63:** Cost drivers for the reconfiguration of the rig

Generally, the rig is very well configured for higher temperatures. When facing temperatures up to 85°C no expensive modifications are needed. The various mud hoses represent a serious price driver at 85-90°C. Various gaskets, seals and shale shaker screen cause further expenses in the same region. At a temperature of 88-107°C (depending on the mud system) the BOP causes the biggest single price driver.

Thus, reconfiguration to avoid fast degradation or failure is only reasonable, when drilling for long terms in high temperature geothermal areas without any cooling equipment.

Component Type	Component Name	Component Material	Provider	Temperature Limit [°C]	Cost [€/piece]	Amount	Description
Agitation System, seal	Dichtungen Rührwerke	n.a.	Flygt	n.a.	n.a.	3	Seals at agitation system
Pre-charge Pump, seal	Dichtungen, Ladepumpen Mission Magnum I	Graphitdichtung	Mission Magnum I	300	100	6	Seal at precharge pump
Mono pump, seals	Dichtungen Monopumpe	Perbunan		80	100	2	Seal at mono pump cylinder
Mono pump, joint boot	Gelenkmanschette Monopumpe	Perbunan		80	421	4	Joint boot of pump from sand trap to centrifuge
Butterfly valve, seal	Butterflyschieber 8"	NBR	End Armaturen	85	600	32	Seals for butterfly valves between mud tanks
Expansion joint	Kompensatoren in Saugleitung	n.a.		80	377	8	Connection joint
Gasket	Dichtungen Schlagkupplungen	Viton, NBR		160, 95	45	20	Seals at surface flowline connections
Gasket	Dichtungen Jägerkupplungen 27"	NBR		90	1500	2	Seals for fast connection between tanks
Gasket	Dichtungen Jägerkupplungen 8-10"	NBR		90	565	15	Seals for fast connection between tanks
Seals	Dichtungen in Hochdruckschiebern	NBR	Hydril, NOV	80	100	10	Valves after mud pump and at standpipe
Metax-pump Seal	Dichtungen Hochdruckkolben Metaxp.	Ecopur, Nylatron	NOV	90	380	6	Seals at mud pump (1x splitter, 1x crosshead, 1x Cylinder, 2x valve)
Jumper hose	Jumper hose in Steigleitung	n.a.		n.a.	5600	6	Flexible hose from pump to manifold and from standpipe and drilling rig.

Mud-hose	Mudschläuche am Mast	Ecopur, Nylatron		91 / 85	5600	6	Connecting hoses at the mast
Mud-hose	Mudschläuche am Topdrive	Ecopur, Nylatron		91 / 85	5600	6	Connecting hoses for top drive
Gasket	Dichtungen an SAE-Flansche	Ecopur		90 / 85		32	Connections for high pressure hoses
Gasket	Mudswivel Dichtungspaket	Ecopur, Nylatron		90 / 85	80	4	Sealing ring at swivel of top drive
Gasket	Kellyhahn Dichtungspaket	Ecopur, Nylatron		90 / 85	40	2	Sealing of the ball valves around the top dive
Shale shaker, component	Siebträger	NBR, HNBR	Derrick	55, 110	500	3	Shale shaker stinger protector
Shale shaker, component	Rippen von Shaker	NBR, HNBR	Derrick	55, 110	1000	3	Shale shaker bed material, new screen necessary when limits reached
Polyurethane foam	Abdichtung Flowline	Polyurethane	Würth	80	minor	-	Sealing between bell nipple and flow-line
Gasket	Flanschdichtung Riserrohr	NBR		85	10	1-3	Squeezed flat gasket above BOP connections
BOP Seal	Preventer-Seals	NR (for water based), NBR (for oil based)	T3	107/ 88	100 000	1	Seals at BOP (1x Donut seal for annular preventer, 4x seals for rams)
<b>Total Cost if reaching surface temperatures above 85°C :</b>					<b>130 830 €</b>		
<b>Total Cost if reaching surface temperatures above 90°C, also including BOP rubber change:</b>					<b>244 585 €</b>		

Table 21: Temperature sensitive elastomeric components of the DrillTec rigs

## 3.3 Fluids

### 3.3.1 Drilling mud

The effect on properties and the degradation of drilling fluids with temperature is considered as one of the main problems with high temperature drilling applications. Care must be taken to maintain the desired rheology, the filtration properties, the inhibition and the hydraulics in the system.

There are different programs in the market which estimate the according temperatures and furthermore simulate the complete wellbore hydraulics. Nevertheless, accurate FAN rheometer reading values must be provided or general approximations will be used by the programmes. At wells exceeding the temperature of 120°C additionally mud properties are observed by a HPHT test with a FAN 75.

Temperature limits for the mud system should be designed in advance according to the expected temperatures. Excessive temperatures in the mud may have one or more of the following consequences:

- Rheology problems may occur as additives and solids behave different at elevated temperatures. Muds may thicken or thin with temperature.
- The speed of chemical reactions in the mud is increased. Dispersion of solids is increased with temperature.
- Degradation of additives and loss of their effect. The breakdown of the mud may result in precipitation of solid materials and a low viscosity. (e.g. XCD with low PH or guar gum at 120-130°C).
- The common problem resulting from rheology changes are insufficient hole cleaning caused by poor solid transport. This further leads to a reduced ROP and problems with bit balling, stuck pipe and tight holes. A lower fluid density at the lower part of the annulus where the mud solids get precipitated may result in insufficient weight, an imbalance in the mud system and the potential of a kick.
- In some cases increased interaction between the molecules and a crosslinking action may lead to a high viscosity (e.g. XCD at high PH values). It was reported that viscosity can be so high, that even a liner cannot be run in hole any more.
- A large fall-out of water may occur (e.g. CMC at high temperatures). This leads to a directly proportional amount of solids staying in the annulus and thick filter cakes tend to occur, resulting in differential sticking.
- Water/oil vaporises at surface. This effects some cooling of the mud which is positive. But as a negative consequence care must be taken to maintain the fluid mixture and add the vaporised losses. For oil based muds for example a reverse-osmosis may occur, in which an excessive amount of inhibiting CaCl in the water may dry out shale formations and cause cavings.
- Decrease of lifetime of the down-hole components due to high temperatures. Cooling of the tools is a problem at excessive temperatures. As mentioned corrosion rates increase and corrosion inhibition works less effective. Oil based muds tend to react and degenerate the elastomer components.



- Decrease of lifetime of the surface components. Increased corrosion deteriorates metal components due to aggressive vapour present. Damage to the mud-pump occurs due to the vaporisation in the piston and a resulting clanking.
- Unhealthy vapours on the surface are an HSE issue. Especially oil based muds with larger amounts of highly toxic aromatic hydrocarbons must be treated carefully. The flashpoint of an oil based mud is generally required to be 82°C (180°F) and therefore must be considered at higher temperatures. Sometimes closed tanks are used but as the cooling is minimal there a mud cooler has to be used.

The rheology of drilling mud changes severely in the mud cycle and down-hole rheology differs from surface rheology. While viscosity reaches a minimum at the high temperatures in the lower part of the annulus it increases again when mud is cooled at the surface.

When considering the Bingham Plastic Model generally plastic viscosity decreases with increasing temperature. The Yield Point may increase or decrease with increasing temperature depending upon the solid content of the fluid. Thus, the power-law index (n) generally decreases with increasing temperature, and consistency index (K) generally increases with increasing temperature.

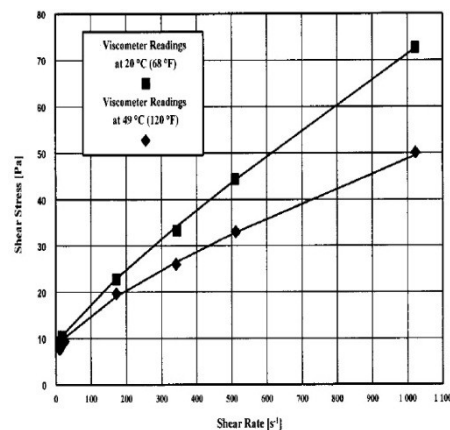


**Fig.64:** Rheological behavior „shear stress vs. shear rate... of the drilling mud at two different temperatures (20 and 49°C)... tested at the viscometer<sup>[95]</sup>

Different companies have developed mud systems that are suitable for elevated temperatures. Several years ago high temperature applications often recommended the usage of oil based muds to maintain the desired parameters sufficiently. The problem with these systems is the environmental issue and the accordingly high disposal costs. The technology for water based mud systems has improved in recent years. The new generation of water based muds is also applicable at temperatures higher than 200°C.

The biggest disparities for temperature come from the base fluid. As mentioned in the previous chapter water has a much higher heat capacity than oil, thus causing different temperature profiles. Water based mud is environmentally friendly and offers easy mud handling. The disadvantages are excessive cost at temperatures >160°C (caused by Fromat additives), bad and instable mud properties, low lubricity and lower inhibition compared to oil based muds. Mud additives are said to have a negligible impact on the heat capacity, though hematite should be considered in the calculation.

Oil based muds offer high temperature stabilities and they are easier to control and maintain. They have comparatively low filtration values, high lubricity, a low kinematic viscosity and therefore low ECD and offer excellent inhibition to shales. Their common disadvantages are the higher costs (around 10 times higher) and the environmental issues. Nevertheless, for high temperatures they may be a reasonable alternative.

The various different types of additives for the mud system show very different dependence on temperature. Suppliers usually provide temperature-limits for their products, which can be used as a guideline. Nevertheless, in reality there is no sharp temperature boundary for mud components but a temperature band, in which the effectiveness given by the various additives decreases.<sup>[56]</sup> Preparing the appropriate mud is more of a trial and error process. Mud properties are watched carefully and if necessary an according additive is added. Depending on the reaction of the system another additive has to be used. The following temperature ranges could be found:

The presence of bacteria may be a problem up to 100°C. As bacteria develop more rapidly under elevated temperatures and pressure the complete mud system can be degraded in a matter of hours.

A first obstacle can be defined at 100°C for simple mud containing bentonite or bentonite and salt. Bentonite has a higher tendency to flocculate at higher temperatures, which creates excessive viscosity and consequently high ECD's. Deflocculants (=thinner) (polymer deflocculants, dispersants like lignosulfonates, lignite or Leonardite) can be simply used to solve such problems. The application of polymer deflocculants is limited to 120-150°C. Due to the higher demand of additive for higher temperatures also the initial costs of the drilling mud will increase. An according planning of the mud system is essential. Another negative aspect of the usage of deflocculants are the heavy metals they contain (Chrome etc.), which is a HSE problem and results in higher deposition costs.<sup>[61]</sup>

A first real boarder-line can be defined at a mud temperature of around 120°C, depending on the mixture chemistry present. Until this temperature a well can be drilled with standard products with reasonable care and optimisation from the mud engineer.

At higher temperatures especially polymer additives are affected from degradation. Fluid loss additives, viscosifiers, shale inhibitors, flocculation control and some lost circulation materials (e.g. xanthan gum, starch, poly anionic cellulose (PAC), carboxymethyl cellulose (CMC) ) are affected. The quality of manufacturing of the polymer additive hereby affects the temperature resistance. As indicated previously, the arrangement of the monomers as well as chain length and type of atomic bounding is determining the stability.

Oxygen scavenger may further increase the limit for some degrees, as they avoid a reaction and degradation with oxygen. The most common one is sodium sulphite (about 1kg/m<sup>3</sup> is needed). In relation with high temperature stability the PH-value has a big impact on polymers. It should be kept in a basic domain between PH 8 – 10,5.

The second major temperature limit is reached at approximately 150°C, because most temperature extended products breaks down after exceeding this temperature (e.g.

Polysaccharide). Once this temperature is exceeded, “tuned” standard mud components are not applicable anymore and higher quality additives are necessary. This consequently causes an increase in price.

The thermally degraded polymer additives have no great direct chemical effect on the mud. They attach to cuttings and get cleaned out of the system in the mud cleaning equipment with time. However, an increase in low-gravity solids content, rheological and filtration properties can be observed. The latter comes from the development of CO<sub>2</sub> during the degradation of polymers. This in turn degrades carbonate additives and therefore affects the filtration values negatively. Potential formation damage is the consequence. <sup>[59]</sup>

An exception to the stated temperature boundaries can be achieved with the usage of various formates (Sodium-, Calcium- and Cesium-formate). Formates can further stabilize polymer products. They stabilize the monomer binding as it acts as a protective colloid. This is done by scavenging destructive free radicals which are involved in oxidative degradation processes at elevated temperatures. The big disadvantage with the usage of formates is their high price and a low resulting lubricity. <sup>[57], [59]</sup>

As a general statement, a temperature up to 180°C is controllable with the current fluid technology available. The temperature of 220°C was indicated to represent an absolute maximum and is very difficult to handle. From these temperatures onward different approaches have to be found for the mud system and drilling with pure water may be the only chance.

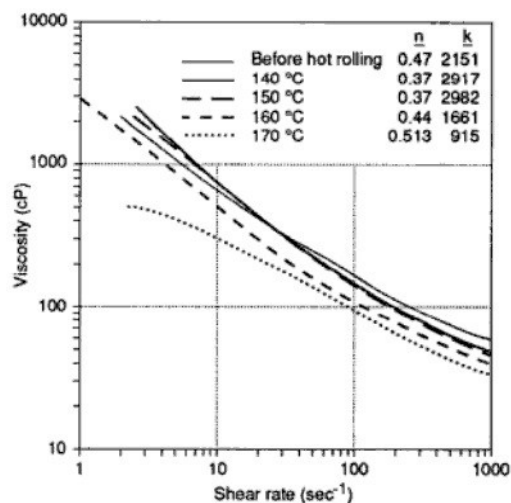


**Fig.65:** Example of the rheology of xanthan in sodium formate brine at different temperatures <sup>[58]</sup>

Recently developed additives do exceed the temperature limits of standard muds by far, but also suffer from limitations. For example the fluid loss control agent Vinylamid is a copolymer offered by several companies under different names (Halliburton: Hostadril). The product is stable up to 205°C. Nevertheless, the additive needs a small amount of Bentonite (15-20 kg/m<sup>3</sup>) present in the mud for its functionality. This causes a high skin effect, which must be cleaned subsequently. An alternative to Vinylamid would just be the usage of oil based mud. <sup>[56]</sup>

Additives like non-polymer lost circulation materials or weighting agents are not affected by high temperature.

Since synthetic based drilling fluids are reported to be more sensitive to temperature and pressure than any other type of drilling fluid. Muds containing ester are reported to get unstable starting from 100°C with a sharp decline of properties at around 150°C. The values are even faster deteriorated at high PH-values. <sup>[60]</sup>

Oil based muds are more stable at higher temperatures and have a temperature limitation of 250 – 280°C. In contrast to their high price, additional price increases with high temperatures were mentioned to be low, so that the price is more constant with temperature.

As mentioned in an earlier chapter, the correct measurement of the PH-value for the drilling mud is also subjected to temperature. On one hand the electronic measuring devices need a correction for the actual temperatures, on the other the PH-value itself depending on the present temperature and chemistry. For high temperatures no common standards exist for measuring.

The impact of the temperature boundaries determined above is evident when looking at the mud prices. Generally there are huge differences between standard and high temperature materials, which can be up to 10 times more expensive. A part of this increase comes from the required development and production efforts of the components, as well as the low availability of additives especially at very high temperatures. Furthermore the markets demand is not too high, resulting in high prices for adequate payback. The following graph shows an approximative evolution for mud price with temperature for various data gathered.

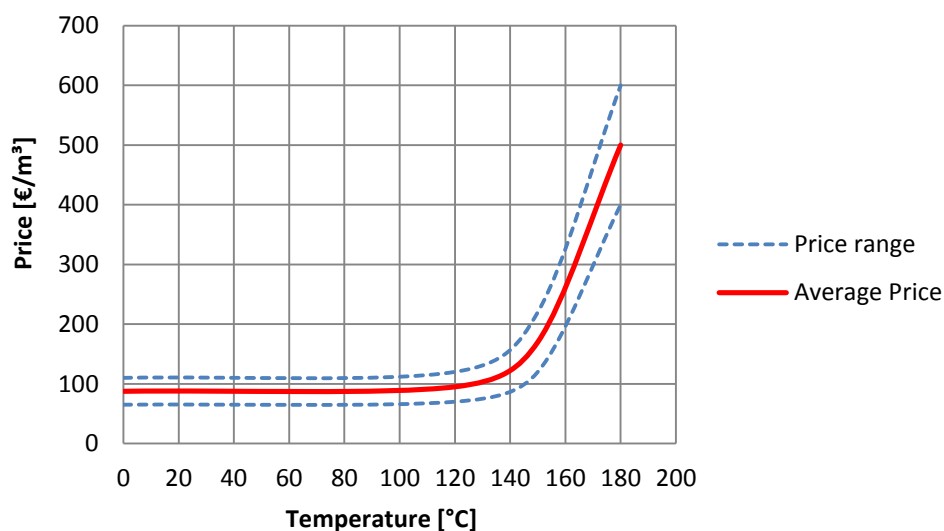


**Fig.66:** Price development with temperature for inhibited KCl water based systems

As shown price data was found for inhibited (KCl) water based systems with a specific gravity smaller than 1,2 kg/lit. The given price development links with the mentioned additives' temperature problems with standard prices up to 120°C, a slight increase increases from 120°C onwards and excessive price increases from 150°C onward. A list of some common additives and their limitations found in the literature is presented in the Appendix.

However, for operators higher costs for mud are often justified when taking into account the overall costs and the daily costs of a project. Comparatively small savings on the mud system may lead to expensive follow up problems when underestimating the effects of temperature.

Depending on the well plan it is often beneficial to use the expensive additives already at the beginning. A loss of the low price additives due to heat may be prevented and also a reduction in transports and storage cost may be reached on the well site. However, the given situation varies with every well and with every mud system, so that no general rules can be formulated. The application of such ideas is depended on company policy and is also a question of gained experience and know-how.

There are also aspects from the operational point of view, as working safety with hot mud present and lifetime reduction of surface equipment.

### 3.3.2 Cement

Due to the many parameters affecting and interacting in cement slurry, the proper mixture is often referred to as an art, rather than a science. Changes in temperature will have significant impact on well cements physical and chemical behavior, cement mixture chemistry, phase development, rheology, setting time, set strength and strength retrogression. Nevertheless, it is not usual nowadays to decide only based on temperature data as other effects like pressure, alkalinity or salinity of brine have an interacting influence.

One problem in determining general statements for cement mixtures regarding temperature limits is the large bandwidth of available materials and their chemistry. Consequently the influence of temperature varies with each component in the system. Many of the materials used are not specified by API and usage depends on regional experience and cheap availability. In Germany for example about 30-40% of the cements used are not certified by API but by EN and DIN. High Manganese Resistance cement, a cheap mixture of furnace cement, flying ash and saltwater supported by available regional experience, is an example of an cheap, alternative cement composition, also used for geothermal wells in Germany.

For wells, where no regional experience from cement providers exist or where operators have no experience and try to mitigate risk, the generally more expensive API cements are used. In Europe API class A,C,G & H are used, depending very much on the closest certified provider. The latter two classes are more suitable for higher temperatures. Portland cement is always the base material and additives are added according to experience.

Two important effects of high temperature environments on cement are a decreased thickening time, strength buildup and strength retrogression. The very popular API thickening time schedule often over- or under-estimates the true temperature.

Portland cement consists principally of four compounds: tricalcium silicate ( $\text{Ca}_2\text{SiO}_5 = \text{C}_3\text{S}$ ;  $\approx 70\%$ ), dicalcium silicate ( $\text{C}_2\text{S}$ ;  $< 20\%$ ), tricalcium aluminate ( $\text{C}_2\text{A}$ ) and tetracalcium aluminoferrite ( $\text{C}_2\text{AF}$ ). The first two are the most abundant, and when adding water they hydrate and form gelatinous calcium silicate hydrate (C-S-H-Gel). This is responsible for the strength and dimensional stability of the set cement. Furthermore also calcium hydroxide (lime) is formed (it has no strength contribution). The hydration of the alluminate phases is mainly important in short times and therefore affects rheology and early strength of the cement.

The hydration rate of the cement and the nature, stability and morphology of the hydration products are strongly dependent on temperature. At higher temperatures the rate of hydration during the early setting period is much higher and the duration of the induction and setting periods is shortened. However, for longer times the degree of hydration and thereby ultimate compressive strength are often reduced. This can be seen in the graph of the calorimeter analysis on the left.

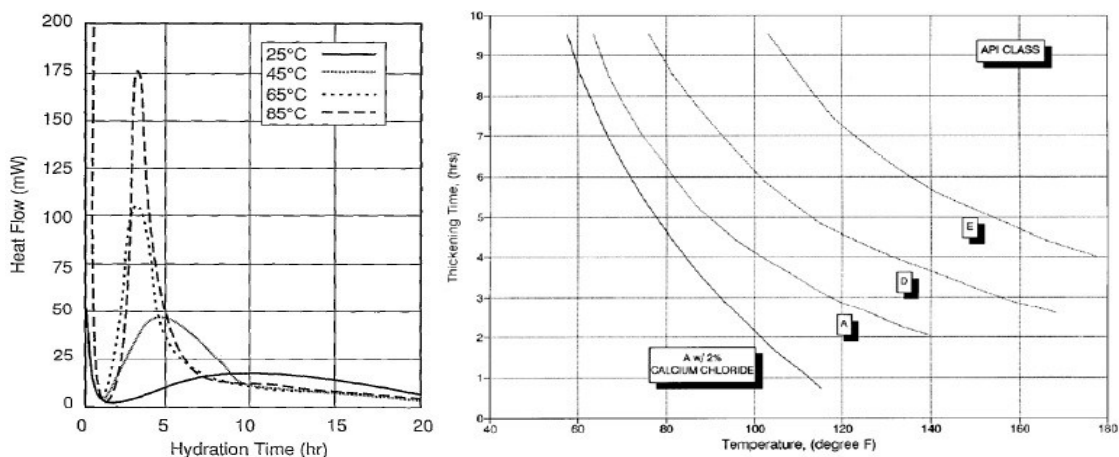


**Fig.67:** Effect of temperature on hydration time on Class G Portland cement observed in a calorimeter <sup>[53]</sup> (right), Effects of Temperature on thickening time <sup>[55]</sup>

Up to 40°C the hydration products are the same as those which occur at ambient conditions. Changes occur in the microstructure and morphology of the C-S-H-Gel at higher temperatures as the material becomes more fibrous and individualized and a higher degree of silicate polymerization is observed. At curing temperatures higher than about 110°C the C-S-H-Gel is no longer stable and crystalline calcium silicate hydrates are formed. This phase is much denser and thus responsible for an increase in permeability and for a decrease of compressive strength, called strength retrogression. The higher dissolution rates of lime with water at higher temperatures further deteriorates the cement quality.

The problem with strength retrogression can be avoided by adding 30 to 50% of silica (BWOC) as flour or fine sand at higher temperatures than around 110°C. The addition of silica increases the bulk lime-to-silica ratio and therefore prevents the formation of undesired phases. As can be seen in the picture below the mole ratio should be around

less or equal 1.0. Phases like Tobermorite ( $C_5S_6H_5$ ), Xonotlite ( $C_6S_6H$ ) and Gyrolite ( $C_6S_3H_2$ ) maintain good strength and low permeability values, sometimes up to 400°C.

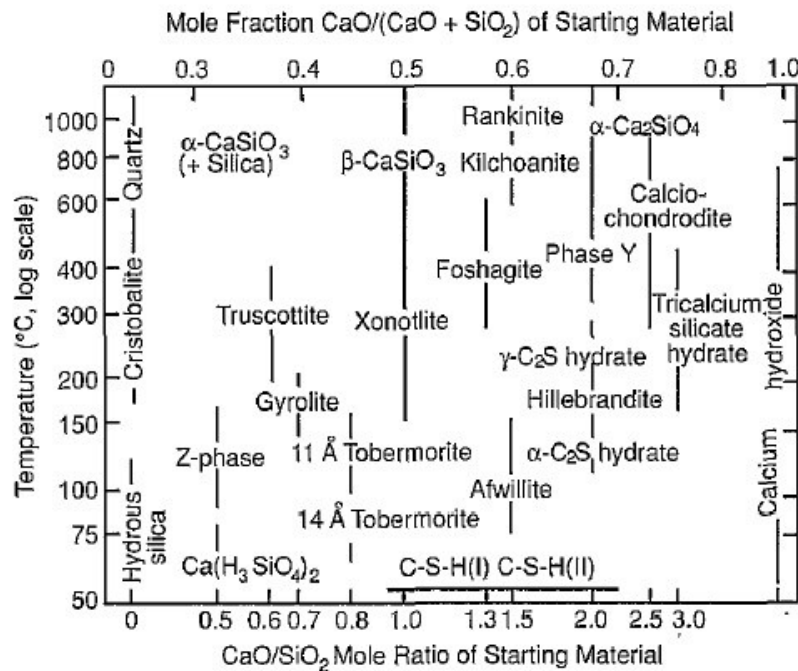


**Fig.68:** Cement phases for various lime to silica ratios at different temperatures <sup>[53]</sup>

Cement additives can be subdivided in several groups which are: Filtration control additives, loss of circulation control additives, specific weight control additives, thickening and setting time control additives, viscosity control additives and special problems control additives. In general, additives which are not chemically reactive with the cement and which require a high water to cement ratio produce a cement of poor temperature stability. <sup>[55]</sup> Similar to the drilling mud additives polymeric components (fluid loss, emulsifiers, retarders,...) cause problems due to degradation, starting at around 120°C. In a cement mixture with many different additives the chance for chemical interaction raises and is strongly depending on the present temperature.

For *retarders* temperature is a big issue, as it determines the type and amount of additive. It is critical that the cement is sufficiently long, but not too long, pumpable. Lignosulfonates are commonly used and have a temperature limit of up to 122°C. With modification by certain acids a temperature of 150°C can be reached and by adding sodium borate it can be reliable up to 315°C. In mixture several retarders can have a higher temperature reliability than a separate one. Some high temperature retarders start retarding only at high temperatures. Generally speaking, the higher the temperature is the more complicated the choice of the retarder gets. The correct selection depends not only on the actual temperature limitation, but also on the influence on the setting process. The time to reach ultimate strength depends on temperature and chosen retarder. In the following hypothetical graph retarder one will be more economic as he reaches ultimate strength faster.

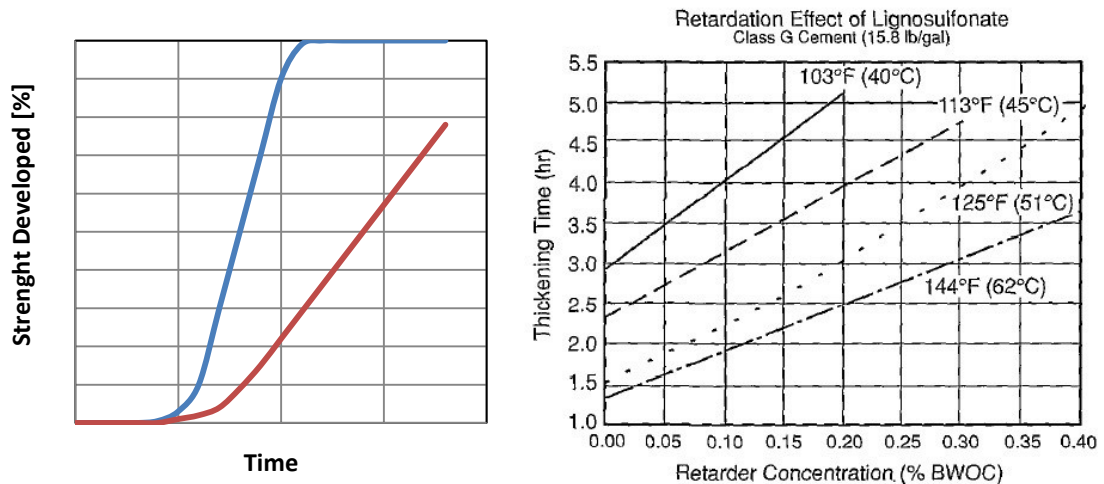


**Fig.69:** Hypothetical graph to show the influence of the retarder selection (left), Retardation of lignosulfonates at different Temperatures (right) <sup>[53]</sup>

Sodium Chloride can act as an accelerator as well as a retarder, depending on concentration and temperature environment. Calcium Chloride is very commonly used as an *accelerator* though it has various side effects on cement such as increased hydration heat generation (up to 27 to 33°C after slurry placement, thus steel movement causes micro-annuli). Gypsum can also be used as an accelerator at lower temperatures. (60-83°C).

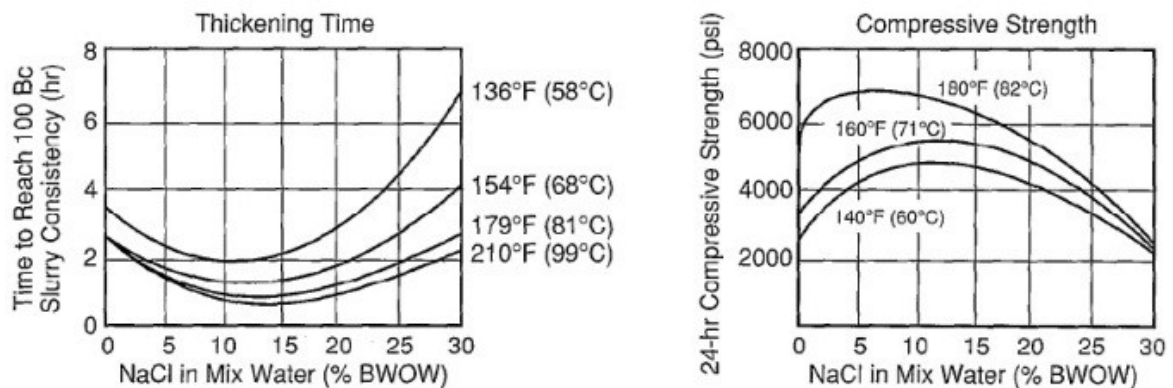


**Fig.70:** Effect of sodium chloride on thickening time and compressive strength/development of cement [53]

A common and cheap *weight control* agent is bentonite, which needs water addition and thereby decreases specific weight of the slurry. Generally this approach results in worse cement properties with reduced compressive strength and thickening time. At temperatures higher than 93°C (200°F), the bentonite additive promotes strength retrogression in cements with time. Other important agents for extending are Pozzolans (Silicious or siliceous and aluminous material: fly ashes, volcanic ashes and diatomaceous earth), which have various temperature efficiencies and limitations. Gilsonite, a naturally occurring asphaltite mineral, is a light weight material as well as a fluid loss additive, but should not be used above 150°C as it starts softening there.



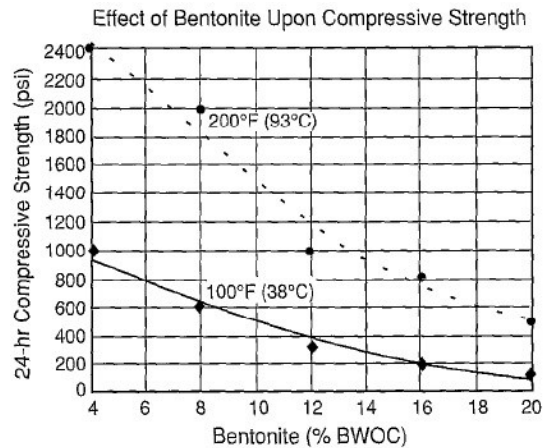


**Fig.71:** Effect of bentonite on compressive strength

*Fluid loss additives* consist of particulate materials, such as vinylidene chloride (50°C), polyvinyl acetate (50°C) or styrene-butadiene (176°C), or water soluble polymers, such as various cellulose derivatives (commonly < 93°C) or cationic polymers (Polyethyleneimine), 225°C).<sup>[53],[55]</sup>

For high temperature cements there are principal types of wells: deep oil and gas wells, geothermal wells, and thermal recovery wells. Thus, when designing cements for high temperature down-hole conditions a separation between HP/HT wells and HT-only wells, as geothermal wells, is reasonable.

For *deep HP/HT* wells pressure has an important effect on the cement chemistry and phase development. Increasing pressure will shorten thickening time although its effects are less pronounced than temperature. Besides earlier compressive strength development also the ultimate compressive strength is higher. In general, the higher the circulating temperature, the higher the sensitivity of Portland cement systems to subtle chemical and physical differences between the slurry ingredients. Therefore generally temperature simulation is conducted some weeks in advance and consequent laboratory tests are performed with samples of the water, cement, and additives which will be used during the job. Besides, in HP/HT wells narrower annuli, over-pressured zones, and corrosive fluids are commonly encountered.

Furthermore, it is important to consider the large pumping times of several hours requiring the usage of retarders. As the length of the casing string or the liner increases, length elongation and proper cement seal gets more difficult to achieve. A differential in temperature from top to bottom of the cement column, static as well as dynamic, has to be considered in long sections. When not considering the exact temperature profile, this can again cause an over-retardation of cement resulting in excessive waiting on cement time.<sup>[53]</sup>

The environment of *geothermal wells* is challenging, as high down-hole temperatures come along with extremely saline and corrosive formation brines. The presence of carbonate in brines presents a serious difficulty for Portland cement systems. To cope the problem with salty brines, a reduction of silica additive grain size is important. Thus, silica flower is used instead of sand, which makes the handling on surface a bit more difficult.

Generally the design for thickening time is not a big issue, as shallow and larger diameter holes will be sufficiently cooled by the circulating mud. The relatively large cement volumes will not be heated up that fast when pumped. This can be observed in the following graph, generated from the temperature data of the simulation from last chapter. Although the low pumping speed the cement temperature increases slowly, as long as it is pumped.

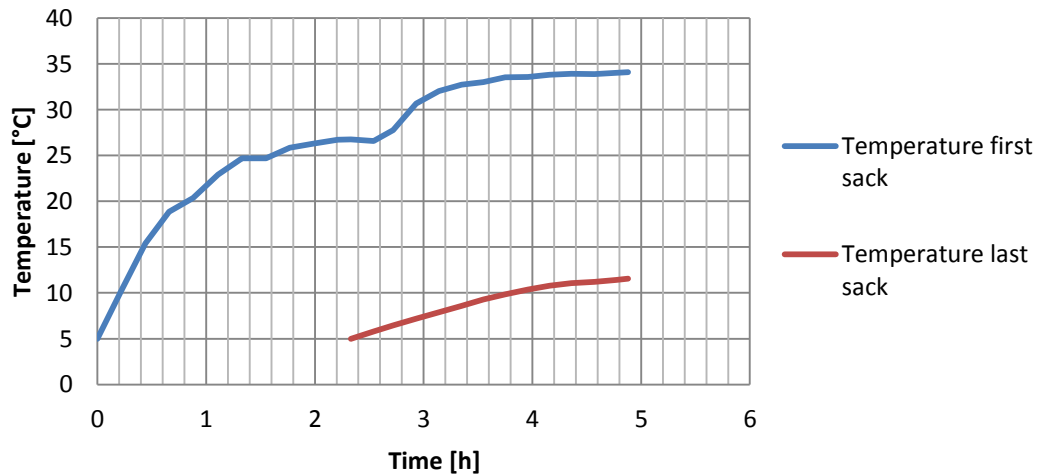


**Fig.72:** Example of the temperature increase of cement with time

The down-hole pressures are seldom above the normal water gradient. On the contrary fluid loss and low fracture gradients will be an issue for geothermal operations and low-density systems are required. Instead fly ash as an extender also bentonite, perlite, and diatomaceous earth are used.

Proper casing design is an issue due to the absence of a tubing. And as mentioned before, especially geothermal wells are frequently cemented to surface, in order to avoid creep and of thermal expansion. <sup>[53]</sup>

From the operational point of view, dealing with high temperatures causes efforts in the handling with the addition of silica. As with other heavy particles, like hematite, silica falls out in batch mixing. It is therefore added late to the mixture to avoid that. The price of the material itself is not an issue, but the different handling may cause price increases of around 10%.

Furthermore casing elongation is an issue for cement and cementing. During hydration, after slurry placement, the temperature of the cement, casing, and surrounding formation can increase by as much as 27°C to 33°C because the wellbore is practically thermally isolated. This results in an elongation of metal tubular, which will contract again with time and which can thereby form thermal micro-annuli. <sup>[53]</sup>

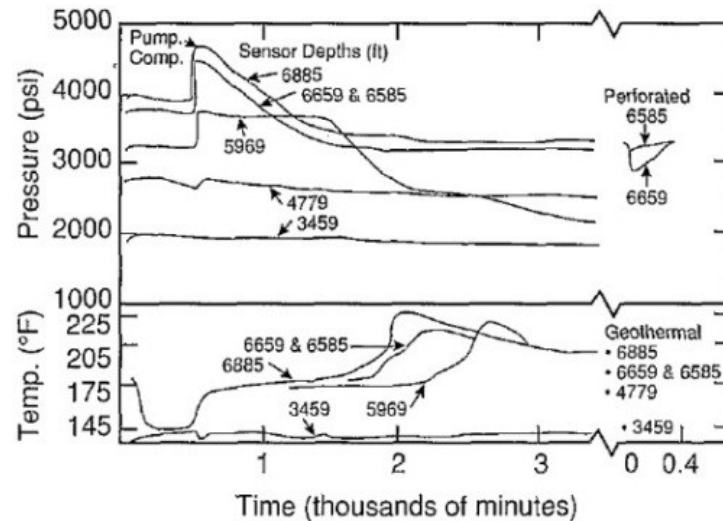


**Fig.73:** Annular pressure and temperature measurements during cementing <sup>[54]</sup>

For planning a cement job early laboratory studies are mandatory. Testing with cement samples and additives as well as with location fluids and conditions is important to predetermine the optimum mixture and possible undesired reactions.

For the actual cement job the static bottom-hole temperature is of interest for investigating cement stability and compressive strength development with time. The circulating temperature on the other hand is important for the calculation of the pumpable time. As a rule of thumb, the static temperature at the depth of the top of cement should not be less than the circulating temperature the slurry is designed for. If this is the case it may take too long to cure. <sup>[97]</sup>

As a very general statement, temperature boundaries for cement mixtures can be defined similar to those of drilling mud. At around 110°C from the silica flower, between 120°C-150°C with the degradation of the polymer additives. Beyond 200°C there is a general difficulty in obtaining sufficient experience and proper additives, which results in highly expensive cement systems. The following diagram gives an estimate of cost increase depending on temperature.

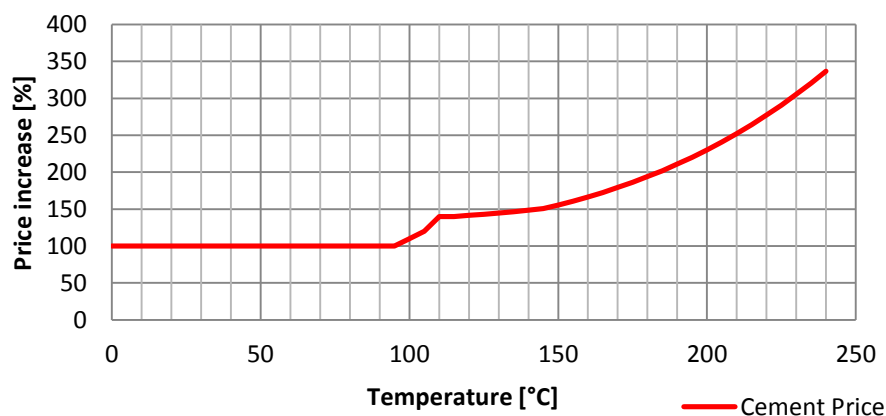


**Fig.74:** Estimated price development of cement vs. temperature

A list of some common additives and their limitations found in the literature are presented in the Appendix.

### 3.4 Electronics

Electronic components represent a major barrier in high temperature drilling applications. Depending on the type of tool used, it is exposed to the dynamic temperature profile, like MWD/LWD, or a profile closer to static, like wireline/slickline tools. The actual temperature the tool is exposed to, depends not only on the temperature conditions on the outside, but further also on the heat dissipated by components on the inside (up to +28°C).

When facing high temperatures during an operation, components in the electronic systems, the high-power electronics, the circuit housing as well as the energy supply, can cause errors or malfunction. Commercial electronics are not designed for temperatures faced in HT operations, and conventional integrated circuit technology is not capable of operating at these temperatures.<sup>[89]</sup>

It is an issue for contractor companies in the petroleum business to get adequate components for a reasonable price, since hardly any other industry needs electronics which are robust enough to handle high pressures, extreme temperatures and kinetic shocks simultaneously. Commercial electronic components are usually designed to operate at conditions below 85°C and further industry specifications for the general industry are just up to 125°C. Thus, for temperatures exceeding 150 °C generally components manufactured, tested and rated for these environments are used, instead of up-screening commercial electronics.<sup>[91]</sup>

For provided electronics different classes exist, which define the materials delivered by ancillary companies. For testing of the electronics standards like consumer-, industrial- and military specification exist, where the latter one includes the toughest tests and is often used for tools.

The actual temperature limitation of the components is given by the material layout and design. Further, the limitation depends on the component's functionality and data output as well as its deterioration with time and temperature cycling. The different responses to temperature of the various components in an electrical system and their interaction cause large development efforts. Although suppliers usually include some tolerance in the proposed temperature limits (usually 5-10°C), they should be taken serious, as failure rate increases exponentially with temperature. A general rule of electrical engineers states, that an increase of 10°C reduces the lifetime of electronic components by the factor two.

For systems semiconductors cause certain limitations for high temperature applications. Silicon based micro-electric devices show a large operational dependence on temperature and have a physical limit of 150-200°C. Furthermore electro-migration causes frequently a lifetime reduction on silicon integrated circuit chips, when metal ions move in the chips thin film conductors. The ion movement depends on current and temperature.

Ceramic chip capacitors are preferred for electronics, as they have a low temperature coefficient of capacitance (change in capacitance with temperature). Still, the dielectric constant depends on temperature non-linearly and causes changes the capacitance,

residual charges. Common surface-mount ceramic chip capacitors show a temperature limit of 150°C.

Resistors show to change their resistivity with time and temperature. For high temperature applications wire-wound resistors and thick film resistors are used, which show small change at high temperatures and thermal cycling. Operation limits are as high as 170°C, sometimes even 550°C. The temperature limiting factor is not the wire itself, but the used coating compound and the neighbouring components.

Further the bonding of integrated circuits is an issue. The combination of different materials in a connection may become resistive at high temperatures, thus causing failures. The common gold-aluminium bonds in the integrated circuits hereby have a limit of 150°C. Aluminium-nickel or aluminium-aluminium wire bonding represents an improvement for higher temperatures.

The usage of the correct solder for connections is also important. The eutectic tin-lead (37/63) solder used for commercial applications will melt at 183°C and is not a good choice for high temperature applications. High lead / low tin content solders (95/5 and 90/10) can be useful for temperatures up to 250°C. Usually the number of solder connections is tried to be kept low, as it is directly proportional to the failure rate. <sup>[91]</sup>

The circuit board itself is also a limitation, as they are generally made of epoxy resins. Normal FR-4 boards (designation for fiberglass reinforced epoxy laminates) will not last above 150°C. Properties such as the glass transition temperature ( $T_g$ ), thermal expansion elastic modulus and yield strength are important. Many boards use bismaleimide-triazine resin, which has a limit of 180°C. Polyimide boards with all the copper traces embedded have been shown to last 6000 hours at 250°C. More specialized applications may require ceramic boards. The thick film conductors on a ceramic board are fired at temperatures from 800°C to 1000°C and are not affected by the much lower application temperature.

The frequently found plastic housings for wires or microcircuits must also be carefully evaluated when temperatures exceed 135°C. When plastic packages become less reliable die-scale chip attach or ceramic packages need to be used, which lean more on solder interconnects.

The sensors themselves used in down-hole tools have various temperature limitations, depending on the type and application. Further also the deviated accuracy of the readings is a major concern. Pressure sensors, for example, Crystal Quartz Gauge are commonly used, but need to be replaced at higher temperatures than around 180°C. Similar limits are given for gravity sensors or shock sensors for accelerometers as they also include semiconductors. The commonly used Fluxgate-Magnetometers for MWD have their operational temperature limit around 175°C – 200°C. For these components generally temperature is an issue as the sensors response (sensitivity, magnetic offset and noise) to the magnetic field varies widely. Conventional gamma sensors are based on scintillation technology cannot be used in high-temperature environments because detector performance degrades. For HT applications Geiger-Müller tubes are used. Neutron porosity sensors have to be largely corrected for pressure and temperature, causing larger inaccuracies. <sup>[88]</sup>

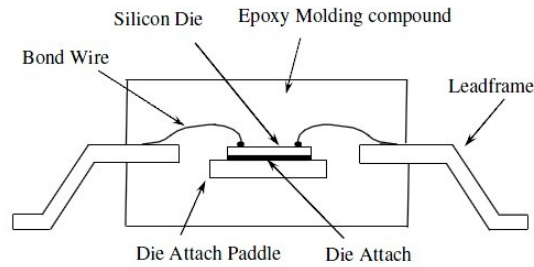


**Fig.75:** Structure of the most common plastic encapsulated microcircuit

At temperatures exceeding 200°C larger modifications are needed. The usage of ceramic packaging technology with dyes (elements without housing but with passivation against corrosion, scratches and dirt) becomes necessary. Electronic devices with a wide bandgap must be considered. Chips are usually connected without wires by using flip chip connection process with high temperature solder, AlN cases and substrates, glass lid and lid seals, high temperature solder joints or welds and metallic housings. <sup>[92]</sup>

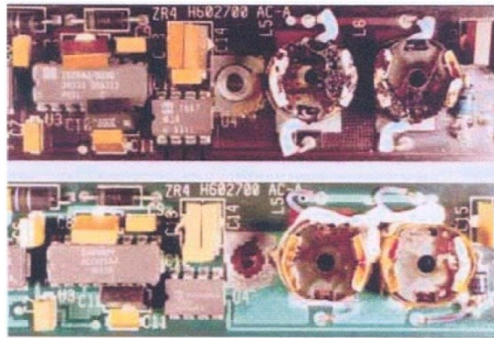


**Fig.76:** Temperature effect on a logging tools circuite board <sup>[88]</sup>

For the power supply of down-hole tools normally lithium-thionyl-chloride batteries are used. The batteries capacities and lifetime vary largely depending on the surrounding temperature. Lithium has a melting point of 180°C and lithium batteries are thus limited to operating temperatures of 160°C and below. In high-temperature batteries magnesium is alloyed with the lithium anode and operating temperature can be increased up to 200°C. Unfortunately this causes a reduction in current capacity and, more problematic, a poor power output below around 100°C. Current development show promising results for non-lithium cells up to 250°C. <sup>[86], [85]</sup>

Alternatively to batteries power generation by using down-hole mud-turbines appears to be a reasonable option, particularly for the high temperature applications. Down-hole generators do not suffer from limitations such as narrow operating temperature ranges or power density variation across an operating temperature range. Also there are no problems with sudden and long high current loads, other than with batteries. Temperature limitations are given by the inside electronics. Dynamic seals are not necessary for HT tools, as magnetic couplings are used to transmit the force from the turbine blades to the power unit, thus only causing a need for a static seal. <sup>[86]</sup> A major limitation, however, is the lack of energy supply without circulation present and the higher initial costs.

Similarly to telemetry systems the temperature limits depend on electronics rather than mechanics.

### 3.4.1 Limitation for logging tools at high temperatures

Conventional logging tools are rated up to 177°C. For an upgrade to high temperature applications sensitive electronics are installed in a pressure rated Dewar flask housing. The Dewar flask protects the electronic circuits from excessive borehole temperatures, thus increasing limits to almost 300°C. However, this is not possible for sensors which must be exposed to the wellbore or where common thermal shielding may prohibit the sensor from conducting the desired measurement correctly.



**Fig.77:** Difference in electronics module housing thickness between a normal (upper) and an HP/HT acoustic tool (lower) <sup>[90]</sup>

Inside the Dewar, the temperature will increase slowly as there is no way to dissipate the heat generated by the electronics itself. As the temperature will rise continuously it is important to conduct appropriate pre-planning and time management on the rig to minimize the logging times. <sup>[88]</sup> Powering the tool for a minimum amount of time, for example, minimizes the internally generated heat. Logging-in while running in hole with the tool is often performed to gain data in the event of a tool failure. For this approach the extra heat generated has to be added to the heat faced down-hole for consideration.

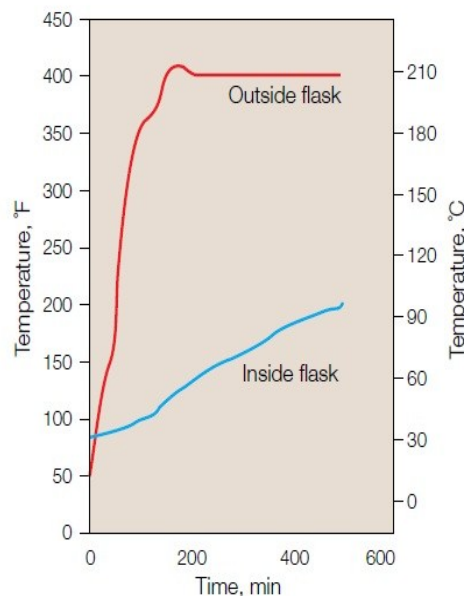


**Fig.78:** Dewar flask housing example <sup>[88]</sup>

It is also important to consider the availability in the special region. It will be easier to get services for locations with many high temperature wells in the vicinity.

In conventional wells wire-line cables no significant degradation for the electrical operation is caused, while for high temperatures higher power losses must be considered. Formation temperatures exceeding 300°C will require the use of MgO-insulated cables or non-conducting cables combined with dewared electronics.

For wire-line tools however the limits are different due to the different insulation mentioned above. The maximum temperatures those tools can be exposed to are generally higher, although large differences do exist:

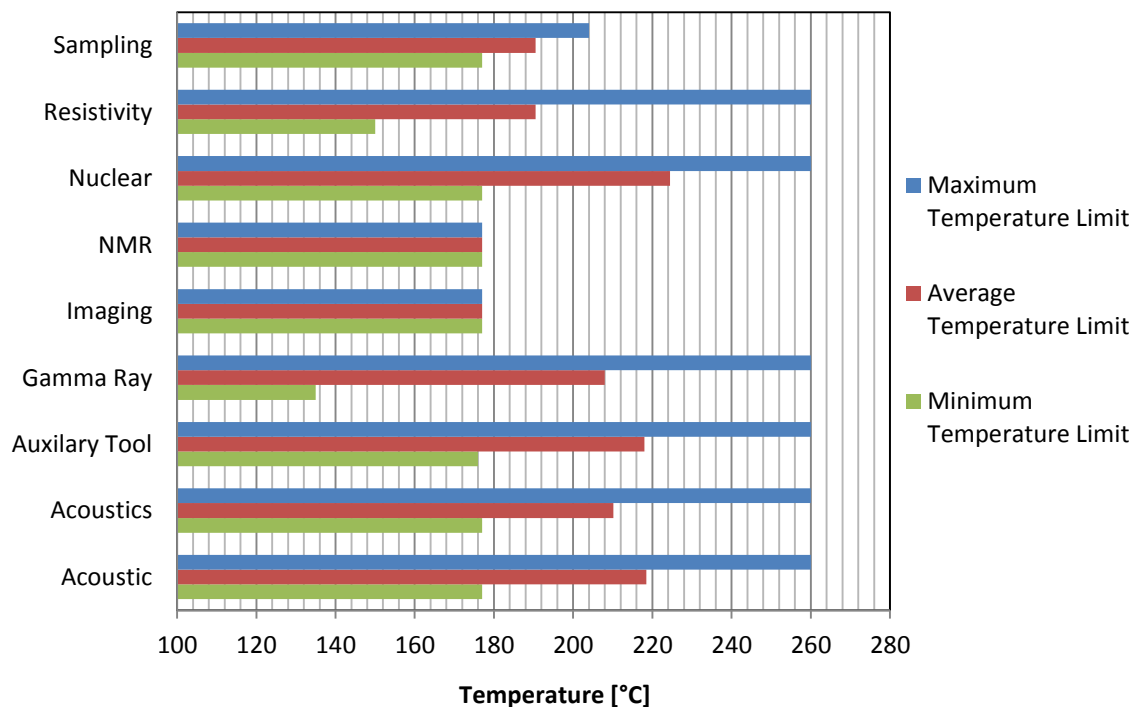


**Fig.79:** Distribution of temperature limitations of wire-line logging tools

Most tools have a temperature limit of around 175°C. However, with an appropriate insulation technique the limits of the tools can be pushed much higher, at least for some time.

### 3.4.2 Limitation for BHA tools at high temperatures

Due to the sensibility of electronics to temperature currently a lot of development effort is conducted by the industry with the data and information being strictly secret. Exact component material selection, build-up and temperature dependent functionality data is hardly published. Recent advances in the industry made it possible to design electric systems, that will operate at ambient temperatures of 230°C.

Besides the increase in temperature capacity of the electronics, also the usage of active cooling systems was evaluated. Significant developments have been made in the area of Silicon-on-Insulator (SOI) components, that are now capable of withstanding operating temperatures above 392°F (200°C). Capacitor technology seems to be making significant development for high temperature as well. <sup>[85]</sup>



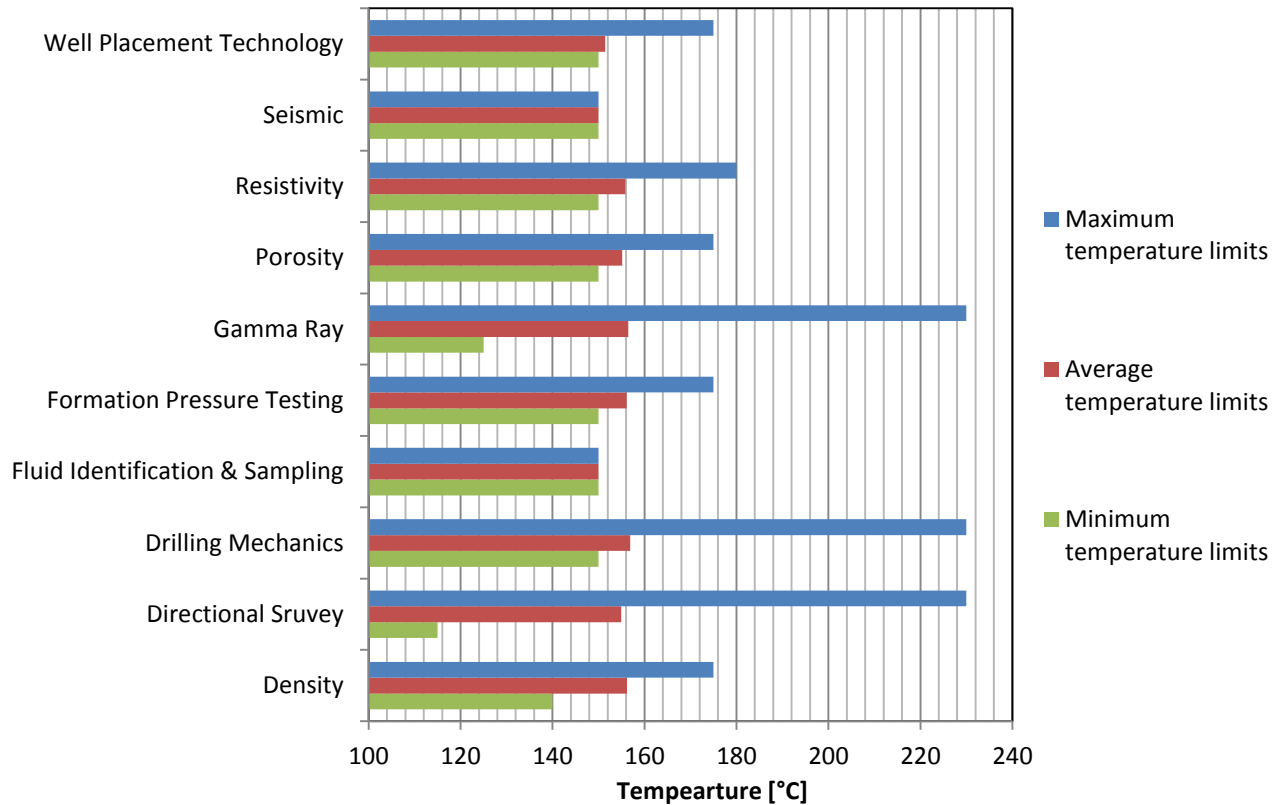


**Fig.80:** Temperature limitations of MWD/LWD tools available

Standard equipment has a minimum temperature limitation of 120°C. But as can be seen in the diagram most MWD/LWD tools available on the market are manufactured to withstand 150°C. The maximum tools capacity is currently at a maximum of 180°C down-hole temperature. A very recent development are two tools, that offer a combination of gamma ray, directional Pressure While Drilling (PWD sensor) and vibration sensors capable of up to 200°C and 230°C.

Depending on the risk wanted to take these tools can also be used in higher temperature applications. In a ultra-high temperature well for example, a retrievable MWD/LWD was used in ultra-hot regions, which were sufficiently cooled down in advance. <sup>[66]</sup> When limitations for BHT tools are reached and risks are not desired, simple alternatives have to be found. Whipstocks and an according BHA can then be a rustic alternative.

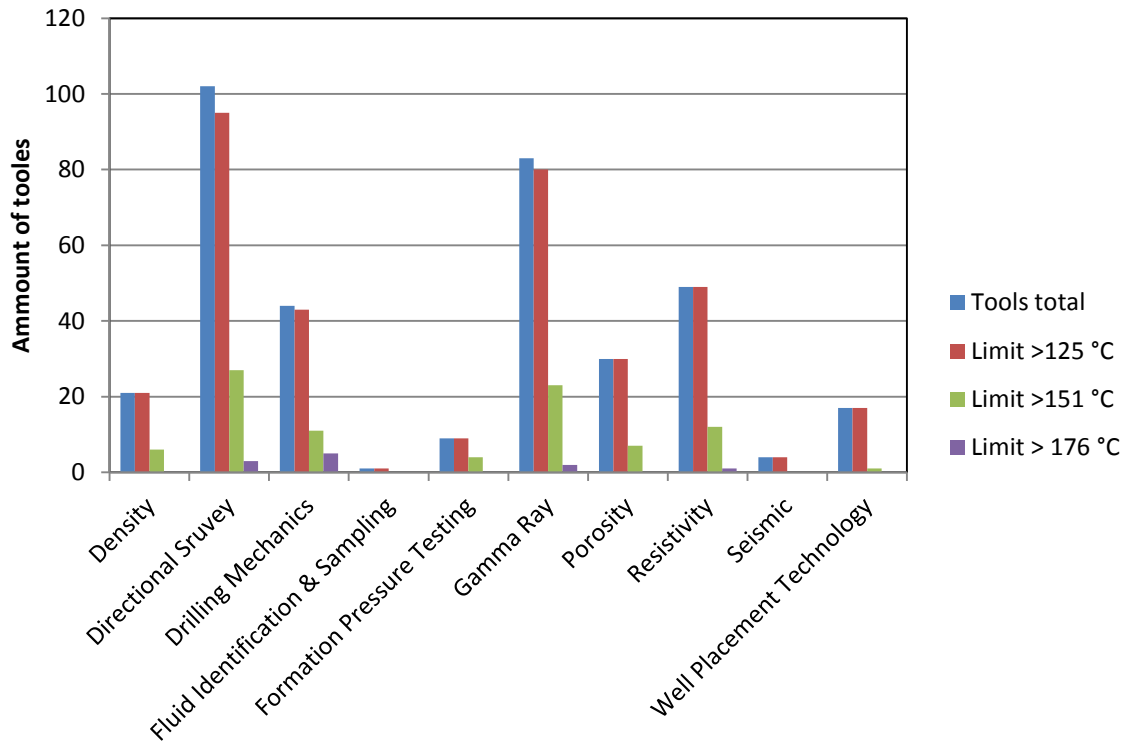


**Fig.81:** Distribution of temperature limitations of MWD/LWD tools

When looking at the distribution of the temperature limits of the tools available, it can be observed that most tool types have a comparatively limited availability above 150°C capacity. A detailed list of tools found in the internet is presented in the Appendix.

According to some price data found during the research the price difference for rental services is usually between 20% and 80%. This depends very much on the actual temperature reached. For 150°C it will be 20% and for 180°C it will be 80% due to the higher wear and the reduced lifetime. Service companies tend to statistically evaluate tool failures related to the operation operational environment and thus find higher price margins depending on the environment.

### 3.5 Review on limits and potential price drivers

For the general industry, materials for manufacturing tools and components are standardized for conditions faced at the surface. Thus, materials needed for subsurface exploration and production face many limitations. Huge engineering effort is put into the development of more stress-resistant tools and components. Drilling in hot environments has various limitations, depending on the desired type of component, the supplier, its availability and its price range.

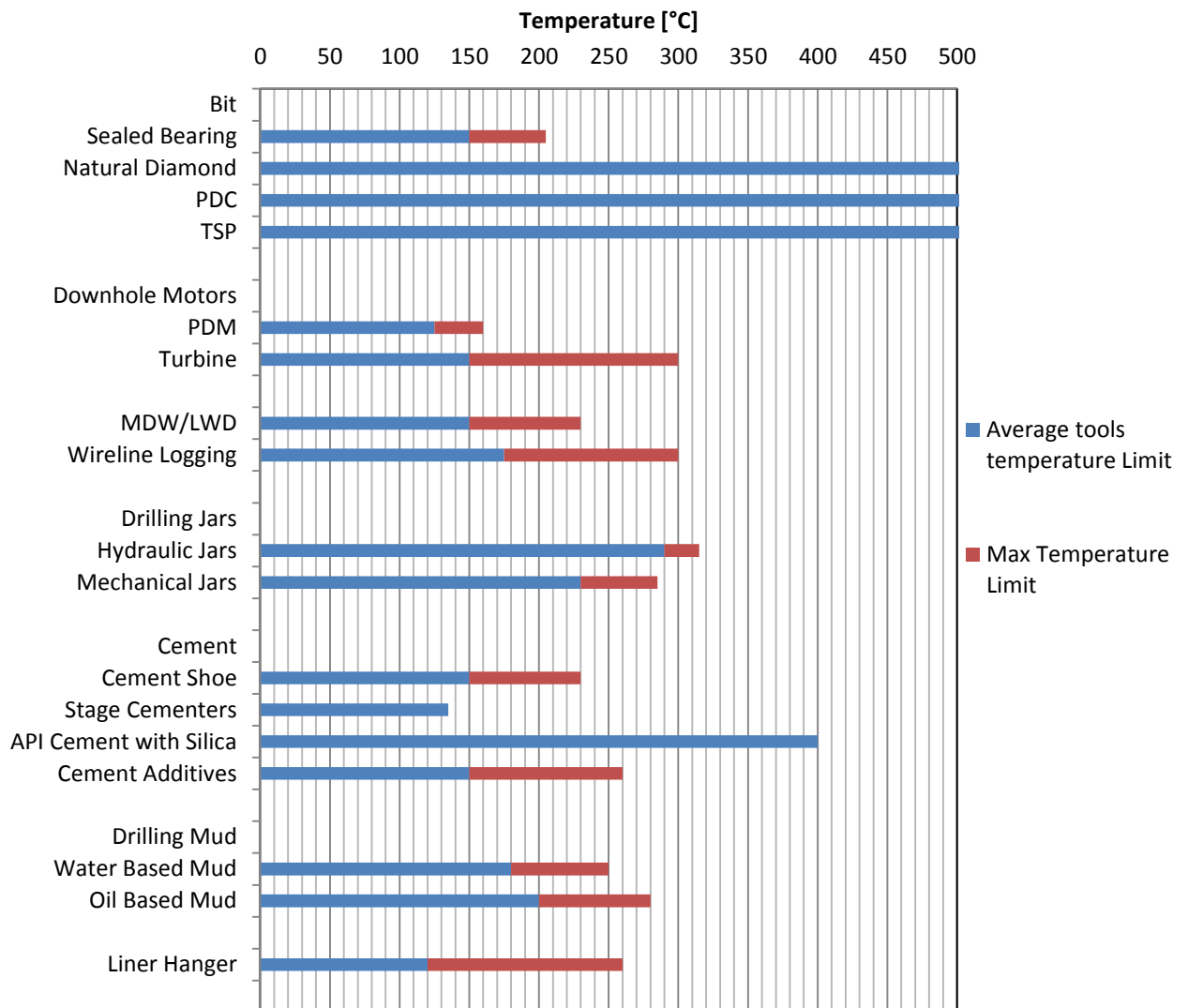


**Fig.82:** Limits of down-hole tools and components

A first basic boundary can be set at 110-120°C. Below this conditions there is almost no concern regarding temperature in drilling applications. A minimum temperature of 120°C is reached by all tools and components.

From this temperature onward, however, some limitations will be faced. Some standard logging or BHA tools already reach their limits. Many of the rubber elements of the down-hole tools need to be modified. Also the addition of silica flour to the cement mixture causes a little extra effort for handling. Polymer mud and cement additives start

to slowly degrade at this temperature. Also the starting of metallurgical concerns for aluminium drill-pipes should be stated here as well as the possible need for better casing couplings.

A second boundary can be generally established around 150°C. The design limit of most electric down-hole devices is set at this temperature. Further polymer components tend to degrade rapidly. This can be seen in BHA components with dynamic seals like down-hole motors or bits, which comprise NBR or HNBR rubber, as well as in mud and cement additives.

A further major boundary can be registered around 180°C, when handling of the drilling mud and cement gets very problematic as well as final limits for almost all BHA electronics are reached.

A maximum of 200 – 250°C for conventional, sophisticated drilling operations can be set, depending on the equipment needed. At higher temperatures large sacrifices have to be accepted and “simple” equipment will prove beneficial: Instead of down-hole motors or steerable systems whipstocks with an appropriately set BHA are acceptable. Turbine motors or the currently developed mud-motors comprising no elastomers are still within their margin. Also unsealed roller cone bits can be used, suffering from reduced lifetime. For logging the dewared slick-line tools are the only option. The drilling mud will also suffer from uncontrolled rheology and the usage of simple water will soon be the only solution.

When down-hole conditions reach these limits, hardly any knowledge is available. Only some scientific deep drilling projects like the KTB in central Europe reached temperatures up to 300°C. Projects like the Iceland Deep Drilling project reached even magmatic rock, before they needed to cease operations. However, also some industrial drilling applications, mainly geothermal ones, were reported, which reached extreme temperatures. In these applications the limits are pushed and the risk of tool failure is accounted for. The tool limitations can be over-gone by appropriate operational measures to a certain degree. For example, the usage of a Top-Drive is very beneficial for high borehole temperatures. With the possibility to circulate while tripping in, the formation can already be cooled. Long circulation intervals, to cool the formation provide a beneficial situation. Mud coolers have sufficient impact on the temperature development, especially for shallower wells. Insulated drill-pipes may be an alternative for future drilling operations, which face excessive temperatures. All these measures have to be evaluated in the planning phase for risk and economics. <sup>[39], [66], [67], [69]</sup>

Due to the different temperatures faced, a separation between down-hole tools and surface tools should be established. As a guideline the following diagram may help for a general overview.

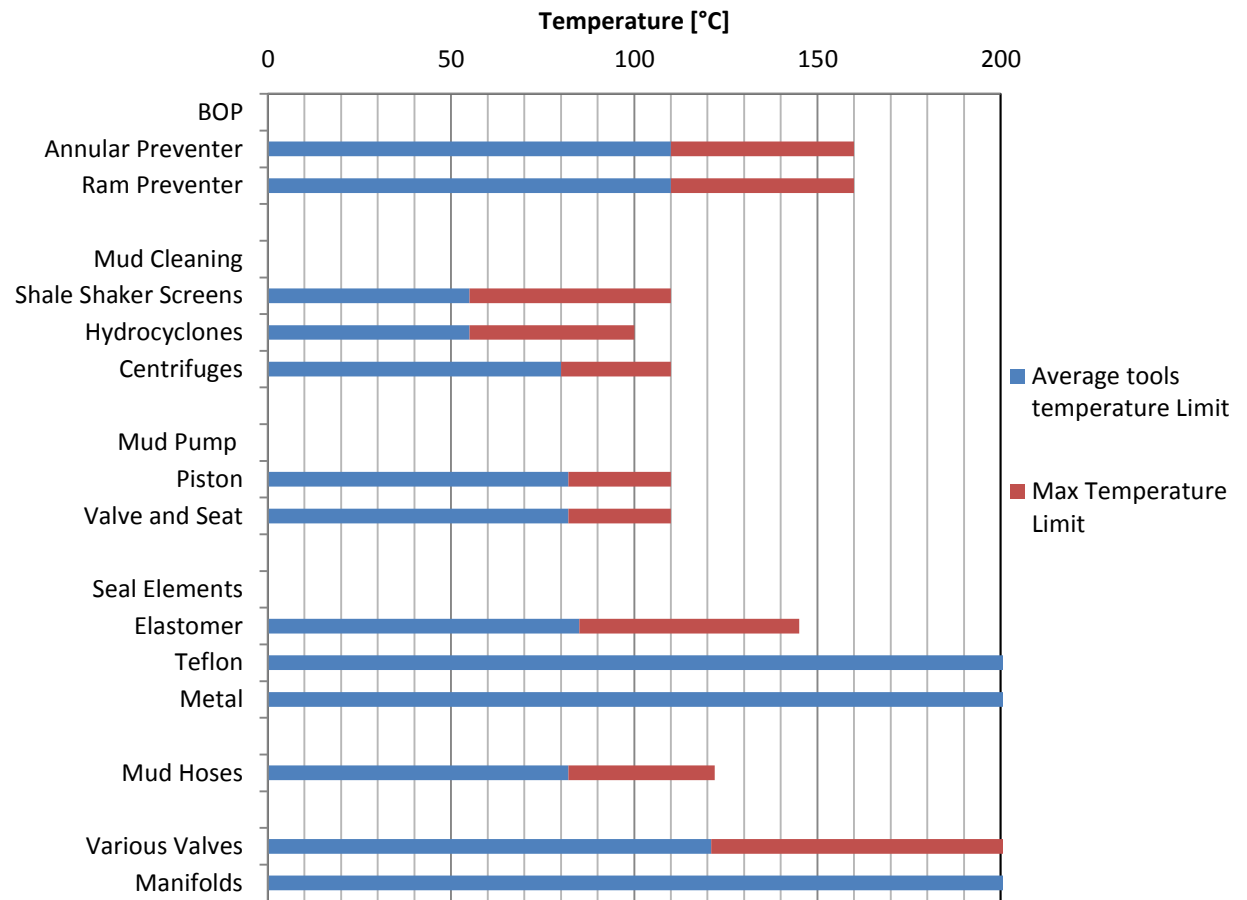


**Fig.83:** Limits of surface equipment

As can be seen the general design layout of mechanical engineering, 80°C, is valid for determining the standard tool limitations. Only the screens and the hydrocyclones have lower average-limitations.

Surface equipment with a rating of greater than 110°C is not available. This seems logical, as drilling mud would boil at surface pressures and would represent a clear HSE issue. Nevertheless, BOPs and valves are present for higher temperatures, which is mandatory for safety.

From the shown limits of down-hole and surface equipment a general range of expected hazards and price increases can be derived. Standard equipment will be supplied at average costs whereas equipment capable of higher temperature will be more expensive.

It must be considered, that the mentioned temperature limits can actually be relativized due to the fact, that increased temperature causes statistically more errors and malfunctions of the tools, even when the design-limits are not exceeded.

Furthermore, issues with corrosion, reduced yield strength of metals as well as degraded material properties of polymer and elastomer components with increasing temperatures,

will cause further drawbacks in overall project economics. Especially also the mud and cement technology needed, which is depending very much on the geology, cause continuous price increases. Thus, these price drivers are hard to quantify and depend very much on experience and appropriate counter-measures.

A statistical evaluation of tool brake-downs, depending on factors deteriorating tools life (pressure, temperature etc.) is conducted within many service companies. Such an approach seems reasonable to qualify the increased costs to be expected for critical environmental factors. However, such data is hardly accessible.

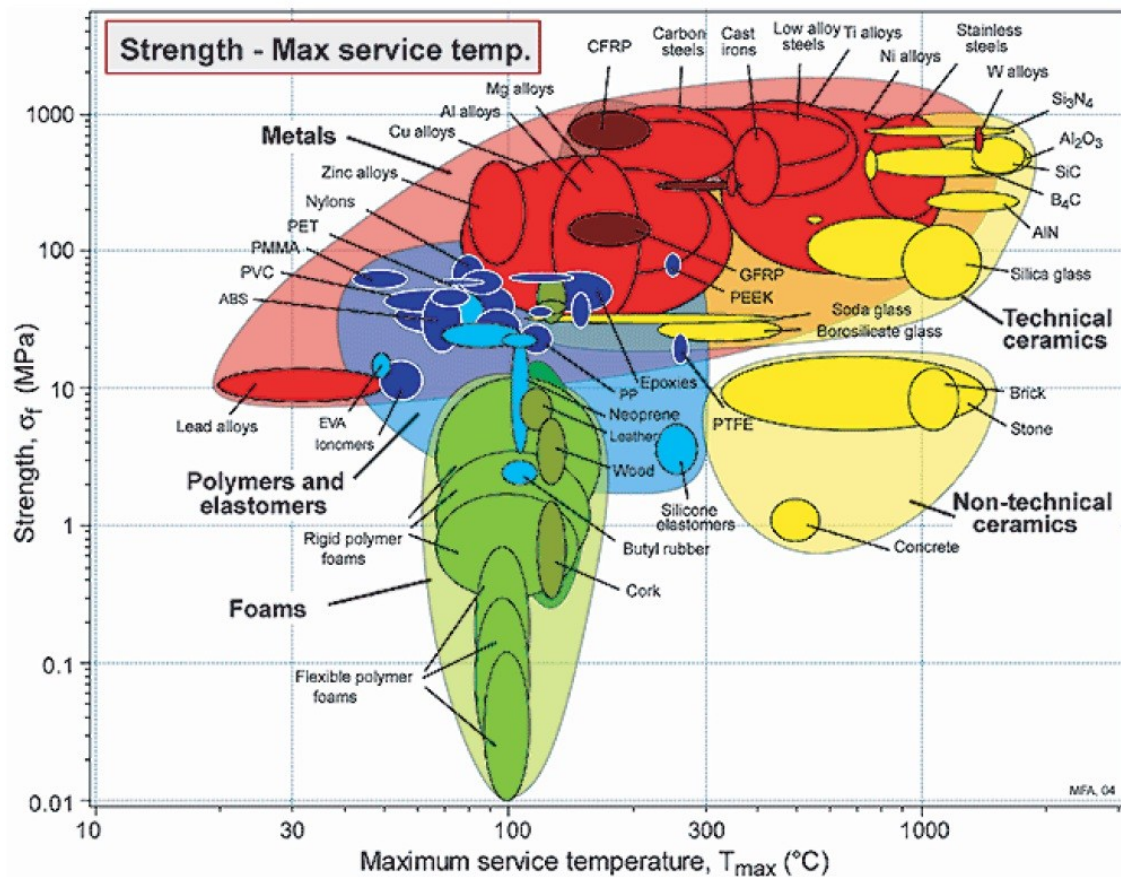


**Fig.84:** Maximum service temperature of materials according to the Ashby chart <sup>[96]</sup>

### 3.6 Cost versus depth comparison

After analysing the potential limiting components in the drilling system an estimate for the potential cost impact on a high temperature drilling application is give below. Therefore the data from the given geothermal well was used again, in order to get an overview of the operational cost with time and depth. The price data was then further processed for a hypothetical well, which would have the same layout, operational sequence and geology, but with a bottom hole static temperature of 175°C instead of 87°C.

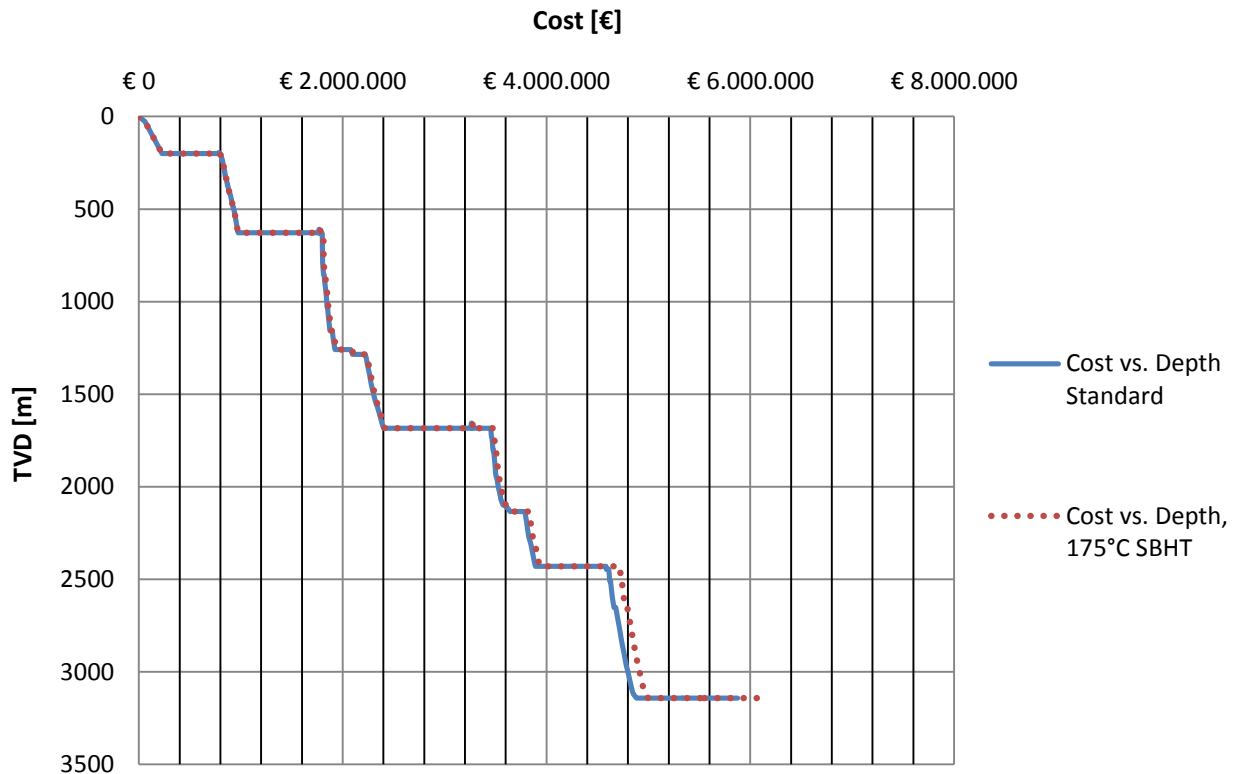


**Fig.85:** Cost vs. Depth of a well with different gradients

As can be seen in the Cost versus Depth Curve the price differences for high temperatures are not really a major cost driver for this well. The increase of costs actually starts at a measured depth of around 2000 meters, as a static temperature of 120°C is reached there. Further, at a depth of around 2600 meters a static temperature of 150°C would be reached. This falls in the construction phase of the last hole section.

For the flow-line temperatures the critical temperature for shale shakers screens and hydrocyclones of 55°C is reached during the construction of the 12 ¼" section, also at around 2000 meters.

According to the price impacts pictured in this chapter, the following increases in operational cost can be observed:

Matter of Expense	Price Increase
Rig	€ 0,00
Drilling Assembly	€ 64.548
BOP	€ 0
Mud	€ 24.417
Mud-regeneation	€ 6.801
Logging	€ 107.872
Casing	€ 9.614
Cement	€ 1.864
<b>Total Cost difference</b>	<b>€ 216.982</b>

**Table 22:** Impact of the equipment on the total costs

An overall price increase of roughly 217.000€ could be observed which represents an increase of 3,6% of the total costs. It gets obvious that the tools containing expensive electronics, like logging and BHA tools are the biggest price drivers. Here the tools were dimensioned for a safe operation according to the static gradient.

Mud and mud regeneration units also have an impact. For cementing the price differences are marginal, as the liner section has a static temperature of around 120°C. Thus, the only issue is the additional silica flour handling.

For the last two casings more expensive float shoes and float collars were necessary. Also a higher rated liner hanger was used. Additional costs for different casing alloys were not considered here.

Additional operations, such as longer circulating intervals as well as further pre-tensioning operation were not included in the observation.

Due to the still acceptable flow-line temperatures indicated by the simulation, a modification of the BOP or the consideration of increased degradation of the rig's surface components did not seem necessary.

The application of mud coolers can be recommended though. Unfortunately no price data is available, but this equipment is generally stated to be cheap for rental. Thus, it is a good alternative to improve the conditions for surface and subsurface equipment to avoid additional wear and safe rental costs for HT- equipment. The diagram shows the two possible temperature profiles in comparison. The installation with the mud cooler was assumed to offer a constant inlet temperature of 45°C. The beneficial overall temperature situation can clearly be observed.



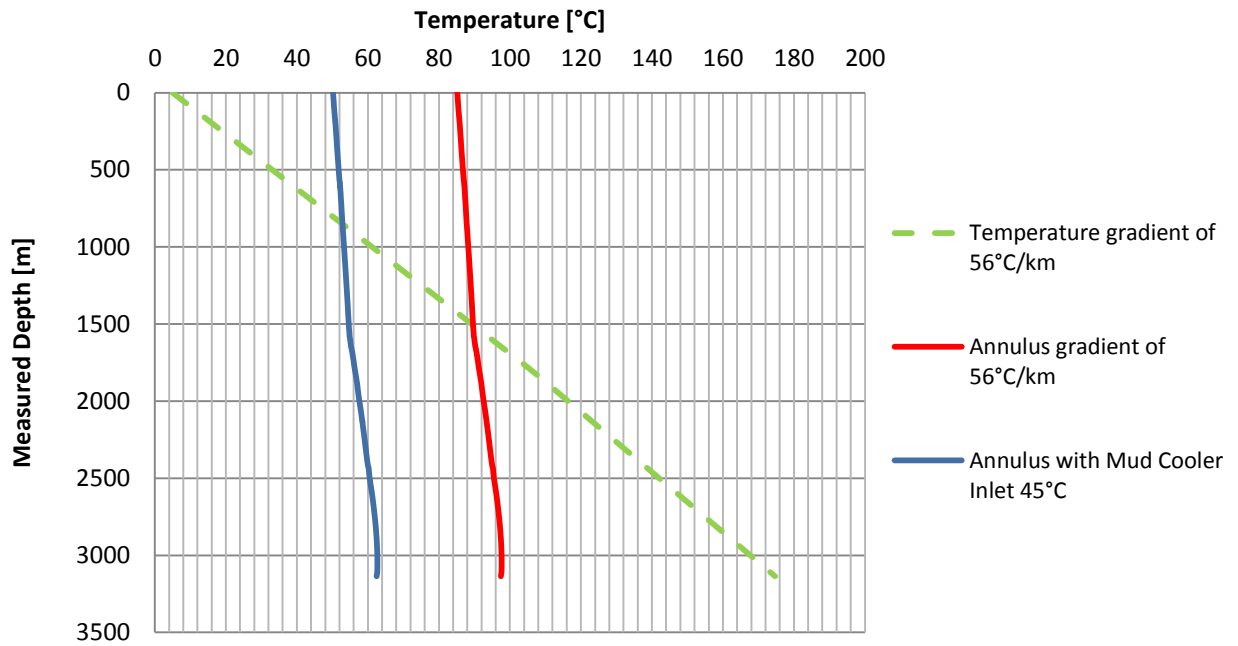


**Fig.86:** Comparison of temperature gradient of a hypothetical well with and without mud-cooler

Nevertheless, when using a mud cooler it must be accounted for the fact, that cooling can only be obtained during circulation. Long shut-in periods will cause a hot mud down-hole and may lead to an imbalance in the mud temperature distribution when starting circulation. Temperature peaks may be then observed, resulting in harmful conditions for not accordingly rated equipment.

## Conclusion

More and more demanding conditions are faced in today's drilling industry. This also includes the frequent occurrence of high temperature sub-surface environments. Either in oil and gas exploration, where HP/HT fields set engineering standards, or in geothermal energy projects, temperature causes engineering concerns for operations and equipment.

The subsurface heat-flow conditions are very diverse from location to location, depending on the geology, mineralogy, morphology and especially the volcanic activity. Also in vertical direction the temperature distribution is very inconsistent, mainly depending on convection by circulating ground waters and conduction properties of the various rock layers.

The drilling process greatly alters the temperature situation in the adjacent rock. Thereby the drilling mud acts like a heat exchanger, bringing heat from the formation to the surface. Many different parameters are interacting and influencing the temperature profile of the circulating fluid with time, such as the thermal properties of fluid and formation, flow rate, mud rheology, surface installations, wellbore geometry, BHA layout and the operational sequence.

When reconstructing the drilling process of a geothermal well with an analytical method or a numerical simulator, it was observed that the energy input from hydraulics and rotation resulted in a large increase in overall system temperature. The available sensor data support these observations. Especially for the shallow, large diameter wells this effect is important and resulted in temperatures above the static gradient of the analysed well. The reconstruction of the complete drilling temperature development showed, that this effect decreases with increasing depth and decreasing diameter.

An energy balance conducted for the uppermost hole-section, which showed the largest increase of the temperature profile above static conditions, gives an explanation. The short circulation cycles and the minimized interaction with the formation for the shallow depth allow for an accumulation of input energy.

As most analytical models don't include energy input from the rig into their predictions, results are wrong, especially for the shallow, large diameter wells. A further model presented, which is basically an improvement by including input energy, gives more correct flow-line temperatures. However, a further limitation of analytical models is the knowledge of the actual mud-inlet temperature. Thus, analytical models proved insufficient for an exact temperature prediction for the given well.

Nevertheless, the models showed to be helpful for the subsequent parameter study. Due to the limited amount of input parameters a quick understanding of down-hole temperature development is possible. It was indicated, that in the beginning of the circulation the final depth, formation temperature, actual mud inlet temperature, well diameter, flow-rate and fluid specific heat are first order effects. Over longer circulation intervals, however, only the mud inlet temperature is a real first order effect. This is in accordance with Fourier's Law of thermal conduction: The heat conduction through formations is relatively small. Thus, little heat flux between the far away formation and

the formation adjacent to a well exist. In transient circulation conditions mud and adjacent formation temperature approach each other and reduce heat flow among each other. Like this an equilibrium is reached in the mud between energy input from the formation and the rig and output to the ambient air.

The subsequent study with the numerical simulator showed similar results. Over long circulation times the mud inlet temperature as well as the geothermal gradient had the biggest impact on the temperature profile, when equilibrium conditions are reached. Further also the need for the input of an exact down-hole lithology and temperature distribution was shown. The latter can be especially important in convective geothermal areas.

The static formation temperature profile and the dynamic circulation profile represent the boundaries, the drilling equipment is exposed to. When facing high temperatures in this operation envelope, considerations regarding metallurgy, polymer components, fluids, cements and electronics are versatile.

For metallurgy the reduction in yield stress has to be accounted for. Especially aluminium alloy tubular suffers from a degradation of mechanical properties and creep. Thermal expansion is mainly an issue for casings. Corrosion evaluation is complicated, but it has the tendency to increase with higher temperatures.

Polymers are a major consideration for high temperatures. Various components include these materials such as mud- or cement additives or tools mud-motors, bits or seals and gaskets. Polymer's mechanical properties basically depend on temperature, due to their chemical composition and build-up.

Elastomers represent the most frequently used polymers in tools and equipment. Very robust and temperature resistant elastomers are available, however depending on the type of elastomer different temperature limits can be stated. Various considerations exist for the equipment, which derive basically from the deviation in mechanical properties, chemical swelling or shrinking and material deterioration with time.

The demand for better elastomer compounds can therefore result in sufficiently higher prices of the equipment. For down-hole equipment the largest impact can be observed at the mud-motor stator, the seals and greasing system at the bit and various other static seals in jars, dampeners and other BHA components. For the surface equipment the biggest impact comes from the BOP rubbers, hoses and mud cleaning equipment.

Also for drilling mud polymer additives represent a limitation. Generally the degradation of hydraulic properties with temperature is a problem, especially for temperatures above 180°C. This causes insufficient hole cleaning or fluid loss with all its consequences.

Cements systems for high temperatures do exist, although general statements are very difficult due to the complexity of the mixtures. For API cements silica flour is mandatory to avoid strength retrogression at temperatures above 110°C. As with drilling mud additives deteriorate at higher temperatures, which can cause problems with fluid loss setting time adjustment or filtration.

Electronics are considered as the most important limiting factor for high temperature applications. The electronic systems, high-power electronics, circuit housing as well as the energy supply, can cause errors or malfunction. Currently the highest commercial tools limitation reached 230°C, but standard tools usually operate up 150°C. With dewar flasks for wire-line tools this limits can be pushed further.

As a rough estimate several temperature-boundaries can be stated, where components complexity, tool limitations and price impact reach a higher level. These are at 120°C, 150°C, 180°C and 200-250°C, where the latter one represents the upper limit for conventional drilling operations. Further on severe sacrifices need to be accepted and operational design has to be adapted largely.

Nevertheless, when considering the overall costs of a drilling project the impact of the usage of high temperature drilling tools is not a major cost factor. Also the usage of mud-coolers is very beneficial. When wells are shallower, even the down-hole equipment will largely benefit from continuous cooling. Thus, it seems reasonable to avoid high follow up costs for temperature related failure and use the appropriate equipment from the beginning.

## References

- [1] "Determination of Virgin Rock Temperature From Drillstem Test"; Christian Hermanrud, Statoil A/S; SPE 19464-PA; 1991
- [2] "Determining Circulating Fluid Temperature in Drilling, Workover, and Well Control Operations"; Kabir, C.S.; Hasan, A.R.; SPE 24581-PA; 1996
- [3] "Advanced Drilling and Well Technology"; Bernt Aadnoy, Iain Cooper, Stefan Miska, Robert F. Mitchell, and Michael L. Payne; Society of Petroleum Engineers; ISBN: 9781555631451
- [4] "Extreme HP/HT completions: Technology Challenges Facing Deep Gas Wells"; Bernardo Maldonado, Mark McCasland, and Alvaro Arrazola, Baker Oil Tools; SPE 97594-PT; 2005
- [5] "Central Graben Extreme Offshore High-Pressure/High-Temperature Cementing Case Study"; John North, Halliburton M&S Ltd.; Martial P. Brangetto, Elf Exploration UK PLC; Elizabeth Gray, Halliburton M&S Ltd.; SPE 59169-MS; 2000
- [6] "HPHT Drilling Fluid Challenges"; Ron Bland, Greg Mullen, Yohnny Gonzalez, Floyd Harvey, and Marvin Pless, Baker Hughes Drilling Fluids; SPE 103731-MS; 2006
- [7] "Ultradeep HP/HT Completions: Classification, Design Methodologies, and Technical Challenges"; B. Maldonado, A. Arrazola, and B. Morton, Baker Oil Tools; Offshore Technology Conference 17927-MS; 2006
- [8] "IEA Statistics, Renewables Information 2010"; International Energy Agency; ISBN: 978-92-64-08416-2; 2010
- [9] "IEA Statistics, Electricity Information 2010"; International Energy Agency; ISBN 978-92-64-08418-6; 2010
- [10] "2010 Present Status of Geothermal Energy in Turkey"; Umran Serpen, Niyazi Aksoy, Tahir Öngürç; Istanbul Technical University; PROCEEDINGS, Thirty-Fifth Workshop on Geothermal Reservoir Engineering; SGP-TR-188; 2010
- [11] "The New Geothermal Law of Turkey and the Opportunities Provided to Entrepreneurs"; Nusret Gungor; Ministry of Energy and Natural Resources, General Directorate of Mining Works Ankara Turkey; Proceedings World Geothermal Congress; 2010
- [12] "Future of Geothermal Energy", Subir K. Sanyal; PROCEEDINGS, Thirty-Fifth Workshop on Geothermal Reservoir Engineering; 2010
- [13] "Hot Dry Rock: A Versatile Alternative Energy Technology"; D. V. Duchane, Earth and Environmental Sciences Div., Los Alamos National Laboratory; SPE 30738-MS; 1995
- [14] "Geothermal energy technology and current status: an overview"; Enrico Barbier; Renewable and Sustainable Energy Reviews, Volume 6, Issues 1-2; 2002
- [15] "Physical Properties of Rocks, Volume 18: Fundamentals and Principles of Petrophysics"; Klaus Helbig and Sven Treitel; ISBN: 008044346X

- [16] "Turkey's Geothermal Energy Potential: Updated Results" E. Didem Korkmaz Basel, Umran Serpen, Abdurrahman Satman; Istanbul Technical University; Stanford Geothermal Workshop; 2010
- [17] "Understanding and Managing Bottom Hole Circulating Temperature Behavior in Horizontal HT Wells - A Case Study Based on Haynesville Horizontal Wells"; Keith Trichel and John Fabian, SPE, Baker Hughes; SPE 40332-MS; 2011
- [18] "Analysis of heat losses and casing temperatures of steam injection wells with annular coolant water flow"; Back, Lloyd H., Cuffel, Robert F; SPE 7148-MS; 1978
- [19] „Projekt TRANSTHERMAL; Nationaler Abschlussbericht für Österreich“; Götzl G., Poltnig W., Domberger G., Lipiarski P.; 2007
- [20] „Bayerischer Geothermieatlas; Bayerisches Geologisches Landesamt“; Dr. Thomas Fritzer, Dr. Erik Settles, Dr. Klaus Dorsch; 2004
- [21] „Application of modern well test analysis techniques to pressure transient tests in Kizildere geothermal field, Turkey“; Mustafa Onur, Ayse Dönmez Zeybek, Umran Serpen; Istanbul Technical University; Geothermics, Volume 32, Issue 2; 2002
- [22] "Finanzierung und Wirtschaftlichkeit von Projekten der Tiefengeothermie“; Alexander von Dobschütz and Dr. Thomas Reif; presentation at the Fachtagung „Klima schützen – Werte schaffen“; 13. Juli 2009
- [23] "Applied Geothermics for Petroleum Engineers“; I. M. Kutasov; Elsevier Science & Techno 1999; ISBN-10:0-444-82887-7
- [24] "Influence of topographically driven convection on heat flow in the Swiss Alps: a model study“; B. Bodri, L. Rybach: Tectonophysics; 1998
- [25] "Geothermal Energy: An Alternative Resource for the 21st Century“; Harsh Gupta and Sukanta Roy; 2006 ISBN-10: 0-444-52875-X
- [26] "Horizontal and Directional Drilling“; Richard S. Carden; PetroSkills; LLC. AN OGCI COMPANY; 2007
- [27] "A Fluid Circulating Temperature Model for Workover Operations“; Hasan, A.R.; SPE 27848-PA; 1996
- [28] "Grundwassertemperatur - Tiefenprofilmessungen der bayerischen Wasserwirtschaftsverwaltung“; Bayerisches Landesamt für Wasserwirtschaft; 2001
- [29] Geothermisches Informationssystem für Deutschland – GeotIS; <http://www.geotis.de/geotis/templates/geotis.php>
- [30] „Geophysik und Geothermie“; Presentation: Joanneum Research; Hon. Prof. Dipl.-Ing. Dr. mont. Christian Schmid; 2010  
[http://www.geophysik.at/input/Herbstkolloquium\\_2010/JOANNEUM\\_Schmid.pdf](http://www.geophysik.at/input/Herbstkolloquium_2010/JOANNEUM_Schmid.pdf)
- [31] "High pressure specific heat capacities of pure water and seawater“; Journal of Chemical Engineering Data, Vol 42, No 4, 1987
- [32] "Practical Advantages of Mud Cooling Systems for Drilling“; Vincent Maury, SPE 25732-PA; 1995
- [33] "Calculation of Formation Temperature Disturbances Caused by Mud Circulation“; EDWARDSO; Journal of Petroleum Technology 124-PA; 1962

- [34] "Thermal Properties and Temperature-Related Behavior of Rock/Fluid Systems"; W.H. SOMERTON; Elsevier Science Publishers H.V.; ISBN 0-444-89001-7; 1992
- [35] "Thermal Geophysics", A.M. Jessop, Developments in Silod Earth Geophysics 17; Elsevier; 1990; ISBN: 0 444 88309 6
- [36] "Wellbore Heat Transmission"; Ramey; Journal of Petroleum Technology 96-PA; 1962
- [37] "Fluid Flow and Heat Transfer in Wellbores"; A.R. Hasan, C.S. Kabir; SPE; ISBN 1-55563-094-4; 2002
- [38] "Time-Dependent Temperature Behaviour in Rock and Borehole"; PhD dissertation; Stavanger University College; 1999
- [39] "Development and Testing of Insulated Drill-Pipe"; J.T. Finger, Drill Cool Systems; SPE 78267-PA; 2002
- [40] "Mathematical Temperature Simulators for Drilling Deepwater HT/HP Wells: Comparisons, Applications, and Limitations"; David Stiles, Mark Trigg; SPE/IADC Drilling Conference 105437-MS; 2007
- [41] "Metallurgy and Corrosion for Petroleum Engineers"; Skript from Dipl. Ing. Dr. Markus Oberndorfer; SS2007
- [42] Script: "Physikalische Grundlagen der Materialkunde"; Gottstein Günter; 2007; ISBN: 978-3-540-71104-9
- [43] Script: „Metallkunde I“; Prof. Dr. Helmut Clemens; Department für Metallkunde und Werkstoffprüfung
- [44] "Petroleum Engineering Handbook, Volume II: Drilling Engineering"; Edited by: Robert F. Mitchell; 2007; ISBN:978-1-55563-114-7
- [45] "Corrosion Control of Drilling Tools Through Chemical Treatments – Effectiveness and Challenges"; Nausha Asrar, SPE, Schlumberger; 2010
- [46] "Current Techniques for Combating Drill-pipe Corrosion"; H. E. Bush, Ray Barbies, Jay P. Simpson, Baroid Division, National Lead Company; 1966
- [47] "The Degradation of Titanium Drill Pipe From Corrosion and Wear in a Drilling Environment"; T.E. Ferg, SPE, Colorado School of Mines, B.D. Craig, SPE, Metallurgical Consultants Inc., and C.S. Aldrich, SPE, Colorado School of Mines; 1993
- [48] "Drillstring with aluminum alloy pipes design and practices"; Mikhail Ya. Gelfgat, Vladimir S. Basovich, Vadim S. Tikhonov, Aquatic Company; 2003
- [49] "Defining the Corrosion Performance Window for Grade 28 Titanium"; R.W. Schutz; NACE 03455; 2003
- [50] "Implement Russian Aluminum Drill Pipe and Retractable Drilling Bits into the USA, Volume I: Development of Aluminum Drill Pipe in Russia, Final Report"; Aquatic Company Moscow, Russia; 1999
- [51] "Unsealed-bearing drill bits are often used in geothermal drilling, where well temperatures prevent the use of any seals"; World Oil; January 2011 issue, pgs 51-54.

- [52] "Standard Handbook of Petroleum Engineering "; William C. -; 2005
- [53] "Well Cementing"; Erik B. Nelson; Schlumberger Educational Services; 1990
- [54] "Field measurements of annular pressure and temperature during Primary Cementing"; C.E. Chooke, 1983
- [55] "Horizontal Directional Drilling"; Richard S. Carden; PETROSKILLS, LLC. AN OGCI COMPANY; 2007
- [56] Vinylsulfonate/Vinylamide Copolymers in Drilling Fluids for Deep, High-Temperature Wells; Hille, M., Hoechst AG; 1985
- [57] The Evolution and Application of Formate Brines in High-Temperature/High-Pressure Operations; D. Bungert, Mobil EEG; S. Maikranz, M-I Drilling Fluids Germany; R. Sundermann, M-I Federal; J. Downs, Norsk Hydro; W. Benton, Cabot Specialty Fluids; M.A. Dick, M-I L.L.C.; 2000
- [58] "Physical chemistry of colloids and interfaces in oil production: proceedings of the 6th IFP Exploration and Production Research Conference, held in Saint-Raphaël, September 4-6, 1991"; page 200
- [59] "Taking Nondamaging Fluids to New Extremes: Formate-Based Drilling Fluids for High-Temperature Reservoirs in Pakistan" R.J. Oswald, OMV; 2006
- [60] "Impact of Heat Aging on Sediment Toxicity of Ester/Olefin-Based Drilling Fluids to *Leptocheirus Plumulosus*"; M.L. Cano, Shell Chemical LP; S. Rabke and J. Candler, M-I SWACO; P.B. Dorn and J.T. Louallen, Shell Global Solutions; and P. Scott, Marathon Oil Corp.; 2005
- [61] "Factors Involved in High-Temperature Drilling Fluids"; Weintritt, D.J., Hughes, R.G., Baroid Div., National Lead Co; 1965
- [62] "Jeotermal Kuyularda Koruma Borusu Tasarimi"; U. Serpen, U. Yalniz; Sondaj Sempozyumu 96 Izmir; 1996
- [63] "Drilling Data Handbook"; Jean-Paul Nguyen, Gilles Gabolde; ISBN: 2710808714; 2006
- [64] "ENI Drilling Fluids Operations Manual";G. Ferrari C. Lanzetta A. Galletta; 1999
- [65] "Kautschuktechnologie: Werkstoffe - Verarbeitung – Produkte"; Fritz Röthemeyer, Franz Sommer; Carl Hanser Verlag GmbH & CO. KG; ISBN: 978-3446404809; 2006
- [66] „Frontier Geothermal Drilling Operations Succeed at 500°C BHST"; Seiji Saito, Sumio Sakuma, SPE 65104-PA; 2000
- [67] "Iceland Deep Drilling Project Finds Magma"; Wilfred A. Elders, Guðmundur Ómar Friðleifsson; article <http://www.geothermal.org/09JulyAugust31.pdf>; 2009
- [68] "Practical advantages of Mud Cooling Systems for Drilling"; Vincent Maury and Alain Guenot; SPE 25732-PA; 1995
- [69] Homepage of the icdp (international continental scientific drilling program): [http://www.icdp-online.org/front\\_content.php?idcat=1446](http://www.icdp-online.org/front_content.php?idcat=1446)
- [70] "Weatherford Drilling Motors Handbook"; Weatherford



- [71] "New Technique Improves Steam Stimulation Completions"; Greer, F. Conrad; SPE 1944-PA; 1968;
- [72] "Hazards Of Yield-Strength Designing"; R. L. McGlasson; American Petroleum Institute 63-012; 1963
- [73] "Geothermal Well Completions: A Critical Review of Downhole Problems and Specialized Technology Needs"; Snyder, Robert E.; SPE 8211-MS; 1979
- [74] "Casing Temperature and Stress Analysis in Steam-Injection Wells"; Jiang Wu; SPE 103882-MS; 2006
- [75] "Effects of Metal Thickness and Temperature on Casing and Tubing Design For Deep, Sour Wells"; J. Brison Greer; Journal of Petroleum Technology 3968-PA; 1973
- [76] „Grundlagen der Elastomertechnologie – Elastomertechnologie 1“; Script, Holzner, Armin, Dipl.-Ing. Dr.techn.; Lehrstuhl für Chemie der Kunststoffe
- [77] "Sperry Drilling Technical Information Handbook"; Halliburton,
- [78] "High Pressure/High Temperature (HP/HT) Seals for Oil and Gas Production"; Ray, Thomas W.; SPE 39573-MS; 1988
- [79] "Elastomeric seals & components for the Oil & Gas industry"; Issue 8; James Walker catalogue; [http://www.jameswalker.biz/system/pdf\\_docs/fichiers/49/original\\_50574\\_JW\\_Elastomeric\\_seals\\_and\\_components\\_for\\_the\\_Oil\\_Gas\\_11.pdf](http://www.jameswalker.biz/system/pdf_docs/fichiers/49/original_50574_JW_Elastomeric_seals_and_components_for_the_Oil_Gas_11.pdf)
- [80] "Technology development for high temperature logging tools"; Veneruso, A.F; Society of Petrophysicists & Well Log Analysts 1979-KK; 1979
- [81] "High-Temperature Variable Bore Ram Blowout Preventer Sealing"; D.J. McWhorter, Offshore Technology Conference 7336-MS; 1993
- [82] "Performance Characteristics of Oilfield Proven Elastomers in Low-Temperature Seal Applications"; K.W. Taylor, Offshore Technology Conference 6583-MS; 1991
- [83] "Accelerated Testing for Lifetime Prediction for Sealing Materials in Drilling and Completion Fluids"; Thomas Schwarz; NACE International 01114; 2001
- [84] "Drilling engineering Workbook" Baker Hughes INTEQ
- [85] "Drilling Completion and Stimulation Program - Development of a High-Pressure/High-Temperature Downhole Turbine Generator" Tim Price; 2006
- [86] "Development of a Mud-Pulse High-Temperature Measurement-While-Drilling (MWD) System - Final Report "; John H. Cohen; Maurer Technology Inc.; 2002
- [88] High Pressure, High Temperature Well Logging, Perforating and Testing"; Schlumberger Oilfield Review Vol. 10 Issue 2; 1998
- [89] "Deep Trek High Temperature Electronics Program"; Edgar R.; United States Department of Energy; 2010
- [90] "Optimizing Wireline Formation Evaluation in HP/HT Wells"; Roderick A. Larson; SPE 97569-MS; 2005
- [91] "Reliable Electronics for High-Temperature Downhole Applications"; B.L. Gingerich, SPE 56438-MS; 1999

- 
- [92] "Integrated PoF and CBM Strategies for Improving Electronics Reliability Performance of Downhole MWD and LWD Tools"; Sheng Zhan, SPE 132665-MS; 2010
- [93] "Quantifying Common Drilling Problems With Mechanical Specific Energy and a Bit-Specific Coefficient of Sliding Friction"; Pessier; SPE 24584-MS; 1992
- [94] "Euler Buckling of Geothermal Well Casing" Robert P. Rechar, Karl W.Schule; Sandia National Laboratorie; SAND82-0863; 1983
- [95] "In-Situ Rheological Characterization of Drilling Mud"; Roberto Maglione; SPE Journal 66285-PA; 2000
- [96] "Materials Selection in Mechanical Design, Third Edition"; Michael Ashby; ISBN: 0750661682; 2005
- [97] "Practical Well Planning and Drilling Manual"; Steve Devereaux; ISBN-10: 0-87814-696-2; 1998

## Appendix

### A. Temperature limitations of fluid additives

List of some common drilling fluid additives and their limitations:

Component Type	Additive Name	Temperature Limit [°C]	Source
Base Fluid	#2 Diesel, 36% Aromatic content	65	[52]
Base Fluid	Mineral Oil 25% Aromatic content	68	[52]
Base Fluid	Mineral Oil 2% Aromatic content	76	[52]
Base Fluid	Mineral Oil 0% Aromatic content	93	[52]
Base Fluid	Mineral Oil 5% Aromatic content	96	[52]
Base Fluid	Mineral Oil 7% Aromatic content	99	[52]
Base Fluid	n-Alkane Paraffin	92	[52]
Base Fluid	LAO Synthetic	115	[52]
Base Fluid	IO Synthetic	115	[52]
Base Fluid	Easter Synthetic	122	[52]
Base Fluid	Synthetic Blend	180	[52]
Mud System	KCL - polymer system	150	[52]
Mud System	Spud Mud	100	[52]
Mud System	Natural Mud	100	[52]
Mud System	Chemically treated mud	150	[52]
Mud System	Saltwater muds	100	[52]
Mud System	Lignite/Lignosulfonate Mud	150	[52]
Mud System	Calcium treated Mud: Lime mud	121	[52]
Mud System	Calcium treated Mud: Gypsum mud	121	[52]
Mud System	Air/Gas drilling mud	260	[52]
Mud System	Mist drilling mud	148	[52]
Mud System	Foam drilling mud	204	[52]
Mud System	Extended Bentonite Muds	93 - 135	[52]
Mud System	Inhibitive Salt/Polymere Mud	121	[52]
Mud System	Surfactant Muds	120	[52]
Mud System	High Temperature Polymere muds	205	[52]
Mud System	Oil based mud	280	[52]
Thinner	Polyphosphate	80	[56]
Thinner	Quebracho	120	[56]
Thinner	Lignosulfonate	170	[56]
Thinner	Lignite	200	[56]
Thinner	Styrenesulfonate/ maleic acid anhydride	200	[56]
Thinner	Polyacrylate polymers and modified	200	[56]

	polyacrylates		
Polymer	Starch and Starch derivatives	100	[56]
Polymer	Cellulose Ethers such as CMC, CMHEC, HEC	140	[56]
Polymer	Biopolymers	140	[56]
Polymer	Acrylate/acrylamide copolymers	200	[56]
Polymer	Vinylsulfonate/vinylamide copolymers	200	[56]
Bactericides	Starch	140	[64]
Emulsifiers	lignosulfonates	150	[64]
Filtrate- or fluid loss	bentonite clays	100	[64]
Filtrate- or fluid loss	sodium carboxymethyl cellulose (CMC)	121	[64]
Filtrate- or fluid loss	Polyanionic Cellulose (PAC)	120	[64]
Filtrate- or fluid loss	pregelatinized starch	140	[64]
Viscosifiers	bentonite	100	[64]
Viscosifiers	XCD Xanthan Harz	120	[64]
Viscosifiers	sclero glukane	140	[64]

**Table 23:** Limits for mud system, base fluids and additives and their limits found in the literature

List of some common cement additives and their limitations:

Additive Type	Additive Name	Temperature Limit [°C]	Provider	Soruce
Weight Control	Bentonite	93	general	[52]
Accelerator	Calcium Chloride	51	general	[52]
Accelerator	Sodium Chloride	70	general	[52]
Accelerator	Gypsum	60	general	[52]
Accelerator	Gypsum-high-temperature grade	83	general	[52]
Retarder	Lignosulfonate	122	general	[53]
Retarder	Lignosulfonate mixed with sodium borate	315	general	[53]
Retarder	Hydroxycarboxylic acids	150	general	[53]
Extender	Gilsonite	150	general	[53]
Extender	Powdered Coal	538	general	[53]
Extender	Fly Ash	232	general	[53]
Dispersant	Polymelamine su&xlafe (PMS)	85	general	[53]
Dispersant	Lignosulfonates	122	general	[53]
Filtrate- or fluid loss	Cellulose	93	general	[53]
Filtrate- or fluid loss	Poly(ethyleneimine)	225	general	[53]
Filtrate- or fluid loss	latices - vinylidene chloride	50	general	[53]
Filtrate- or fluid loss	latices - polyvinyl acetate	50	general	[53]
Filtrate- or fluid loss	latices - Styrene-butadiene latex	176	general	[53]
Retarder	R-3,	82	BJ Services	[63]
Retarder	D13(DB1)	82	Dowell	[63]

Retarder	HR4/HR7 (HR4L/HR7L)	82	Halliburton	[63]
Retarder	R3 (RI0L/R12L/R21L)	107	BJ Services	[63]
Retarder	DBOO (DB01)	107	Dowell	[63]
Retarder	HR5 (HR6L)	107	Halliburton	[63]
Retarder	R6/Diacel LWL	150	BJ Services	[63]
Retarder	D8 (DI0)	150	Dowell	[63]
Retarder	Diacel LWL	150	Halliburton	[63]
Retarder	RB (RBL)		BJ Services	[63]
Retarder	D2B (D150)		Dowell	[63]
Retarder	HR12/HR15 (HR12L/HR15L)		Halliburton	[63]
Retarder	HR20		Halliburton	[63]
Retarder	SR30 (R14/R15LS/R20L) Synthetic Retarder	121	BJ Services	[63]
Retarder	SCR100 (SCR100L) Synthetic Retarder	121	Halliburton	[63]
Retarder	HR25 (HR25L)	218	Halliburton	[63]
Fluid loss additive	FL62 (SAIOI)	49	BJ Services	[63]
Fluid loss additive	0127/0156	49	Dowell	[63]
Fluid loss additive	LAP1 (LA2)	49	Halliburton	[63]
Fluid loss additive	FL33/FL63 (FL33L/FL63L)	49	BJ Services	[63]
Fluid loss additive	D146	49	Dowell	[63]
Fluid loss additive	Halad 322/344/413 (I)	49	Halliburton	[63]
Fluid loss additive	FL62 (SAIOL)	93	BJ Services	[63]
Fluid loss additive	LAP1/Halad 447 (LA2)	93	Halliburton	[63]
Fluid loss additive	D300	93	Dowell	[63]
Fluid loss additive	(Halad 10L)	93	Halliburton	[63]
Fluid loss additive	D60	93	Dowell	[63]
Fluid loss additive	Halad 9/322 (9L/322L)	93	Halliburton	[63]
Fluid loss additive	D59	93	Dowell	[63]
Fluid loss additive	FL62 (FL62L)	121	BJ Services	[63]
Fluid loss additive	D0160 (0603/0159)	121	Dowell	[63]
Fluid loss additive	Halad 22A/344 (22Al)	121	Halliburton	[63]
Fluid loss additive	D065A (080A/0604AM)	121	Dowell	[63]
Fluid loss additive	Halad 14 (14LXP/600LE+)	149	Halliburton	[63]
Fluid loss additive	FL25/FL52	149	BJ Services	[63]

**Table 24:** Limits for cement additives found in the literature

## B. Temperature limitations of various down-hole tools

List of MWD and LWD tools available on the market:

Tool Type	Tool Name	Company	Temperature Limit [°C]
Density	LithoTrak	Baker Hughes	150
Density	Azimuthal Lithodensity (ALD), standard	Halliburton/Sperry Drilling	150
Density	Azimuthal Lithodensity (ALD), optional	Halliburton/Sperry Drilling	175
Density	Stabilized Lithodensity (SLD)	Halliburton/Sperry Drilling	140
Density	Slim Density/Neutron Stand-off Caliper	PathFinder	150
Density	Survivor Slim Density/Neutron Stand-off Caliper	PathFinder	175
Density	Density/Neutron Stand-off Caliper	PathFinder	150
Density	iFinder Density Imaging	PathFinder	175
Density	adnVISION475, standard	Schlumberger	150
Density	adnVISION475, optional	Schlumberger	175
Density	adnVISION675	Schlumberger	150
Density	adnVISION825	Schlumberger	150
Density	adnVISION825s	Schlumberger	150
Density	EcoScope Standard	Schlumberger	150
Density	EcoScope optional	Schlumberger	175
Density	proVISION	Schlumberger	150
Density	StethoScope 675	Schlumberger	150
Density	StethoScope 825	Schlumberger	150
Density	StethoScope 475	Schlumberger	150
Density	Azimuthal Density (AZD), standard	Weatherford	150
Density	Azimuthal Density (AZD), optional	Weatherford	165
Directional Sruvey	APS SureShot	APS Technology	150
Directional Sruvey	APS SureShot HT	APS Technology	175
Directional Sruvey	APS SureShot gamma	APS Technology	150
Directional Sruvey	APS SureShot gamma, HT	APS Technology	175
Directional Sruvey	AutoTrak	Baker Hughes	150
Directional Sruvey	AutoTrak, HT	Baker Hughes	175
Directional Sruvey	AutoTrak X-treme	Baker Hughes	150
Directional Sruvey	AutoTrak X-treme, HT	Baker Hughes	175
Directional Sruvey	AutoTrak eXpress	Baker Hughes	150
Directional Sruvey	AutoTrak V	Baker Hughes	150
Directional Sruvey	AutoTrak V, HT	Baker Hughes	175
Directional Sruvey	CoilTrak	Baker Hughes	150
Directional Sruvey	GyroTrak	Baker Hughes	115
Directional Sruvey	Multiple Propogation Resistivity	Baker Hughes	115
Directional Sruvey	NaviTrak	Baker Hughes	150
Directional Sruvey	OnTrak	Baker Hughes	150
Directional Sruvey	OnTrak, HT	Baker Hughes	175
Directional Sruvey	AziTrak	Baker Hughes	150

Directional Sruvey	EMTrak	Baker Hughes	150
Directional Sruvey	TruTrak	Baker Hughes	150
Directional Sruvey	VertiTrak	Baker Hughes	150
Directional Sruvey	TeleTrak	Baker Hughes	150
Directional Sruvey	Advanced Slim MWD System	Baker Hughes	150
Directional Sruvey	Positive Pulse MWD Probe Based	DrillTech LLC	150
Directional Sruvey	Positive Pulse MWD Probe Based, HAT	DrillTech LLC	175
Directional Sruvey	GeoLink	GE Energy Oilfield Technology	150
Directional Sruvey	GeoLink, HT	GE Energy Oilfield Technology	175
Directional Sruvey	Centerfire Resistivity System	GE Energy Oilfield Technology	175
Directional Sruvey	CPR Propagation Resistivity	GE Energy Oilfield Technology	175
Directional Sruvey	E-Link	GE Energy Oilfield Technology	150
Directional Sruvey	Geolink UltraSlim	GE Energy Oilfield Technology	150
Directional Sruvey	WellTracer	GE Energy Oilfield Technology	150
Directional Sruvey	Pilot	GE Energy Oilfield Technology	150
Directional Sruvey	Tensor	GE Energy Oilfield Technology	150
Directional Sruvey	Electromagnetic Telemetry System	Halliburton/Sperry Drilling	125
Directional Sruvey	Negative Pulse Telemetry System	Halliburton/Sperry Drilling	150
Directional Sruvey	Positive Pulse Telemetry System	Halliburton/Sperry Drilling	150
Directional Sruvey	Positive Pulse Telemetry System, HT	Halliburton/Sperry Drilling	175
Directional Sruvey	MWD Gyro	Halliburton/Sperry Drilling	150
Directional Sruvey	UltraHT-230™ MWD/LWD Sensors	Halliburton/Sperry Drilling	230
Directional Sruvey	MWD Services LLC.	MWD Services LLC.	150
Directional Sruvey	Drift	Navigate Energy Services	150
Directional Sruvey	Directional	Navigate Energy Services	150
Directional Sruvey	HDS-1L Directional Survey	PathFinder	150
Directional Sruvey	HDS-1M Directional	PathFinder	150
Directional Sruvey	HDS-1R Directional	PathFinder	150
Directional Sruvey	HDS-1S Directional	PathFinder	150
Directional Sruvey	Survivor HDS-1 Directional	PathFinder	175
Directional Sruvey	Survivor HDS-1R Directional	PathFinder	175
Directional Sruvey	Survivor HDS-1R Directional	PathFinder	175
Directional Sruvey	Payzone Inclination Gamma	PathFinder	150
Directional Sruvey	Gyro HDS1	PathFinder	150
Directional Sruvey	Gravity HDS1	PathFinder	150
Directional Sruvey	Survivor Gravity HDS1	PathFinder	175
Directional Sruvey	APS SureShot	PathFinder	175
Directional Sruvey	Slim Array Wave Resistivity	PathFinder	150
Directional Sruvey	Survivor Slim Array Wave Resistivity	PathFinder	175
Directional Sruvey	Array Wave Resistivity	PathFinder	150
Directional Sruvey	Survivor Array Wave Resistivity	PathFinder	175
Directional Sruvey	2D Rotary Steering Tool	PathFinder	150
Directional Sruvey	PathMaker Rotary Steerable	PathFinder	150
Directional Sruvey	Ryan EM	Ryan Energy Technologies	150
Directional Sruvey	Ryan Mud Pulse	Ryan Energy Technologies	150

Directional Sruvey	PowerDrive Xtra	Schlumberger	125
Directional Sruvey	PowerDrive X5	Schlumberger	150
Directional Sruvey	Power Drive Xceed	Schlumberger	150
Directional Sruvey	PowerV Vertical drilling	Schlumberger	150
Directional Sruvey	PowerDrive vorteX475	Schlumberger	150
Directional Sruvey	PowerDrive vorteX675	Schlumberger	150
Directional Sruvey	PowerDrive vorteX825	Schlumberger	150
Directional Sruvey	PowerDrive vorteX900	Schlumberger	150
Directional Sruvey	PowerDrive vorteX1100	Schlumberger	150
Directional Sruvey	PowerPak ERT high performance positive displacement motors	Schlumberger	175
Directional Sruvey	ImPulse	Schlumberger	150
Directional Sruvey	ImPulse, HAT	Schlumberger	175
Directional Sruvey	ShortPulse	Schlumberger	150
Directional Sruvey	ShortPulse, HAT	Schlumberger	175
Directional Sruvey	PowerPulse	Schlumberger	150
Directional Sruvey	PowerPulse, HAT	Schlumberger	175
Directional Sruvey	TeleScope	Schlumberger	150
Directional Sruvey	TeleScope, HAT	Schlumberger	175
Directional Sruvey	SlimPulse	Schlumberger	150
Directional Sruvey	SlimPulse, HAT	Schlumberger	175
Directional Sruvey	E-Pulse	Schlumberger	125
Directional Sruvey	E-Pulse XR	Schlumberger	125
Directional Sruvey	GyroPulse	Schlumberger	150
Directional Sruvey	Orienteer Retrievable	Sondex Drilling (Rentals Division)	150
Directional Sruvey	Orienteer Standard	Sondex Drilling (Rentals Division)	150
Directional Sruvey	Orienteer E-Link	Sondex Drilling (Rentals Division)	150
Directional Sruvey	Orienteer Microlite	Sondex Drilling (Rentals Division)	150
Directional Sruvey	Orienteer Ultralite	Sondex Drilling (Rentals Division)	150
Directional Sruvey	Orienteer Ultraslim	Sondex Drilling (Rentals Division)	150
Directional Sruvey	WellTracer	Sondex Drilling (Rentals Division)	150
Directional Sruvey	Pilot MWD	Sondex Drilling (Rentals Division)	150
Directional Sruvey	Target Retrievable System	Target MWD Inc.	150
Directional Sruvey	Revolution Rotary Steerable	Weatherford	150
Directional Sruvey	High Temperature Rotary Steerable (Revolution HT)	Weatherford	160
Directional Sruvey	High Temperature Rotary Steerable (Revolution HT)	Weatherford	180
Directional Sruvey	EMpulse (Electromagnetic)	Weatherford	150
Directional Sruvey	Hostile Environment Logging	Weatherford	150
Directional Sruvey	Hostile Environment Logging	Weatherford	180
Directional Sruvey	HyperPulse	Weatherford	150
Drilling Mechanics	APS Technology (Rental Division)	APS Technology (Rental Division)	150



Drilling Mechanics	Acoustic Caliper	Baker Hughes	150
Drilling Mechanics	AutoTrak G3 (Rotary Steerable System, including OnTrak or AziTrak Integrated MWD/LWD)	Baker Hughes	150
Drilling Mechanics	AutoTrak G3 (Rotary Steerable System, including OnTrak or AziTrak Integrated MWD/LWD)	Baker Hughes	175
Drilling Mechanics	AutoTrak Generation 3.0 (includes OnTrak or AziTrak MWD), can also be run in combination with Modular X-treme motor.	Baker Hughes	150
Drilling Mechanics	AutoTrak Generation 3.0 (includes OnTrak or AziTrak MWD), can also be run in combination with Modular X-treme motor.	Baker Hughes	175
Drilling Mechanics	AutoTrak eXpress	Baker Hughes	150
Drilling Mechanics	AutoTrak V	Baker Hughes	150
Drilling Mechanics	AutoTrak V	Baker Hughes	175
Drilling Mechanics	CoilTrak	Baker Hughes	150
Drilling Mechanics	CoPilot	Baker Hughes	150
Drilling Mechanics	Drill Collar Pressure	Baker Hughes	150
Drilling Mechanics	EMTrak	Baker Hughes	150
Drilling Mechanics	NaviTrak II Advanced Pressure	Baker Hughes	150
Drilling Mechanics	TeleTrak	Baker Hughes	150
Drilling Mechanics	OnTrak MWD	Baker Hughes	150
Drilling Mechanics	OnTrak MWD	Baker Hughes	175
Drilling Mechanics	AziTrak MWD	Baker Hughes	150
Drilling Mechanics	3.1/8" Advanced Slim MWD System + Drilling Performance Sub	Baker Hughes	150
Drilling Mechanics	Sentinel, Shock and Vibration	GE Energy Oilfield Technology	150
Drilling Mechanics	Guardian, Pressure During Drilling	GE Energy Oilfield Technology	150
Drilling Mechanics	AcoustiCaliper	Halliburton/Sperry Drilling	150
Drilling Mechanics	Drillstring Dynamics	Halliburton/Sperry Drilling	150
Drilling Mechanics	Pressure While Drilling	Halliburton/Sperry Drilling	175
Drilling Mechanics	Pressure While Drilling	Halliburton/Sperry Drilling	230
Drilling Mechanics	Vibration Severity	Halliburton/Sperry Drilling	230
Drilling Mechanics	Vibration Severity	Halliburton/Sperry Drilling	175
Drilling Mechanics	Annular Mud Temperature	Halliburton/Sperry Drilling	150
Drilling Mechanics	Drilling Formation Tester	PathFinder	150
Drilling Mechanics	Dynamic Pressure Module	PathFinder	150
Drilling Mechanics	Survivor Dynamic Pressure Module	PathFinder	150
Drilling Mechanics	Payzone Inclination Gamma	PathFinder	150
Drilling Mechanics	2D Rotary Steering Tool	PathFinder	150
Drilling Mechanics	PathMaker Rotary Steerable	PathFinder	150
Drilling Mechanics	PathMaker Rotary Steerable (only 4 3/4)	PathFinder	175
Drilling Mechanics	Sentinel, Shock and Vibration 2	Sondex Drilling	150
Drilling Mechanics	Guardian, Pressure During Drilling	Sondex Drilling	150
Drilling Mechanics	BAP (Borehole/Annular Pressure)	Weatherford	150
Drilling Mechanics	BAP (Borehole/Annular Pressure)	Weatherford	180
Drilling Mechanics	TVM (True Vibration Monitor)	Weatherford	150
Drilling Mechanics	TVM (True Vibration Monitor)	Weatherford	180

Drilling Mechanics	ESM (Environmental Severity Measurement)	Weatherford	150
Drilling Mechanics	ESM (Environmental Severity Measurement)	Weatherford	180
Drilling Mechanics	RAT (Rapid Annular Temperature)	Weatherford	150
Drilling Mechanics	RAT (Rapid Annular Temperature)	Weatherford	180
Formation Fluid Identification and Sampling	GeoTap IDS	Halliburton/Sperry Drilling	150
Formation Pressure Testing	TesTrak	Baker Hughes	150
Formation Pressure Testing	GeoTap	Halliburton/Sperry Drilling	150
Formation Pressure Testing	Drilling Formation Tester	PathFinder	150
Formation Pressure Testing	StethoScope 675, standard	Schlumberger	150
Formation Pressure Testing	StethoScope 675, optional	Schlumberger	165
Formation Pressure Testing	StethoScope 825, standard	Schlumberger	150
Formation Pressure Testing	StethoScope 825, optional	Schlumberger	165
Formation Pressure Testing	StethoScope 475, standard	Schlumberger	150
Formation Pressure Testing	StethoScope 475, optional	Schlumberger	175
Gamma Ray	APS SureShot	APS Technology (Rental Division)	150
Gamma Ray	APS SureShot	APS Technology (Rental Division)	175
Gamma Ray	APS SureShot with Gamma	APS Technology (Rental Division)	150
Gamma Ray	APS SureShot with Gamma	APS Technology (Rental Division)	175
Gamma Ray	AutoTrak G3 (Rotary Steerable System, including OnTrak or AziTrak Integrated MWD/LWD)	Baker Hughes	150
Gamma Ray	AutoTrak G3 (Rotary Steerable System, including OnTrak or AziTrak Integrated MWD/LWD)	Baker Hughes	175
Gamma Ray	AutoTrak X-treme	Baker Hughes	150
Gamma Ray	AutoTrak X-treme, HT	Baker Hughes	175
Gamma Ray	AutoTrak eXpress	Baker Hughes	150
Gamma Ray	CoilTrak	Baker Hughes	150
Gamma Ray	EMTrak	Baker Hughes	150
Gamma Ray	Multiple Propagation Resistivity	Baker Hughes	150
Gamma Ray	NaviGamma	Baker Hughes	150
Gamma Ray	TeleTrak	Baker Hughes	150
Gamma Ray	OnTrak MWD	Baker Hughes	150
Gamma Ray	OnTrak MWD	Baker Hughes	175
Gamma Ray	AziTrak MWD	Baker Hughes	150
Gamma Ray	Near Bit Gamma	Baker Hughes	150
Gamma Ray	TruTrak	Baker Hughes	150
Gamma Ray	3.1/8" Advanced SLIM MWD System	Baker Hughes	150
Gamma Ray	Positive Pulse MWD and API Gamma Ray Probe Based	DrilTech LLC	150

Gamma Ray	Positive Pulse MWD and API Gamma Ray Probe Based	DrilTech LLC	175
Gamma Ray	Geolink Modular Gamma	GE Energy Oilfield Technology	150
Gamma Ray	Pilot Gamma	GE Energy Oilfield Technology	150
Gamma Ray	Scinturion Gamma	GE Energy Oilfield Technology	150
Gamma Ray	Dual Gamma Ray (DGR)	Halliburton/Sperry Drilling	150
Gamma Ray	Gamma Ray Probe	Halliburton/Sperry Drilling	150
Gamma Ray	Gamma Ray Probe	Halliburton/Sperry Drilling	175
Gamma Ray	Azimuthal Gamma Ray (AGR)	Halliburton/Sperry Drilling	150
Gamma Ray	Geo-Pilot Gamma Ray (ABG)	Halliburton/Sperry Drilling	150
Gamma Ray	Geo-Pilot Gamma Ray (ABG)	Halliburton/Sperry Drilling	175
Gamma Ray	Gamma Ray/At-Bit Inclination (GABI)	Halliburton/Sperry Drilling	150
Gamma Ray	UltraHT-230™ MWD/LWD Sensors	Halliburton/Sperry Drilling	230
Gamma Ray	MWD Shuttle	MWD Services Inc.	150
Gamma Ray	Directional Gamma	Navigate Energy Services	150
Gamma Ray	HDS-1L Directional Gamma	PathFinder	150
Gamma Ray	HDS-1L Directional Gamma	PathFinder	150
Gamma Ray	HDS-1R Directional Gamma	PathFinder	150
Gamma Ray	Survivor HDS-1L Directional Gamma	PathFinder	175
Gamma Ray	Survivor HDS-1S Directional Gamma	PathFinder	175
Gamma Ray	Survivor HDS-1R Directional Gamma	PathFinder	175
Gamma Ray	Payzone Inclination Gamma	PathFinder	150
Gamma Ray	APS SureShot with Gamma	PathFinder	175
Gamma Ray	Compensated Wave Resistivity	PathFinder	150
Gamma Ray	Slim Array Wave Resistivity	PathFinder	150
Gamma Ray	Survivor Slim Array Wave Resistivity	PathFinder	175
Gamma Ray	Array Wave Resistivity	PathFinder	150
Gamma Ray	Survivor Array Wave Resistivity	PathFinder	175
Gamma Ray	PathMaker Rotary Steerable	PathFinder	150
Gamma Ray	PathMaker Rotary Steerable	PathFinder	175
Gamma Ray	PowerDrive X5	Schlumberger	150
Gamma Ray	ShortPulse	Schlumberger	150
Gamma Ray	ImPulse	Schlumberger	150
Gamma Ray	PowerPulse	Schlumberger	150
Gamma Ray	TeleScope	Schlumberger	150
Gamma Ray	SlimPulse	Schlumberger	150
Gamma Ray	E-Pulse	Schlumberger	125
Gamma Ray	ShortPulse	Schlumberger	175
Gamma Ray	ImPulse	Schlumberger	175
Gamma Ray	PowerPulse	Schlumberger	175
Gamma Ray	TeleScope	Schlumberger	175
Gamma Ray	SlimPulse	Schlumberger	175
Gamma Ray	E-Pulse XR	Schlumberger	125
Gamma Ray	geoVISION675	Schlumberger	150
Gamma Ray	geoVISION825	Schlumberger	150
Gamma Ray	arcVISION312	Schlumberger	150

Gamma Ray	arcVISION475	Schlumberger	150
Gamma Ray	arcVISION675	Schlumberger	150
Gamma Ray	arcVISION675	Schlumberger	175
Gamma Ray	arcVISION825	Schlumberger	150
Gamma Ray	arcVISION900	Schlumberger	150
Gamma Ray	EcoScope	Schlumberger	150
Gamma Ray	EcoScope	Schlumberger	175
Gamma Ray	PeriScope	Schlumberger	150
Gamma Ray	Orienteer Modular Gamma	Sondex Drilling (Rentals Division)	150
Gamma Ray	Orienteer Modular Gamma	Sondex Drilling (Rentals Division)	150
Gamma Ray	Target Retrievable Gamma System	Target MWD Inc.	150
Gamma Ray	EMpulse (Electromagnetic)	Weatherford	150
Gamma Ray	HyperPulse	Weatherford	150
Gamma Ray	150 15 HAGR (High-temperature Azimuthal GR)	Weatherford	150
Gamma Ray	SAGR (Spectral Azimuthal GR)	Weatherford	150
Gamma Ray	At-Bit Measurement System	Weatherford	150
Gamma Ray	150 15 HAGR (High-temperature Azimuthal GR)	Weatherford	180
Porosity	LithoTrak	Baker Hughes	150
Porosity	SoundTrak	Baker Hughes	150
Porosity	MagTrak (Advanced Magnetic Resonance While Drilling)	Baker Hughes	150
Porosity	Bi-modal AcousTic (BAT)	Halliburton/Sperry Drilling	150
Porosity	Compensated Neutron Porosity	Halliburton/Sperry Drilling	150
Porosity	Compensated Thermal Neutron (CTN), standard	Halliburton/Sperry Drilling	150
Porosity	Compensated Thermal Neutron (CTN), optional	Halliburton/Sperry Drilling	175
Porosity	Magnetic Resonance Imaging Logging While Drilling (MRIL-WD)	Halliburton/Sperry Drilling	150
Porosity	Compensated Long-Spaced Sonic	PathFinder	150
Porosity	E Sonic	PathFinder	150
Porosity	Slim Density/Neutron Standoff Caliper	PathFinder	150
Porosity	Survivor Slim Density/Neutron Stand-off Caliper	PathFinder	175
Porosity	Density/Neutron Stand-off Caliper	PathFinder	150
Porosity	iFinder Density Imaging	PathFinder	175
Porosity	SonicScope475	Schlumberger	150
Porosity	sonicVISION675	Schlumberger	150
Porosity	sonicVISION825	Schlumberger	150
Porosity	sonicVISION900	Schlumberger	150
Porosity	adnVISION475, standard	Schlumberger	150
Porosity	adnVISION475, optional	Schlumberger	175
Porosity	adnVISION675	Schlumberger	150
Porosity	adnVISION825	Schlumberger	150
Porosity	adnVISION825s	Schlumberger	150
Porosity	proVISION	Schlumberger	150

Porosity	EcoScope Standard	Schlumberger	150
Porosity	EcoScope optional	Schlumberger	175
Porosity	Thermal Neutron Porosity (TNP), Standard	Weatherford	150
Porosity	Thermal Neutron Porosity (TNP), optional	Weatherford	165
Porosity	Shockwave Sonic (SST), Standard	Weatherford	150
Porosity	Shockwave Sonic (SST), optional	Weatherford	165
Resistivity	APS SureShot Gamma + Propagation Resistivity	Baker Hughes	150
Resistivity	APS SureShot Gamma + Propagation Resistivity	Baker Hughes	175
Resistivity	AutoTrak X-treme (Rotary Steerable System, including OnTrak or AziTrak Integrated MWD/LWD and hard-wired, precontoured modular X-treme mud motor)	Baker Hughes	150
Resistivity	AutoTrak X-treme (Rotary Steerable System, including OnTrak or AziTrak Integrated MWD/LWD and hard-wired, precontoured modular X-treme mud motor)	Baker Hughes	175
Resistivity	Multiple Propagation Resistivity	Baker Hughes	150
Resistivity	OnTrak MWD	Baker Hughes	150
Resistivity	OnTrak MWD	Baker Hughes	175
Resistivity	AziTrak MWD	Baker Hughes	150
Resistivity	StarTrak	Baker Hughes	150
Resistivity	ZoneTrak (Bit Resistivity)	Baker Hughes	150
Resistivity	TRIM Induction Resistivity Tool	GE Energy Oilfield Technology	150
Resistivity	Centerfire Propagation Resistivity Tool	GE Energy Oilfield Technology	175
Resistivity	Compact Propagation Resistivity (CPR) Tool	GE Energy Oilfield Technology	150
Resistivity	EWR-PHASE 4	Halliburton/Sperry Drilling	150
Resistivity	EWR-PHASE 4D	Halliburton/Sperry Drilling	150
Resistivity	SuperSlim EWR-PHASE 4	Halliburton/Sperry Drilling	150
Resistivity	SuperSlim EWR-PHASE 4	Halliburton/Sperry Drilling	150
Resistivity	EWR-M5	Halliburton/Sperry Drilling	150
Resistivity	Azimuthal Focused Resistivity (AFR)	Halliburton/Sperry Drilling	150
Resistivity	Azimuthal Deep Resistivity (ADR)	Halliburton/Sperry Drilling	150
Resistivity	Compensated Wave Resistivity	PathFinder	150
Resistivity	Slim Compensated Wave Resistivity	PathFinder	150
Resistivity	Slim Array Wave Resistivity	PathFinder	150
Resistivity	Survivor Slim Array Wave Resistivity	PathFinder	175
Resistivity	Array Wave Resistivity 6	PathFinder	150
Resistivity	Survivor Array Wave Resistivity	PathFinder	175
Resistivity	mcrVISION	Schlumberger	150
Resistivity	ImPulse standard	Schlumberger	150
Resistivity	ImPulse optional	Schlumberger	175
Resistivity	geoVISION675	Schlumberger	150
Resistivity	geoVISION825	Schlumberger	150
Resistivity	arcVISION312	Schlumberger	150
Resistivity	arcVISION475	Schlumberger	150

Resistivity	arcVISION675 standard	Schlumberger	150
Resistivity	arcVISION675 optional	Schlumberger	165
Resistivity	arcVISION825	Schlumberger	150
Resistivity	arcVISION900	Schlumberger	150
Resistivity	PeriScope	Schlumberger	150
Resistivity	EcoScope Standard	Schlumberger	150
Resistivity	EcoScope optional	Schlumberger	175
Resistivity	Orienteer TRIM Resistivity	Sondex Drilling (Rentals Division)	150
Resistivity	Compact Propagation Resistivity (CPR) Tool, standard	Sondex Drilling (Rentals Division)	150
Resistivity	Compact Propagation Resistivity (CPR) Tool, optional	Sondex Drilling (Rentals Division)	175
Resistivity	Multi-Frequency Resistivity (MFR), standard	Weatherford	150
Resistivity	Multi-Frequency Resistivity (MFR), optional	Weatherford	165
Resistivity	Multi-Frequency Resistivity (MFR) - High Temperature, standard	Weatherford	150
Resistivity	Multi-Frequency Resistivity (MFR) - High Temperature, optional	Weatherford	180
Resistivity	Multi-Frequency Resistivity-PLUS(MFR-PLUS)	Weatherford	150
Resistivity	GuideWave Azimuthal Multi-Frequency Resistivity (Az-MFR)	Weatherford	150
Seismic	seismicVISION675	Schlumberger	150
Seismic	seismicVISION825	Schlumberger	150
Seismic	seismicVISION675	Schlumberger	150
Seismic	seismicVISION900	Schlumberger	150
Well Placement Technology	AziTrak MWD	Baker Hughes	150
Well Placement Technology	ZoneTrak (Bit Resistivity)	Baker Hughes	150
Well Placement Technology	DeepTrak	Baker Hughes	150
Well Placement Technology	StarTrak	Baker Hughes	150
Well Placement Technology	Azimuthal Deep Resistivity (ADR)	Halliburton/Sperry Drilling	150
Well Placement Technology	Azimuthal Focused Resistivity (AFR)	Halliburton/Sperry Drilling	150
Well Placement Technology	At-Bit Inclination (ABI)	Halliburton/Sperry Drilling	150
Well Placement Technology	Payzone Inclination Gamma	PathFinder	150
Well Placement Technology	PeriScope	Schlumberger	150
Well Placement Technology	geoVISION675	Schlumberger	150
Well Placement Technology	geoVISION825	Schlumberger	150
Well Placement Technology	EcoScope Standard	Schlumberger	150
Well Placement Technology	EcoScope optional	Schlumberger	175
Well Placement Technology	arcVISION312	Schlumberger	150
Well Placement Technology	Multi-Frequency Resistivity- PLUS(MFR-PLUS)	Weatherford	150

---

Well Placement Technology	GuideWave Azimuthal Multi-Frequency Resistivity (Az-MFR)	Weatherford	150
Well Placement Technology	At-Bit Measurement System	Weatherford	150

**Table 25:** Temperature limits of MWD/LWD tools